AD-A082 025 ARMY MISSILE COMMAND REDSTONE ARSENAL AL TECHNOLOGY LAB F/G 17/1
A POLYVINYLIDENE FLUORIDE DIFFERENTIAL MEMBRANE PRESSURE ACOUST--ETC(U)
SEP 79 J A SCHAEFFEL
UNCLASSIFIED DRSMI-T-79-25 NL

1 of 2

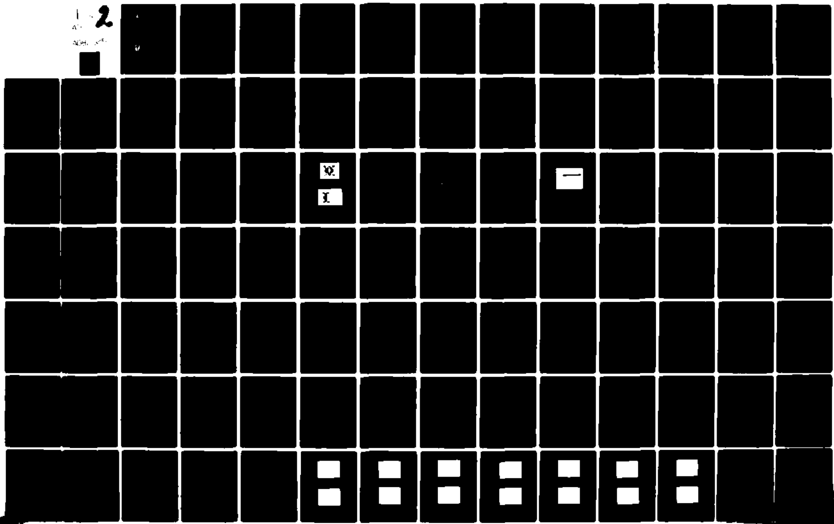

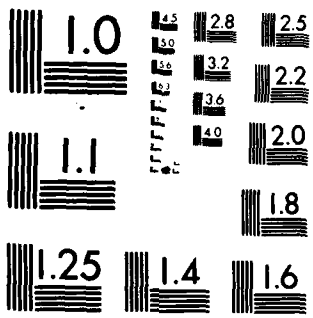

MICROCOPY RESOLUTION TEST CHART
NATIONAL BUREAU OF STANDARDS 1963 A

12

LEVEL II

AD A 082025

TECHNICAL REPORT T-79-95

A POLYVINYLIDENE FLUORIDE DIFFERENTIAL MEMBRANE PRESSURE ACOUSTICAL TRANSDUCER

John A. Schaeffel, Jr.
Ground Equipment and Missile
Structures Directorate
US Army Missile Laboratory

DTIC
ELECTE
MAR 19 1980
A

28 September 1979

U.S. ARMY MISSILE COMMAND
Redstone Arsenal, Alabama 35809

Approved for public release; distribution unlimited.

DDC FILE COPY

SMI FORM 1021, 1 JUL 79 PREVIOUS EDITION IS OBSOLETE

80 3 18 033

DISPOSITION INSTRUCTIONS

DESTROY THIS REPORT WHEN IT IS NO LONGER NEEDED. DO NOT RETURN IT TO THE ORIGINATOR.

DISCLAIMER

THE FINDINGS IN THIS REPORT ARE NOT TO BE CONSTRUED AS AN *OFFICIAL DEPARTMENT OF THE ARMY POSITION* UNLESS SO DESIGNATED BY OTHER AUTHORIZED DOCUMENTS.

TRADE NAMES

USE OF TRADE NAMES OR MANUFACTURERS IN THIS REPORT DOES NOT CONSTITUTE AN OFFICIAL ENDORSEMENT OR APPROVAL OF THE USE OF SUCH COMMERCIAL HARDWARE OR SOFTWARE.

(14) DRSMI-T-79-25

UNCLASSIFIED

SECURITY CLASSIFICATION OF THIS PAGE (When Data Entered)

REPORT DOCUMENTATION PAGE

READ INSTRUCTIONS BEFORE COMPLETING FORM

1. REPORT NUMBER T-79-95	2. GOVT ACCESSION NO.	3. RECIPIENT'S CATALOG NUMBER (9)
4. TITLE (and Subtitle) (6) A POLYVINYLIDENE FLUORIDE DIFFERENTIAL MEMBRANE PRESSURE ACOUSTICAL TRANSDUCER.		5. TYPE OF REPORT & PERIOD COVERED Technical Report,
		6. PERFORMING ORG. REPORT NUMBER
7. AUTHOR(s) (10) John A. Schaeffel, Jr		8. CONTRACT OR GRANT NUMBER(s) (12) 117
9. PERFORMING ORGANIZATION NAME AND ADDRESS Commander US Army Missile Command ATTN: DRSMI-RL Redstone Arsenal, Alabama 35809		10. PROGRAM ELEMENT, PROJECT, TASK AREA & WORK UNIT NUMBERS
11. CONTROLLING OFFICE NAME AND ADDRESS Commander US Army Missile Command ATTN: DRSMI-RPT Redstone Arsenal, Alabama 35809	(11)	12. REPORT DATE 28 Sep[redacted]79
		13. NUMBER OF PAGES 116
14. MONITORING AGENCY NAME & ADDRESS(if different from Controlling Office)		15. SECURITY CLASS. (of this report) Unclassified
		15a. DECLASSIFICATION/DOWNGRADING SCHEDULE

16. DISTRIBUTION STATEMENT (of this Report)

Approved for public release; distribution unlimited.

17. DISTRIBUTION STATEMENT (of the abstract entered in Block 20, if different from Report)

18. SUPPLEMENTARY NOTES

19. KEY WORDS (Continue on reverse side if necessary and identify by block number)

Polyvinylidene
Polyvinylidene Fluoride (PVDF)
Acoustical Transducer
Membrane Transducer
Differential Membrane Pressure Transducer
Ultrasonic
Transducer Arrays

20. ABSTRACT (Continue on reverse side if necessary and identify by block number)

This work describes an ultrasonic acoustical transducer used to generate and receive ultrasonic waves. Transducer construction includes a membrane of polyvinylidene fluoride (PVDF), a piezoelectric polymer, which is deflected by liquid or gas pressure to form a concave or convex surface. When an RF signal is applied to the membrane transducer ultrasonic waves are generated. Calculations for the performance of the transducer are given along with the results of a series of ten tests. A 1.27 cm diameter transducer was (cont.)

> over

/ 13427

JOB

20. constructed for this study. Results indicate that, although the acoustical power output of the device is lower than conventional transducers, the lower construction costs and variable focal length capability may make it ideal for fabrication into large transducer arrays.

CONTENTS

Accession For
NTIS GRA&I
DDC TAB
Unannounced
Justification
A

ILLUSTRATIONS

ILLUSTRATIONS (Continued)

ILLUSTRATIONS (Continued)

ILLUSTRATIONS (Continued)

Figure | Page

ILLUSTRATIONS (Concluded)

TABLES

TABLES (Concluded)

I. INTRODUCTION

Polyvinylidene Flouride (PVDF) is a remarkable polymer with piezoelectric properties which may be used in the fabrication of ultrasonic acoustical transducers. The material is currently being manufactured in the United States on a pilot plant scale by the Pennwalt Corporation. It is currently available in 10 cm x 20 cm x approximately 27 micrometer thick sheets for experimental purposes.

PVDF films are currently manufactured by the electrical polarization of stretched sheets of the material [1]. A typical method of manufacture consists of uniaxial stretching PVDF sheets from two to seven times their original length at a temperature of 80 degrees C [2]. The films are then placed between copper plate electrodes and preheated to a specific temperature of around 110 degrees C. The copper plate electrodes are then connected to a high voltage power supply and the films are polarized (poled) in an electric field of 500 to 1000 kV/cm. After about 30 minutes poling time the films are cooled for at least 15 more minutes. Before or after poling, metallic electrodes are vapor deposited onto the surface of the PVDF film as contact electrodes. The exact method used by the Pennwalt Corporation in the manufacture of piezoelectric PVDF films cannot be disclosed for proprietary reasons.

Although this report will not seek to explain the piezoelectric phenomena in PVDF in any detail, a brief description of the effect will be given. Apparently the mechanical stretching of the PVDF sheet stock results in a stress-induced orientation of polyvinylidene fluoride dipoles [3]. The poling process at elevated temperatures preferentially aligns these dipoles normal to the film surface resulting in a piezoelectric material. Another possible mechanism is that the polarization is induced by a combination of inhomogeneous strain due to stretching and the space charge distribution in the film. Whichever theory is correct, the end result is a material having excellent piezoelectric properties in relation to cost and method of manufacture.

At the present time ultrasonic transducers operating from 1 to 10 MHz are needed which have the following features:

- low costs in fabrication and operation,
- high acoustical energy output,

When a mechanical stress is applied to an area of piezoelectric material a polarization per unit area P_i (or dipole moment per unit volume) is generated [7],

where:

$$P_i = d_{ij} \sigma_j \tag{1}$$

$i = 1,2,3$ and $j = 1,2,3,4,5,6$

$P_i \equiv$ polarization per unit area

$d_{ij} \equiv$ piezoelectric moduli (matrix representation)

$\sigma_j \equiv$ applied stress (matrix representation)

Equation (1) refers to the direct piezoelectric effect.

The converse piezoelectric effect occurs when an electric field is applied to a piezoelectric material and it becomes strained by an amount directly proportional to the electric field strength. For this case:

$$\epsilon_j = d_{ij} E_i \tag{2}$$

$\epsilon_j \equiv$ matrix representation of strain

$E_i \equiv$ electric field strength.

As illustrated in Equations (1) and (2) the piezoelectric moduli are measures of the conversion efficiency from an electrical signal to a mechanical strain in the material and vice versa. *Table 1* compares the d piezoelectric constants of various piezoelectric materials in a case of transverse effect [5].

Figure 2 shows a cross sectional view of a PVDF circular membrane deflected under a differential pressure (P) to form a focused transducer as shown in *Figure 1*. If the ultrasound is emitted normal to the surface of the membrane, the focal point of the transducer will be located at

$$r = \frac{a^2 + w^2}{2w} \tag{3}$$

where,

$r \equiv$ membrane transducer focal radius

$a \equiv$ membrane radius

$w \equiv$ membrane deflection.

Equation 3 assumes a spherical shaped membrane deflection.

For the membrane under uniform pressure load P the Hencky deflection equation is [8].

$$w = .662\ a\ \sqrt[3]{\frac{Pa}{Et}} \tag{4}$$

where:

$w \equiv$ membrane deflection under differential pressure load
$a \equiv$ membrane radius
$t \equiv$ membrane thickness
$P \equiv$ differential membrane pressure
$E \equiv$ membrane modulus of elasticity

These equations assume the absence of a radial tensile force under no differential pressure load. Equations 3 and 4 were used to predict the focal length of .25 inch, .50 inch and .75 inch diameter PVDF transducers under a differential membrane pressure of 0 to 120 cm H_2O. The modulus of elasticity used in the computations was 8.438×10^6 cm H_2O. *Figure 3* illustrates the results.

If the transducer is operated as a diverging acoustic radiator, the angle of divergence θ will be given as

$$\Theta = \text{Arcsin} \left\{ \frac{2wa}{a^2 + w^2} \right\} \tag{5}$$

Equations 3 and 5 assume normal transmission from the surface of the membrane into the external acoustical medium which is not exactly true. For instance a plane circular surface radiator of ultrasound will have a beam divergence given as [9],

$$\gamma = 68.8\ \lambda/D \tag{6}$$

where

$\gamma \equiv$ angle of divergence in degrees
$\lambda \equiv$ ultrasonic wave length
$D \equiv$ diameter of circular radiator.

Equation 6 assumes small λ/D ratios.

Another important parameter is the length of the near field [9]. For circular flat radiators of ultrasound

$$N = \frac{(D^2 - \lambda^2)}{4\lambda} \tag{7}$$

where,

$D \equiv$ diameter of ultrasonic radiator
$\lambda \equiv$ wavelength of ultrasonic wave
$N \equiv$ nearfield length

Figure 4 illustrates the variation of N with frequency for a 1500 m/sec wave velocity in water and a .5 inch diameter transducer. For uniform test results all calibration tests should be performed at ranges greater than N.

A PVDF device was constructed for testing in the laboratory. *Figures 5* through *9* iillustrate the device. The PVDF membrane is placed between the two electrode holders shown in *Figure 5* and *6*. *Figure 6* illustrates the acoustical cavity electrode which was .25 inch thick. Two plexiglas end supports were used to hold the electrodes against the PVDF as shown in *Figures 7* through *9*.

The membrane material selected for testing was KYNAR® PVDF piezoelectric film obtained from the Pennwalt Corporation. The film measured 10 cm x 10.8 cm in area x 27 μm thick. Nickel-chrome electrodes were deposited on both sides of the film. The film for the transducer was cut 1.2 inches square and placed in the transducer. To prevent electrical leakage RTV silicone rubber cement was used to seal the electrodes as shown in *Figure 9*.

III. EXPERIMENTAL CONFIGURATION

The experimental configuration used to test the PVDF transducer is shown in *Figures 10* and *11*. *Figure 10* illustrates the electrical system for testing the differential pressure membrane transducer. The components and their functions are:

- Tektronix Type 191 Constant Amplitude Signal Generator - Used to generate the RF transmit signal.

- ENI 350L Power Amplifier - A 50 dB power amplifier used to amplify the RF transmit signal.

- Triplet RF Ammeter - A resistor thermocouple type of unit. used to measure the current drawn by the transmitter transducer.

- Tektronix Type 485 Oscilloscope - Monitors the RF transmitter signal voltage and RF receiver signal voltage.

- Hewlett-Packard 8405A Vector Voltmeter - Measures the RF RMS signal voltage of the receiver transducer.

- Moseley Autograf XY-Recorder-Used to plot the receiver RMS signal voltage as a function of pressure.

- Bell and Howell Type 4-356-0144 Pressure Transducer - Used to monitor the PVDF differential membrane pressure.

- PMC Regulated Power Supply - Supplies electrical power to the Bell and Howell pressure transducer.

Figure 11 illustrates the PVDF transducer gas supply system. In the gas system air from a supply tank is valved to a Matheson pressure regulator. A main air control valve is used to control the air pressure to the PVDF transducer in conjunction with a micrometer air-bleed valve. A Mercury manometer and Bell and Howell pressure transducer are used to monitor the PVDF gas pressure. *Figure 12* illustrates the normalized output of the Bell and Howell transducer versus the gas pressure as measured by the manometer. Easily seen, the output is linear with input pressure and may be used to drive the XY-plotter.

Experiments were performed using the PVDF membrane transducer in water. Two tanks were used in the experiments. A large 1.52 m x 3.05 m x 1.22 m deep tank was used for transmission tests and a small .762 m x .305 m x .305 m deep tank was used for cross sectional scans of the PVDF beam intensity. In order to test the PVDF transducer, an Aerotech .50 inch diameter Gamma 2.25 MHz resonance frequency transducer was used. *Figure 13* shows the PVDF and Aerotech reference transducers mounted on a plexiglas base which was submerged in the acoustical tanks for experimental purposes.

In all of the tests approximately 612 cm of Type RG-59 B/U cable was used between the Aerotech reference transducer and electrical readout equipment. 607 cm of Type RG-59 B/U cable was used for the main RF transmission line to and from the PVDF transducer.

IV. EXPERIMENTAL TESTS AND RESULTS

A series of tests were conducted to study the performance of the PVDF differential membrane pressure transducer. Each test is assigned a code letter followed by a frequency parameter. As an example A2.25 refers to test A performed at 2.25 MHz. An explanation of each test series and the results are given below.

A. Test Series A

In this series of tests the PVDF transducer served as the transmitter and the Aerotech transducer was the receiver. The membrane differential pressure was varied from -100.76 cm H_2O (focused radiator condition) to +188.85 cm H_2O (diverging acoustical radiator condition). The transmission length in water was 27.43 cm and the PVDF voltage was 15.0 volts peak-to-peak. *Figures 14* through *20* show the results of transmitting from 1.00 MHz to 3.50 MHz. A definite perturbation is seen at about 0.0 cm H_2O differential pressure. This perturbation becomes rather pronounced as the PVDF signal amplitude was increased. The graphs are all rather flat which makes the transducer an ideal variable focus unit.

The unusual behavior at 0.0 cm H_2O differential pressure is a result of the d_{31} and d_{32} modes of vibration having no component of deformation in the z direction of the transducer. It was found that, if water was allowed to fill the acoustical cavity, the acoustical energy transmitted at this condition was negligible. This is the result of energy being lost from the back side of the membrane into the acoustical cavity.

B. Test Series B

This series of tests was the same as the Test A series except that the PVDF transducer acted as a receiver while the Aerotech transducer served as a transmitter. Again perturbations are found in *Figures 21* through *27* at 0.0 cm H_2O differential membrane pressure. The relatively flat response of the PVDF transducer at each of the tested operating pressures indicates that it is a good receiver even though the signal voltage output is low.

C. Test Series C

In this series of tests the PVDF transducer apparent power was measured as a function of the PVDF applied peak-to-peak voltage. The apparent power is obtained from

$$P_{app} = V_{rms} I_{rms} \tag{8}$$

where,

P_{app} ≡ Apparent power consumed by the PVDF transducer

V_{rms} ≡ Root mean square voltage applied to PVDF transducer

I_{rms} ≡ Root mean square current flow through the PVDF transducer when V_{rms} is applied.

The pressure for the test was -100.76 cm H_2O and *Figures 28* through *34* show the apparent power consumption at various frequencies as a function of applied signal voltage.

Another important parameter measured in this test series was the gain in transmitting from the PVDF transducer to the Aerotech transducer as a function of the PVDF apparent power consumption. The gain in transmitting from the PVDF to the Aerotech transducer is given as

$$\beta = 20 \ \mathrm{Log}_{10} \left\{ \frac{V_{arms}}{V_{prms}} \right\} \tag{9}$$

where,

β ≡ dB gain in transmitting from PVDF to the Aerotech transducer

V_{arms} ≡ RMS voltage output of the Aerotech transducer

V_{prms} ≡ RMS voltage input to the PVDF transducer.

Figure 35 illustrates β as a function of P_{app} for various frequencies at -100.76 cm H_2O membrane differential pressure and a transmission length spacing between transducers in water of 27.43 cm. The flat response at most of the measured frequencies is ideal. At 2.25 MHz the gain was greatest since this is the natural frequency of the Aerotech transducer.

D. Test Series D

This series of tests was the same as test series C except that the differential membrane pressure was +188.85 cm H_2O. This condition made the PVDF transducer a diverging radiator instead of a focused transducer as in the C series of tests. Results are similar and are shown in *Figures 36* through *43*.

E. Test Series E

In this test series the PVDF and Aerotech transducers were separated by 27.43 cm of water. First a specified voltage was applied to the PVDF transducer and the output of the Aerotech transducer was recorded. Next, the same voltage was applied to the Aerotech transducer and the output of the PVDF transducer was recorded. The test was performed at

-100.76 cm H_2O differential membrane pressure. Three important parameters resulted from this series of tests.

The PVDF transmission coefficient is a measure of how well the PVDF transducer converts an electrical signal to ultrasound and how well the Aerotech transducer converts the ultrasound to an electrical signal. This coefficient is defined as,

$$T_F = \left\{ \frac{V_{ARMS}}{V_{PVFD}} \right\} X \quad 1000 \tag{10}$$

where,

$T_F \equiv$ PVDF transmission coefficient

$V_{PVDF} \equiv$ Peak-to-peak voltage applied to the PVDF transducer (peak-to-peak volts)

$V_{ARMS} \equiv$ RMS voltage output of the Aerotech transducer. (RMS-MV)

The reference transmission coefficient is a measure of how well the Aerotech reference transducer converts an electrical signal to ultrasound and how well the PVDF transducer converts the ultrasound to an electrical signal. The coefficient is defined as,

$$T_R = \left\{ \frac{V_{PRMS}}{V_A} \right\} X \; 1000 \tag{11}$$

where,

$T_R \equiv$ Reference transmission coefficient.

$V_A \equiv$ Peak-to-peak voltage applied to the Aerotech reference transducer. (peak-to-peak volts)

$V_{PRMS} \equiv$ RMS voltage output of the PVDF transducer. (RMS-MV)

Finally, the reverse transmission coefficient is a measure of performance of the PVDF transducer as a receiver as compared to its performance as a transmitter.

$$T_T = \frac{\tau_R}{\tau_F} \tag{12}$$

Tables 2 through *8* tabulate the T_F, T_R and T_T coefficients as functions of the transmitter voltage whether it be the reference or PVDF transducers. The measured values of T_F, T_R and T_T were averaged over the range of data in each table and plotted as a function of frequency in *Figures 44, 45* and *46*.

F. Test Series F

This test series was the same as Test Series E except that the differential membrane pressure was +188.85 cm H_2O. For this case the membrane transducer was a diverging radiator of ultrasound. Data is tabulated in *Tables 9* through *15* and the results are plotted in *Figures 47* through *49* versus frequency.

G. Test Series G and H

In this series of tests the Aerotech transducer was placed 27.43 cm from the PVDF membrane transducer. It was then scanned along an axis perpendicular to the primary z axis of the PVDF transducer. The normalized response of the Aerotech transducer is plotted as a function of distance along the scan axis. The membrane z axis is located approximately at 51.0 cm. The G series of tests were conducted at +279.75 cm H_2O differential membrane pressure. The H series of tests were conducted at -8.509 cm H_2O differential membrane pressure. The non-uniformity in many of the figures is attributed to poor clamped-edge boundary conditions on the membrane and possible membrane non-uniformity in structure and performance. The slight non-uniform differential pressure across the surface of the membrane due to the water pressure being greater at the bottom of the membrane than at the top may have made some contribution here.

H. Test Series I and J

This series of tests involved scanning the Aerotech transducer along the z axis of the PVDF membrane transducer. The output of the Aerotech transducer was recorded as a function of position along the z axis. *Figures 64* through *77* indicate the normalized response of the Aerotech transducer versus distance from the PVDF transmitter transducer. The far left position of each figure corresponds to the minimum spacing between transducers. *Table 16* gives the pertinent data for each figure. The I series of tests were conducted at -15.62 cm H_2O differential membrane pressure and the J series were conducted at 291.59 cm H_2O differential pressure. In many of the figures the maxima and minima signal lobes are seen which form the near field. The dashed line at the bottom of each figure represents the zero base.

V. CONCLUSIONS

A series of ten tests were performed to determine how well the PVDF differential membrane pressure transducer functions. Tests indicate that the acoustical power output of the PVDF transducer is significantly lower than conventional transducers. Improved features

of the PVDF over conventional transducers include low cost and variable focal length capabilities. This might make it an ideal transducer for fabricating into large arrays.

There are several problems which need to be addressed in the future. Indications from the axial and cross sectional scans are that the method of clamping the PVDF membrane to the electrodes needs to be improved. A simplified gas pressure control system is needed for the transducer. Studies need to be made of the dynamic behavior of the membrane and the ratio of power consumption to acoustical power output of the device needs to be decreased.

REFERENCES

1. Ohigashi, H., *Electromechanical Properties of Polarized Polyvinylidene Fluoride Films As Studied By the Piezoelectric Resonance Method*, Journal of Applied Physics, Vol. 47, No. 3, March 1976.

2. Shuford, R. J., Wilde, A. F., Ricca, J.J., Thomas, G. R., *Dependence of the Piezoelectric Activity of Polyvinylidene Fluoride upon High Speed Uniaxial Stretching and Subsequent Poling*, Proceedings of Piezoelectric and Pyroelectric Symposium-Workshop Held at Gaithersburg, Maryland, April 15-16, 1975, Report No. NBSIR 75-760, September 1975.

3. Oshiki, M., Fukada, E., *Piezoelectric Effect in Stretched and Polarized Polyvinylidene Fluoride Film*, Japanese Journal of Applied Physics, Vol. 15, No. 1, January 1976.

4. US Patent No. 3,792,204.

5. Tamura, M., Yamaguchi, T., Oyaba, T., Yoshimi, T., *Electroacoustic Transducers with Piezoelectric High Polymer Films*, Journal of the Audio Engineering Society, Vol. 23, No. 1, January/February 1975.

6. Murayama, N., Nakamura, K., OBara, H., Segawa, M., *The Strong Piezoelectricity in Polyvinylidene Fluoride (PVDF) Ultrasonics*, Vol. 14, No. 1, January 1976.

7. Pollard, H. F., "Sound Waves in Solids," Pion Limited, London, England, 1977.

8. Roark, R. J., "Formulas for Stress and Strain," 3rd Edition, McGraw Hill Book Co., N.Y., 1954.

9. Boyer, H. E., Editor, "Metals Handbook - Nondestructive Inspection and Quality Control," American Society of Metals, 8th Edition, Vol. 11, 1976.

PRECEDING PAGE BLANK-NOT FILMED

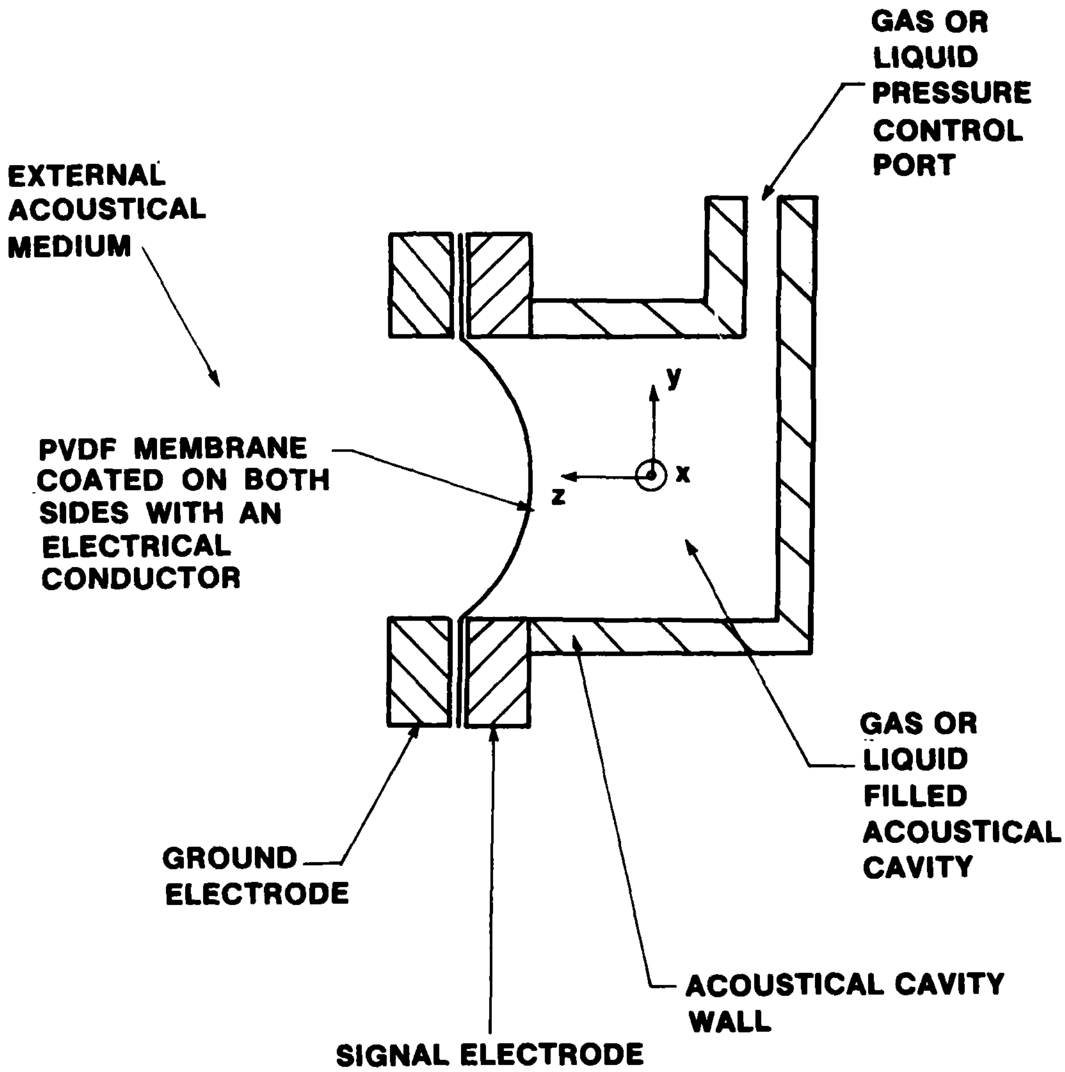

Figure 1. Cross sectional view of PVDF ultrasonic transducer design concept.

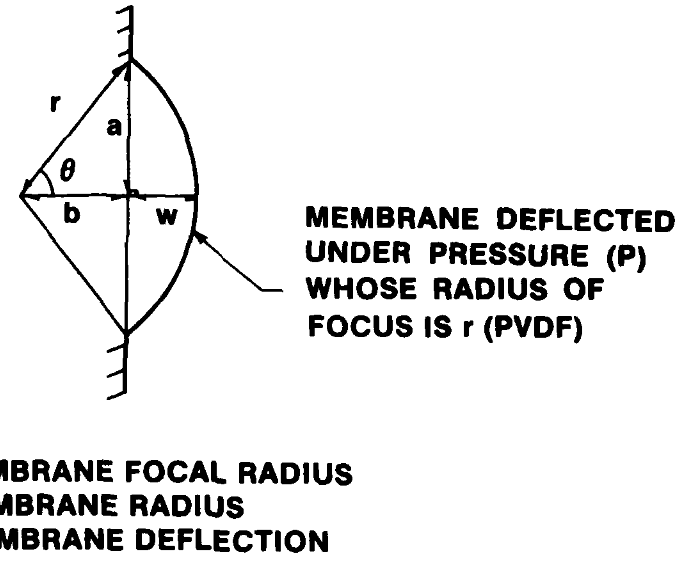

Figure 2. Circular membrane of radius (a) deflected under a differential pressure (P).

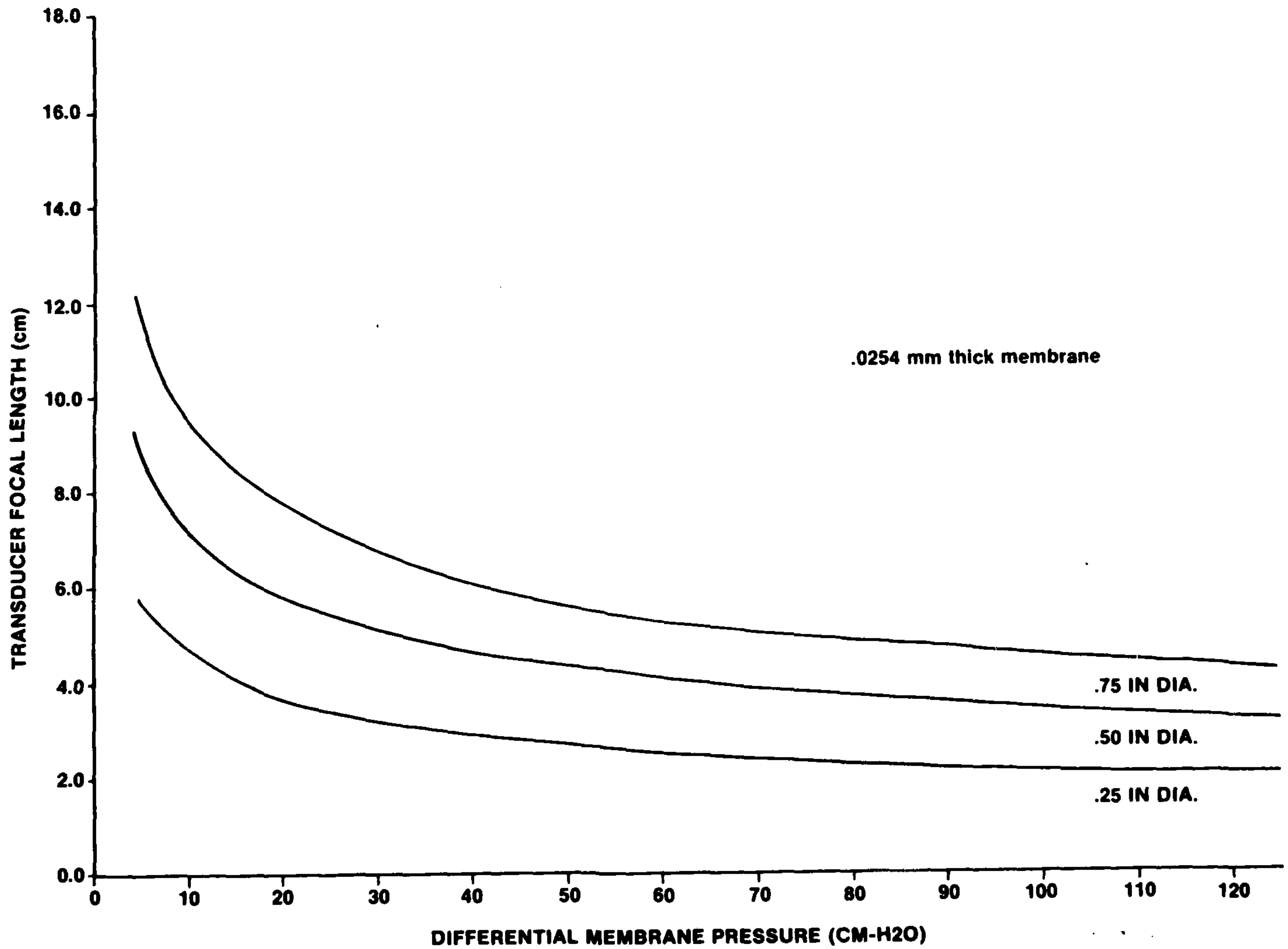

Figure 3. Transducer focal length versus differential membrane pressure

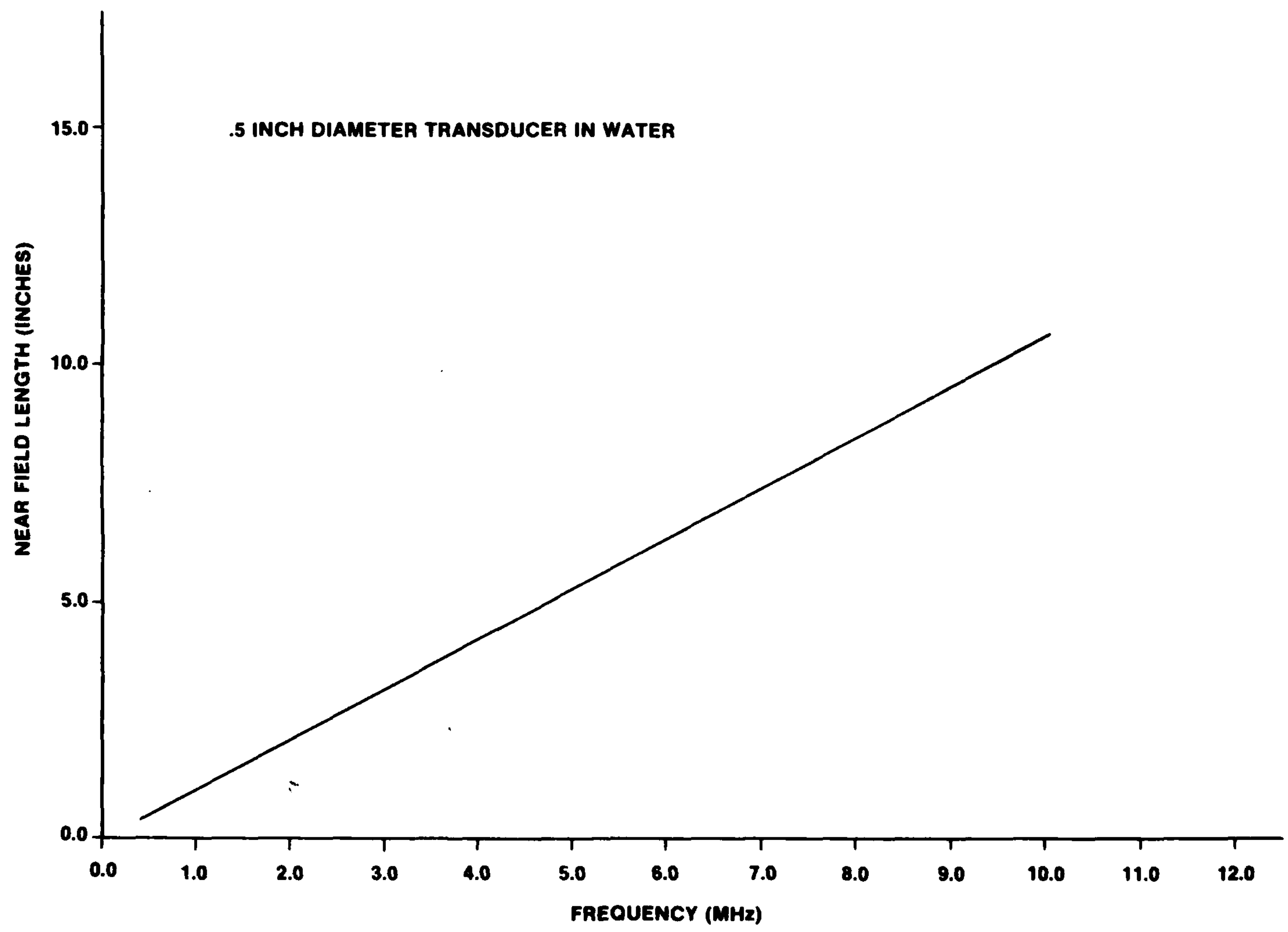

Figure 4. Near field length versus frequency for a .5 inch diameter transducer in water.

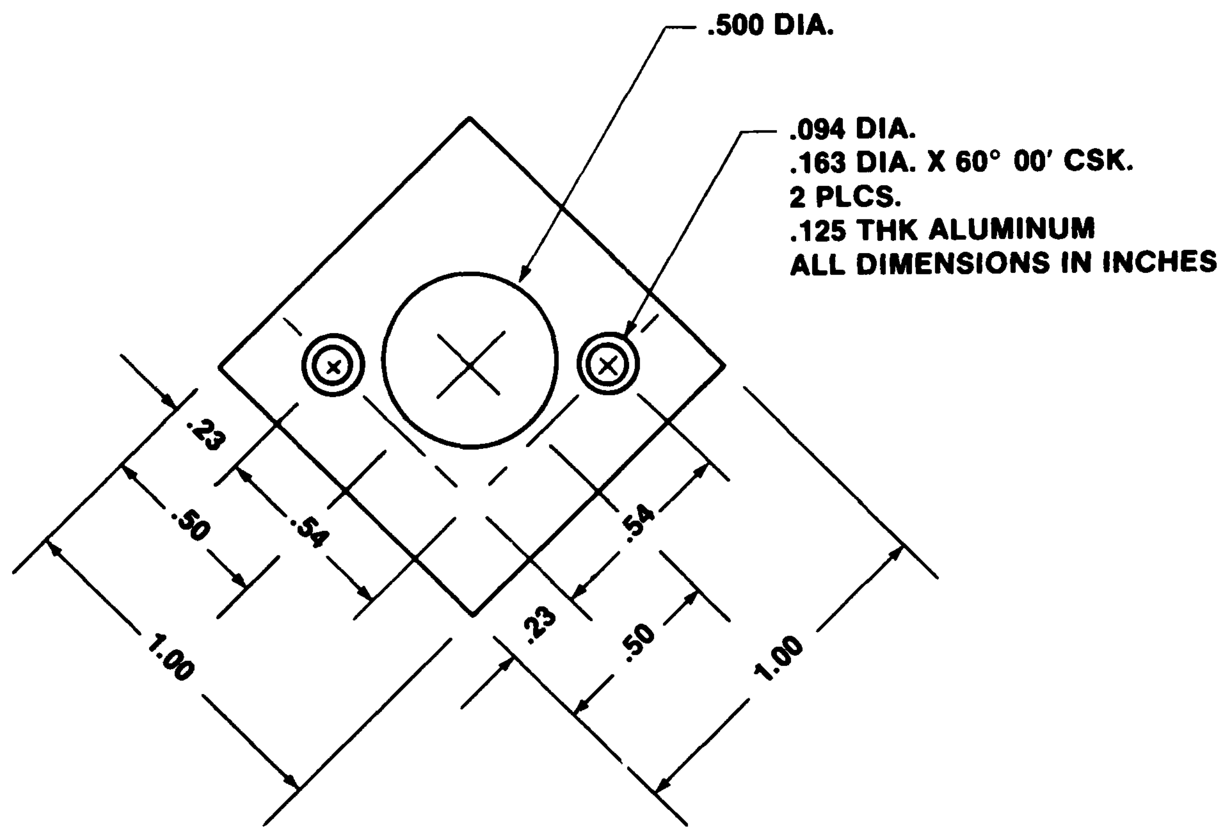

Figure 5. PVDF transducer ground electrode.

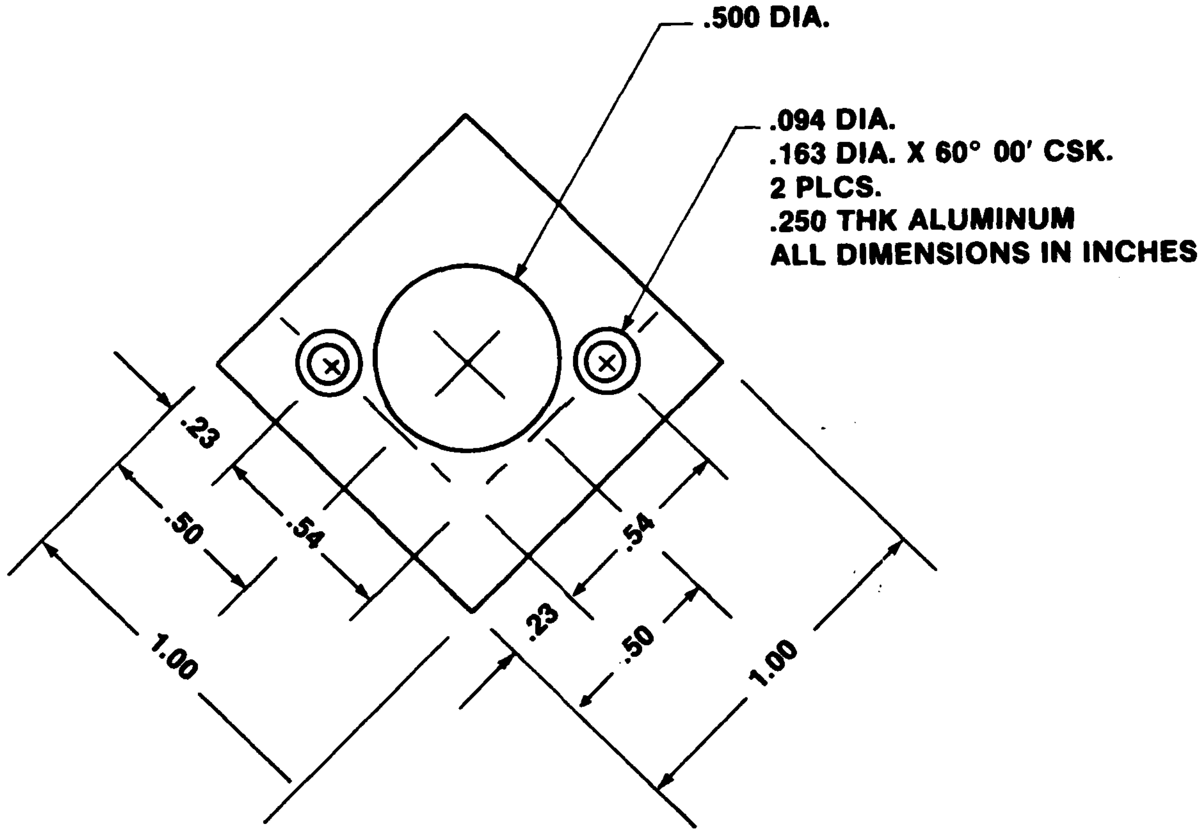

Figure 6. PVDF transducer signal electrode.

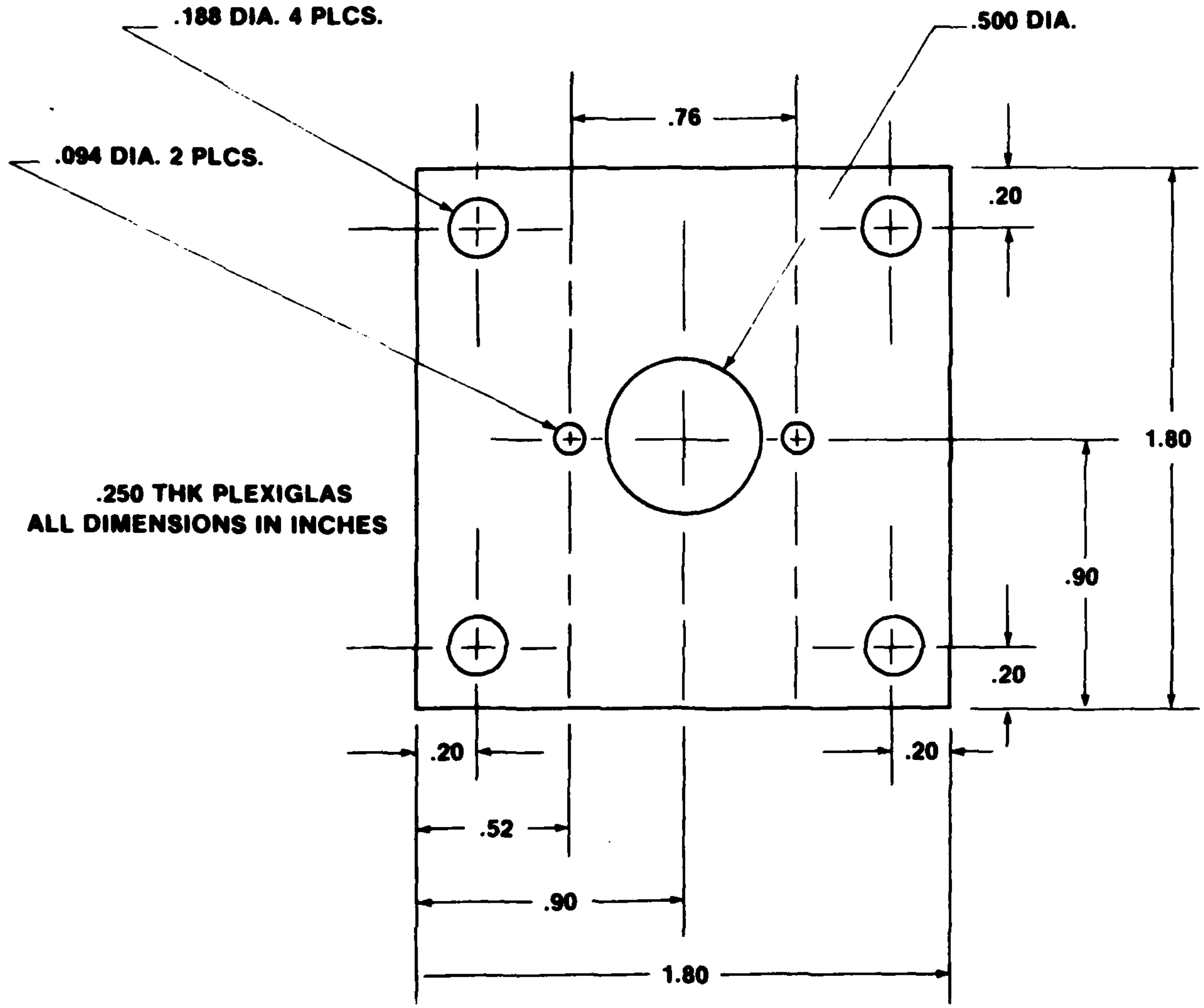

Figure 7. PVDF transducer ground electrode holder.

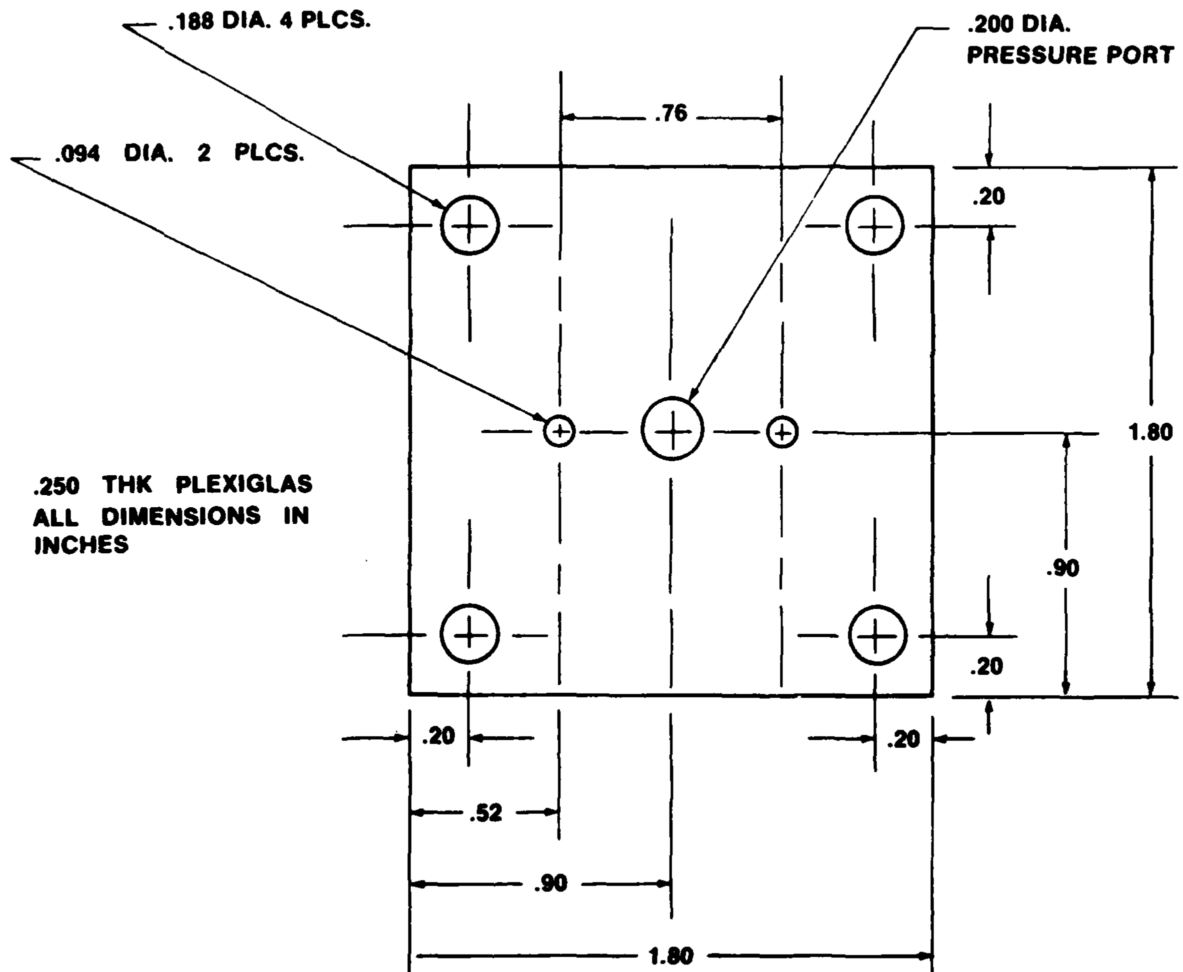

Figure 8. PVDF transducer signal electrode holder and pressure port.

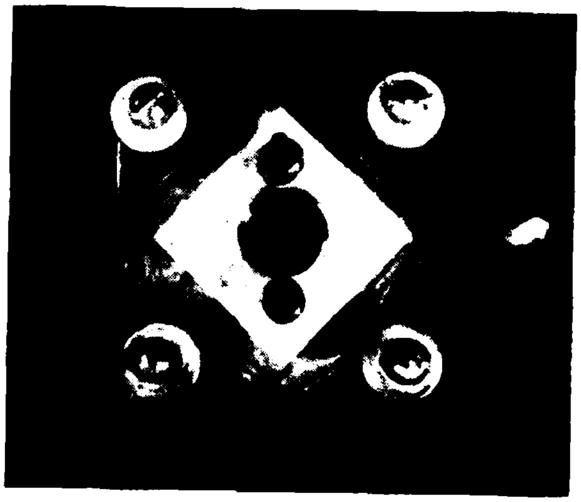

a. FRONT VIEW.

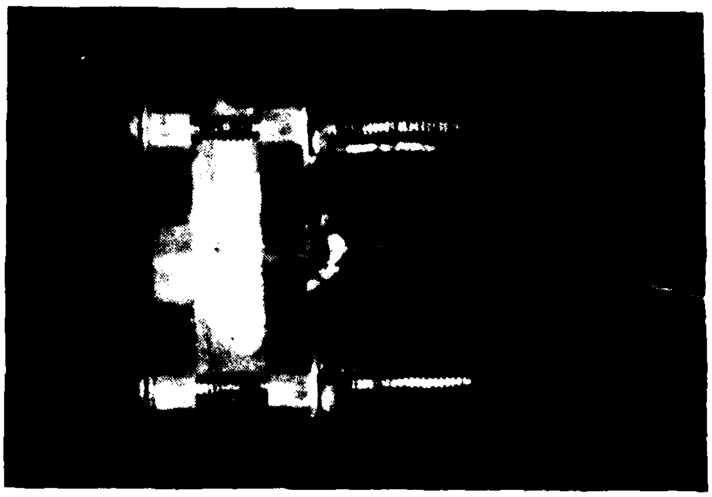

b. SIDE VIEW.

Figure 9. Assembled PVDF transducer.

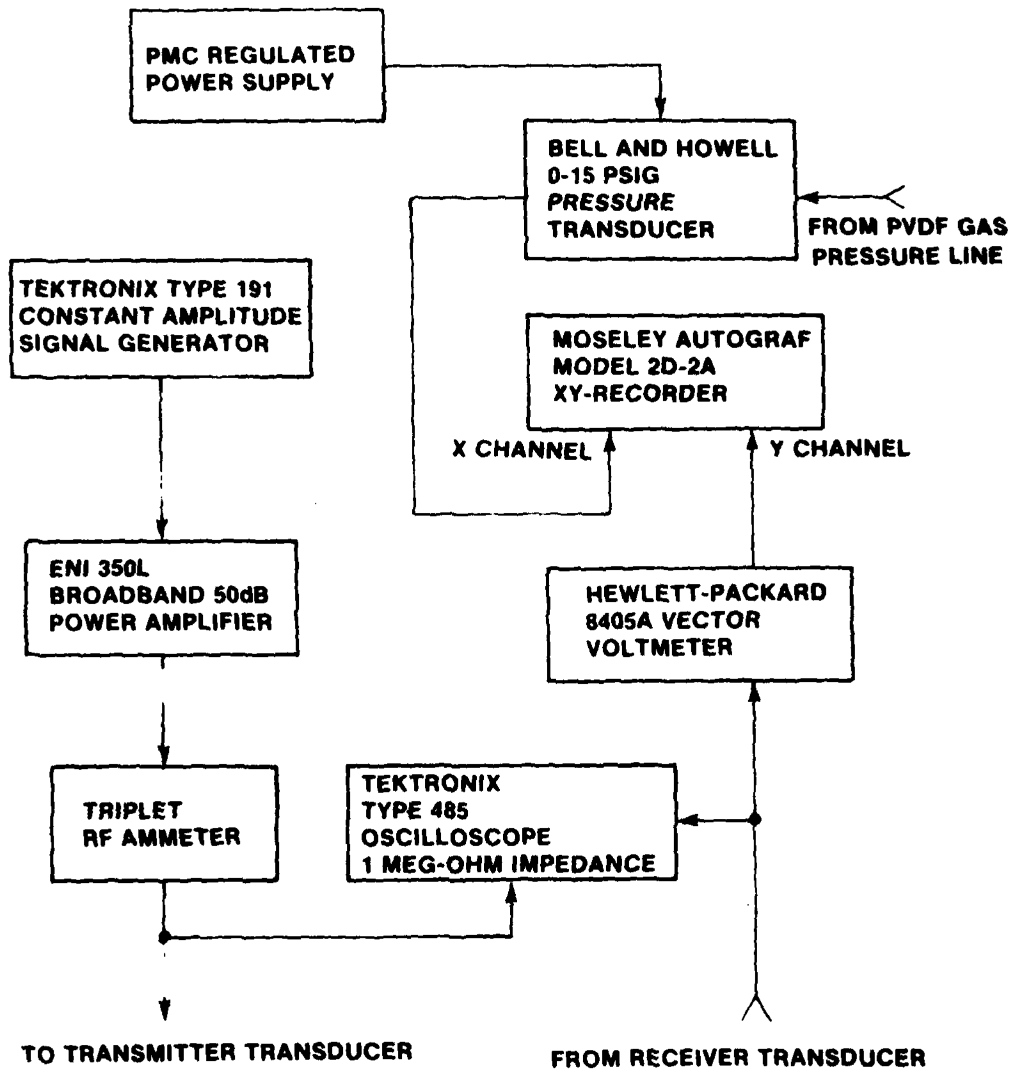

Figure 10. Electrical block schematic for testing PVDF transducer.

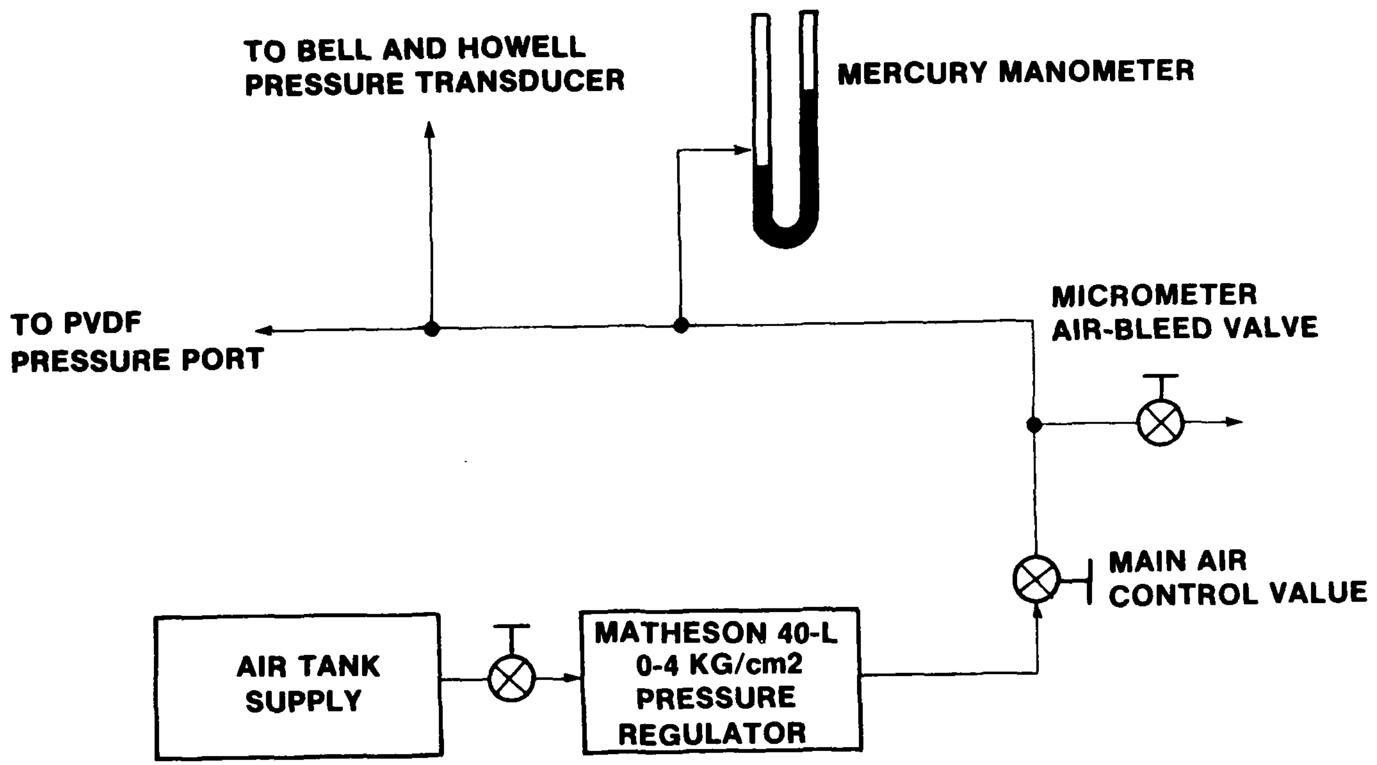

Figure 11. Mechanical block schematic of PVDF transducer gas supply system.

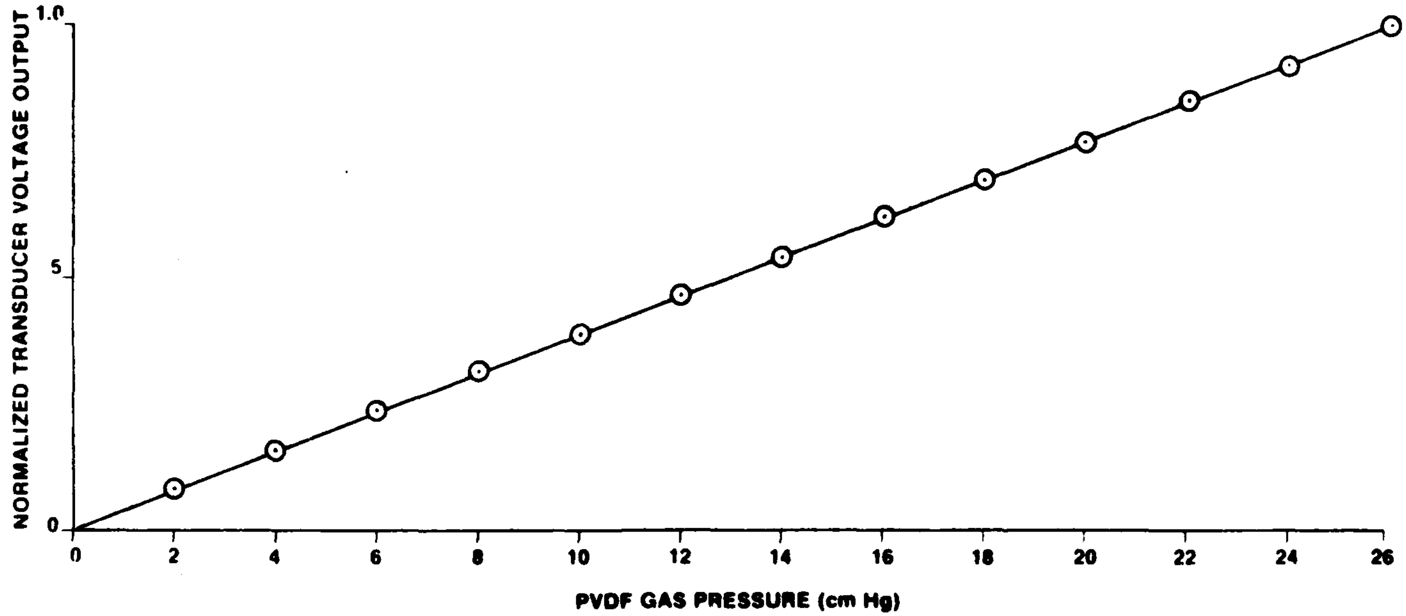

Figure 12. Normalized Bell and Howell transducer output versus PVDF gas pressure.

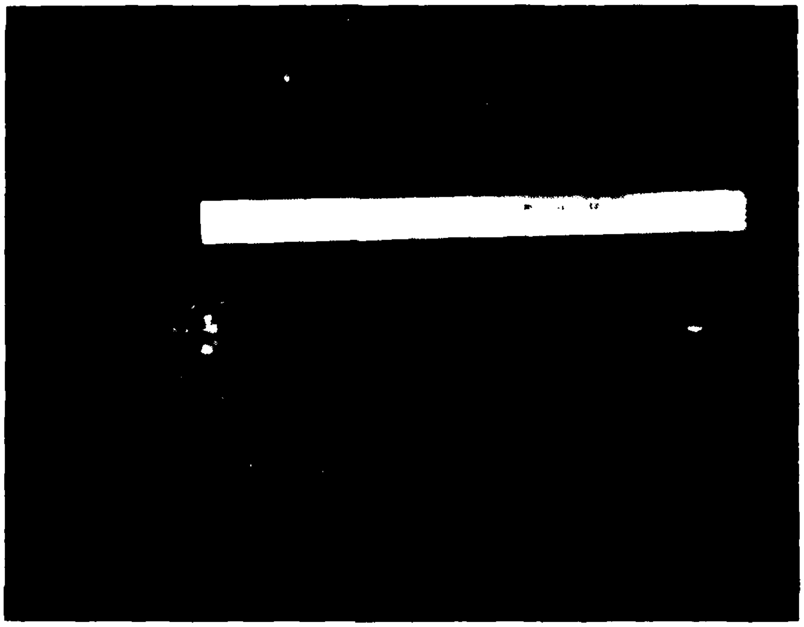

Figure 13. Acoustical PVDF and reference transducers mounted for transmission tests.

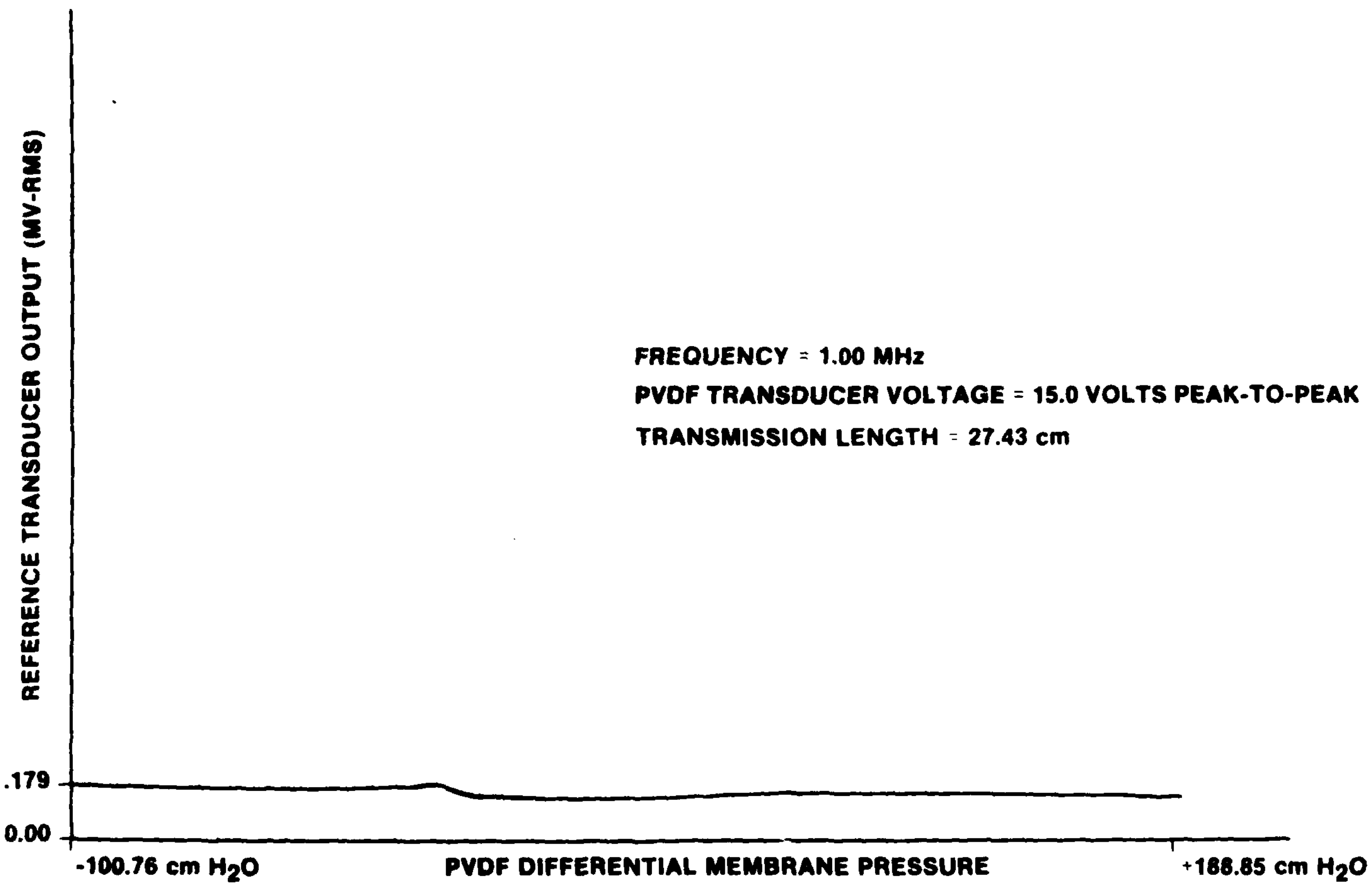

Figure 14. Test A1.00

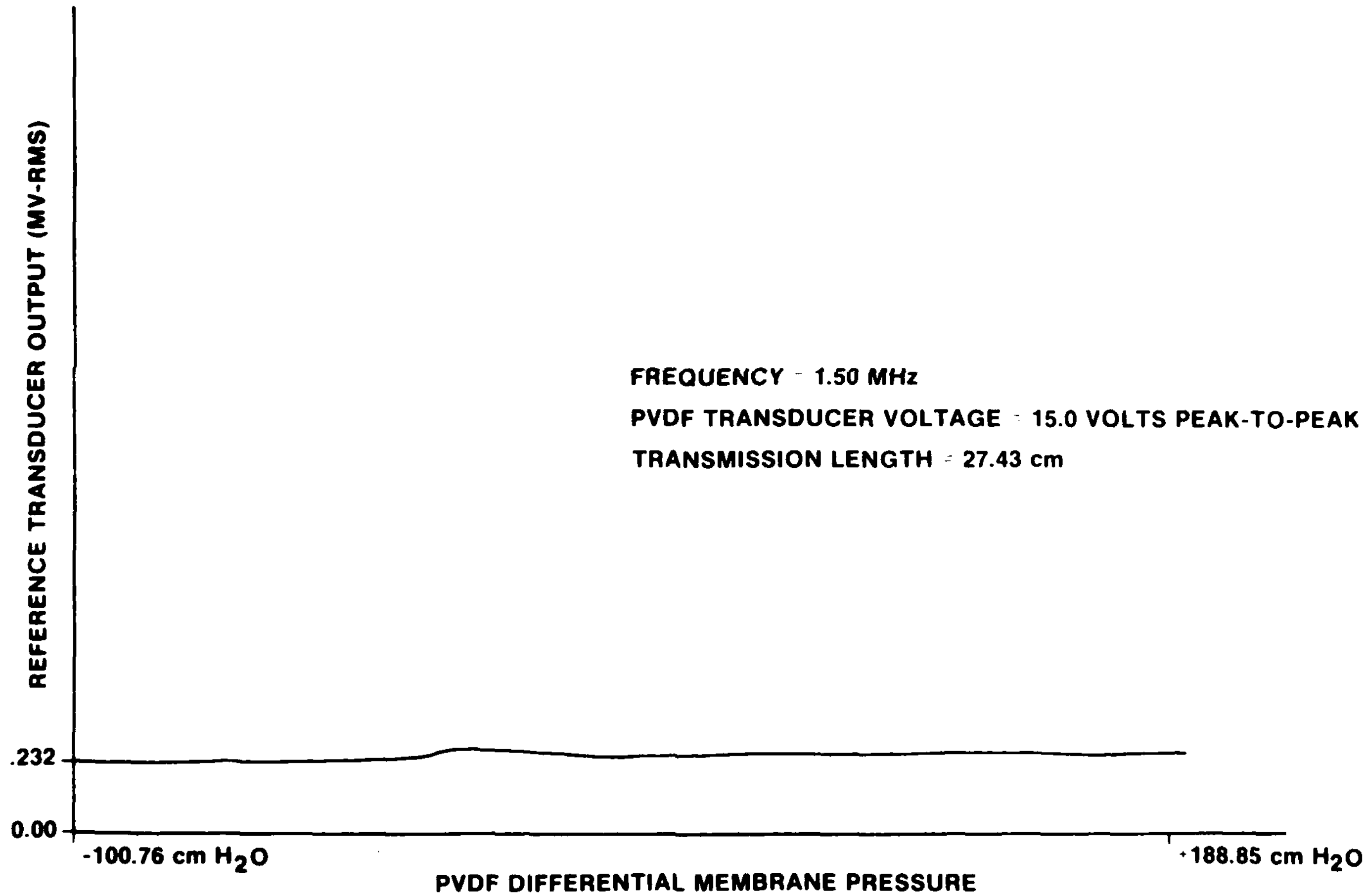

Figure 15. Test A1.50

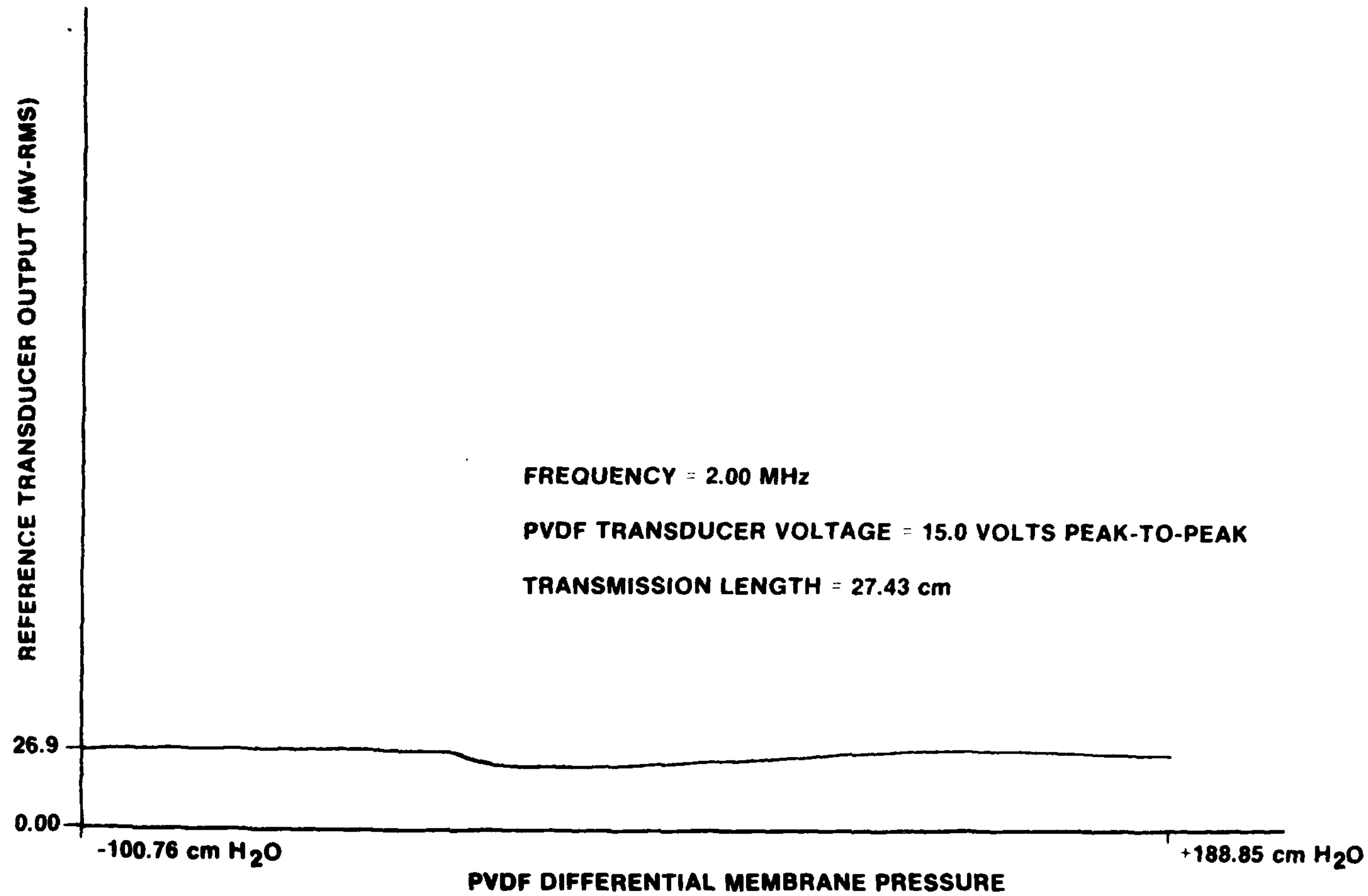

Figure 16. Test A2.00

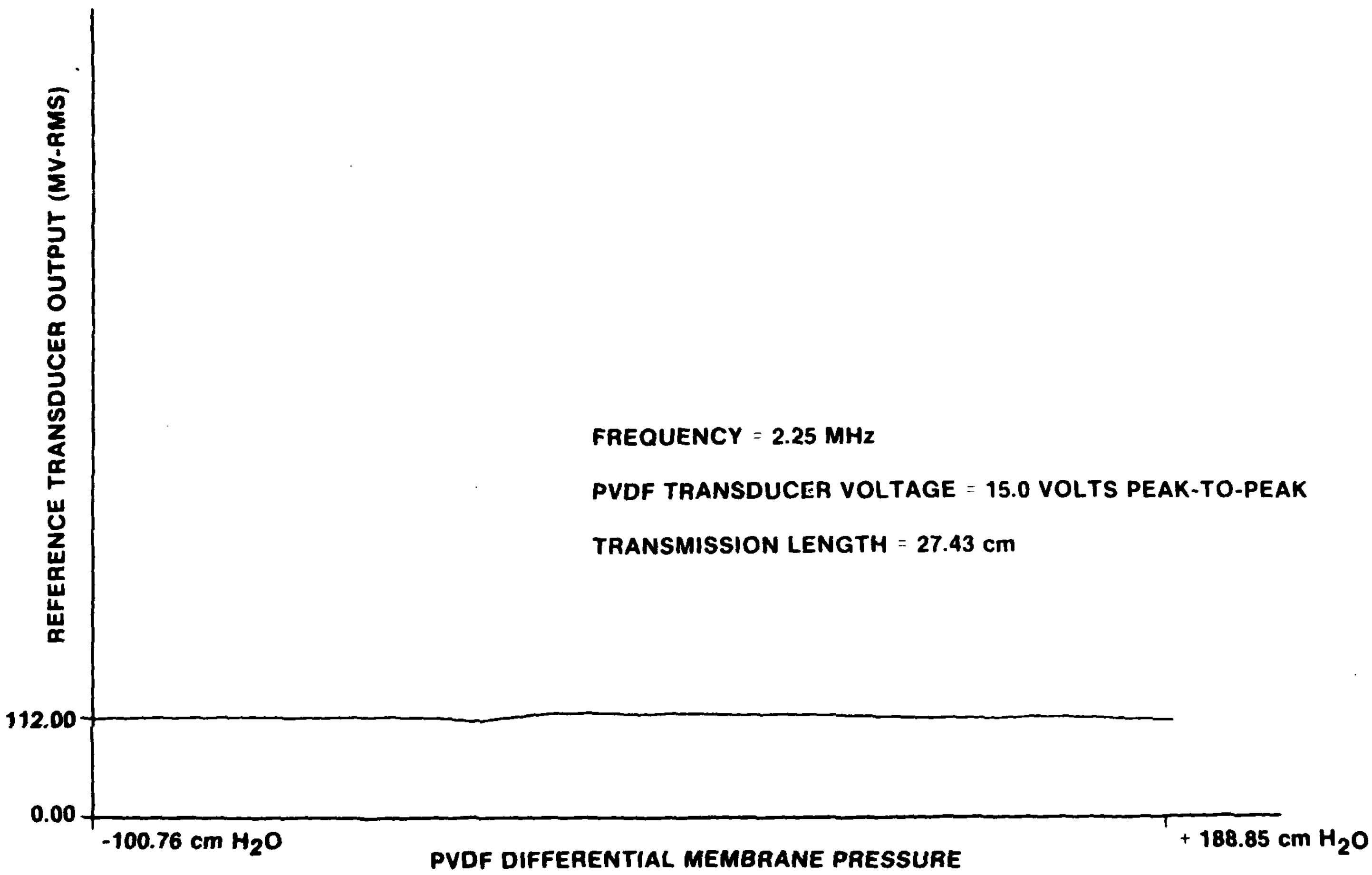

Figure 17. Test A2.25

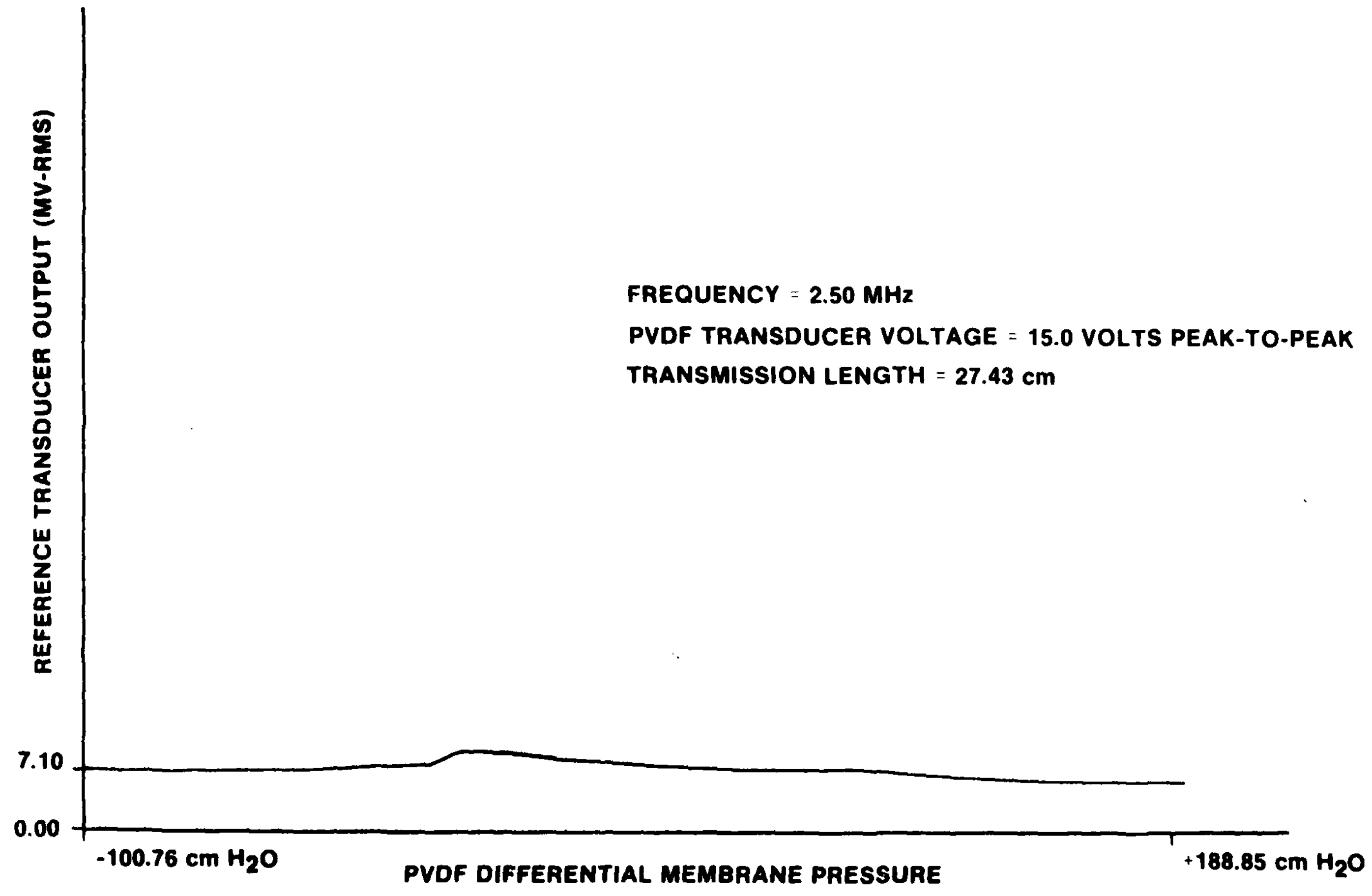

Figure 18. Test A2.50

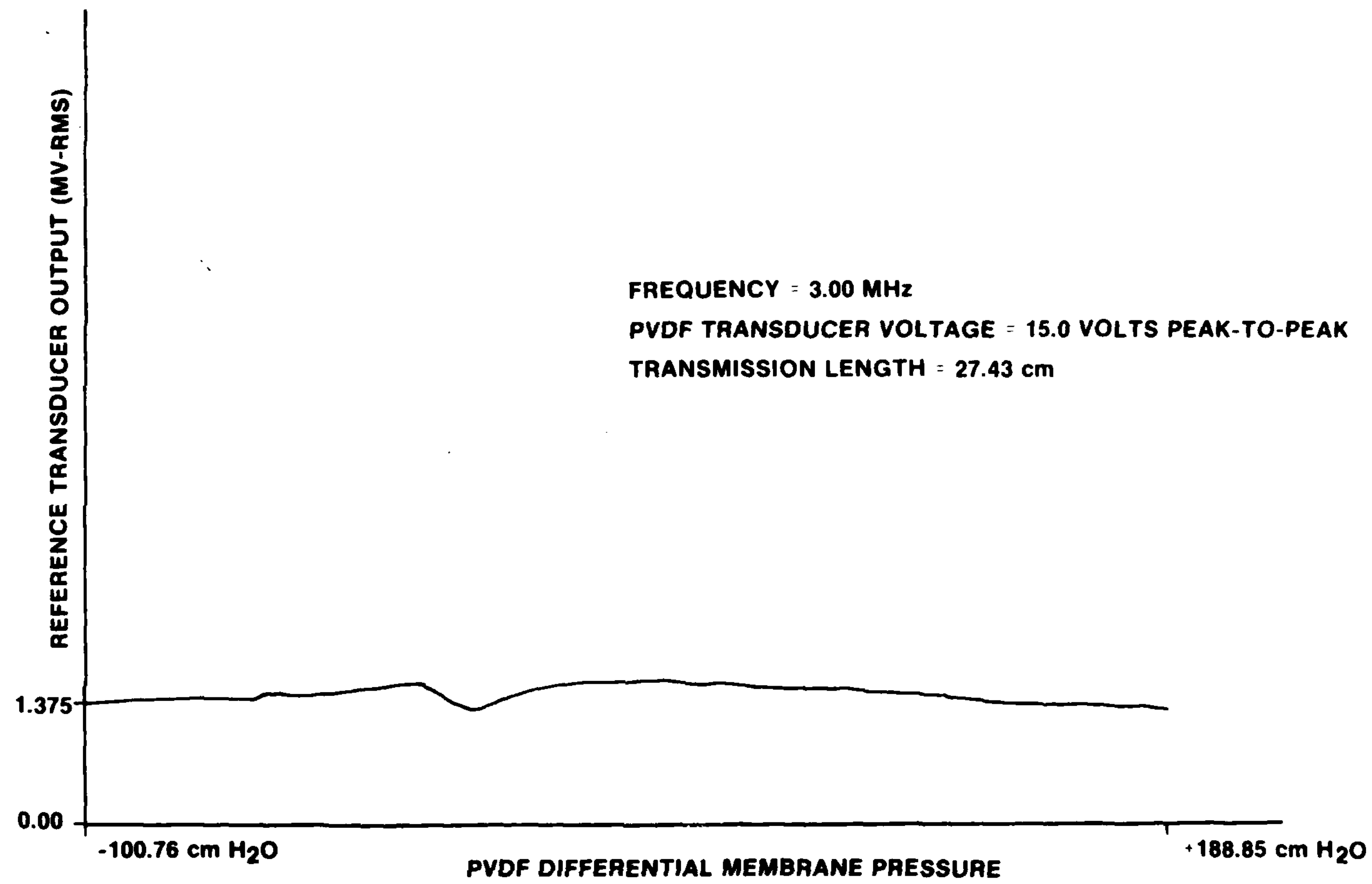

Figure 19. Test A3.00

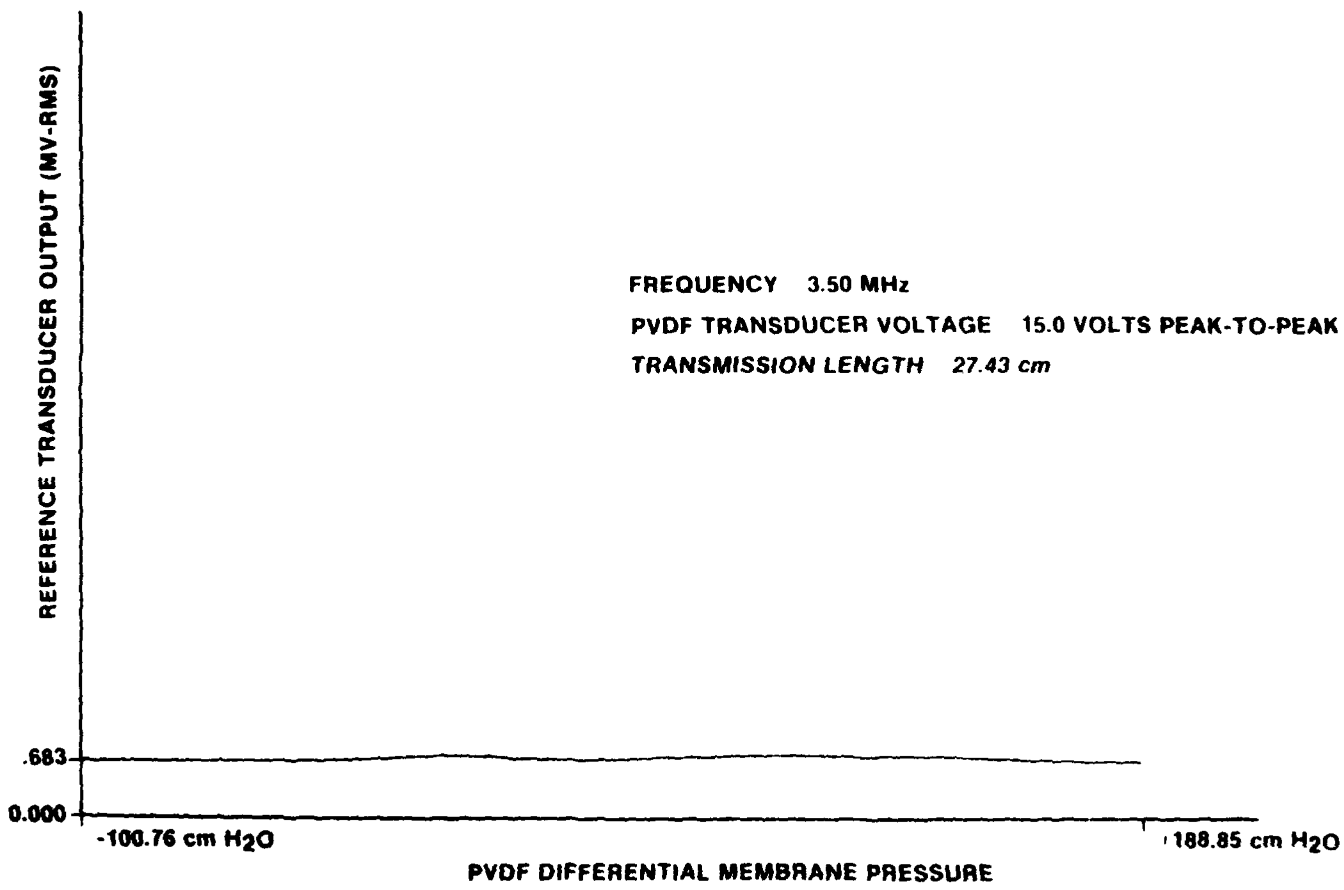

Figure 20. Test A3.50

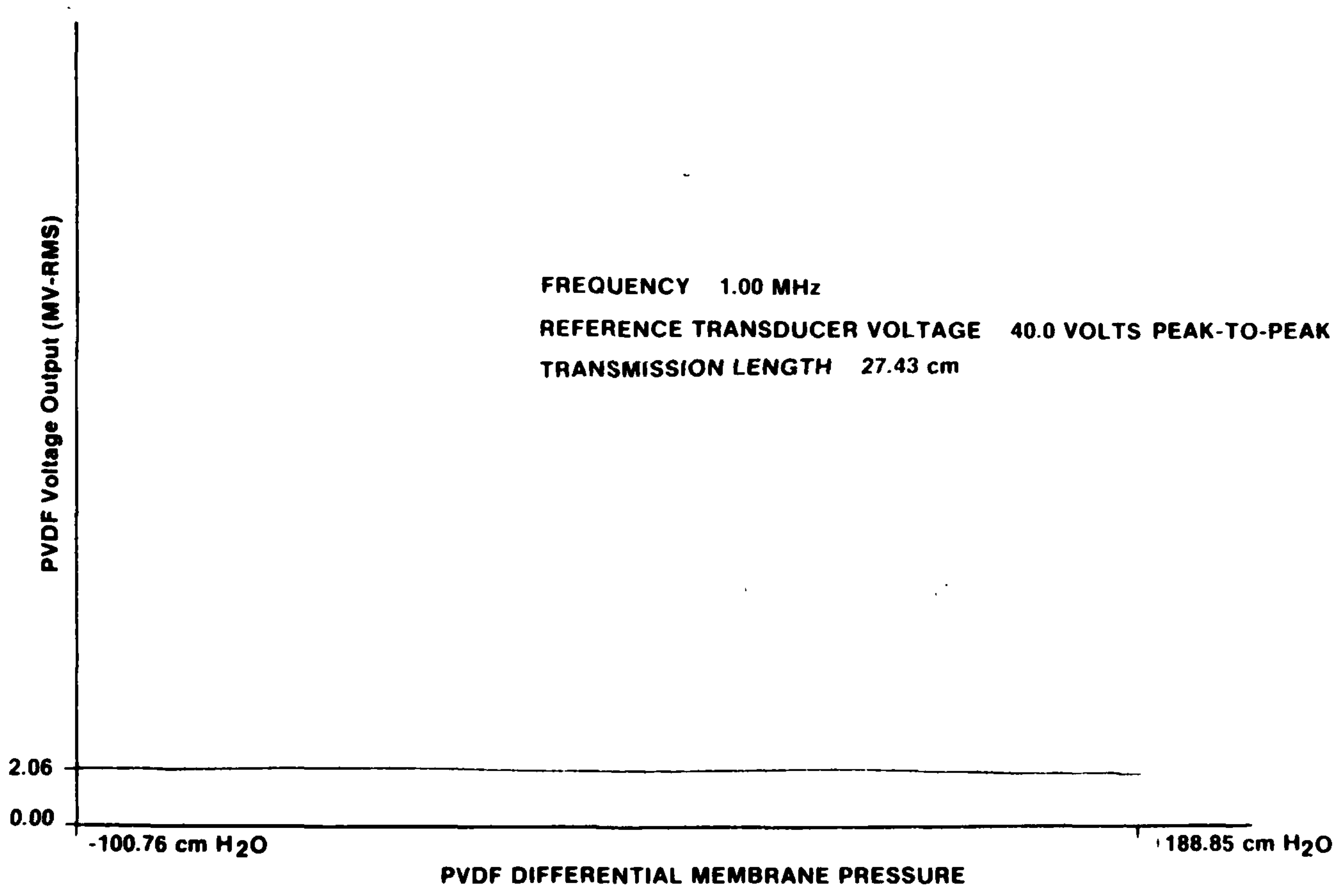

Figure 21. Test B1.00

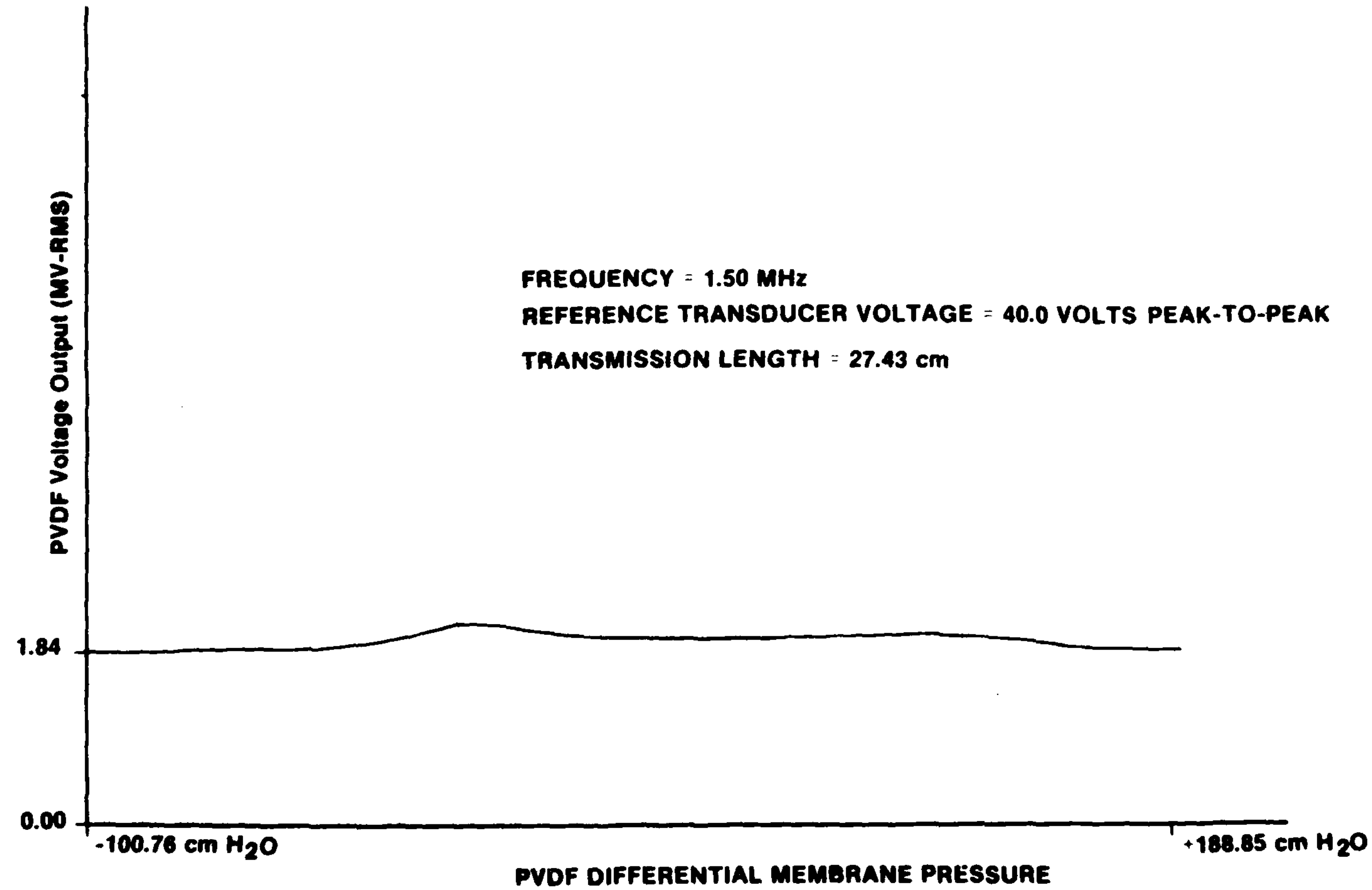

Figure 22. Test B1.50

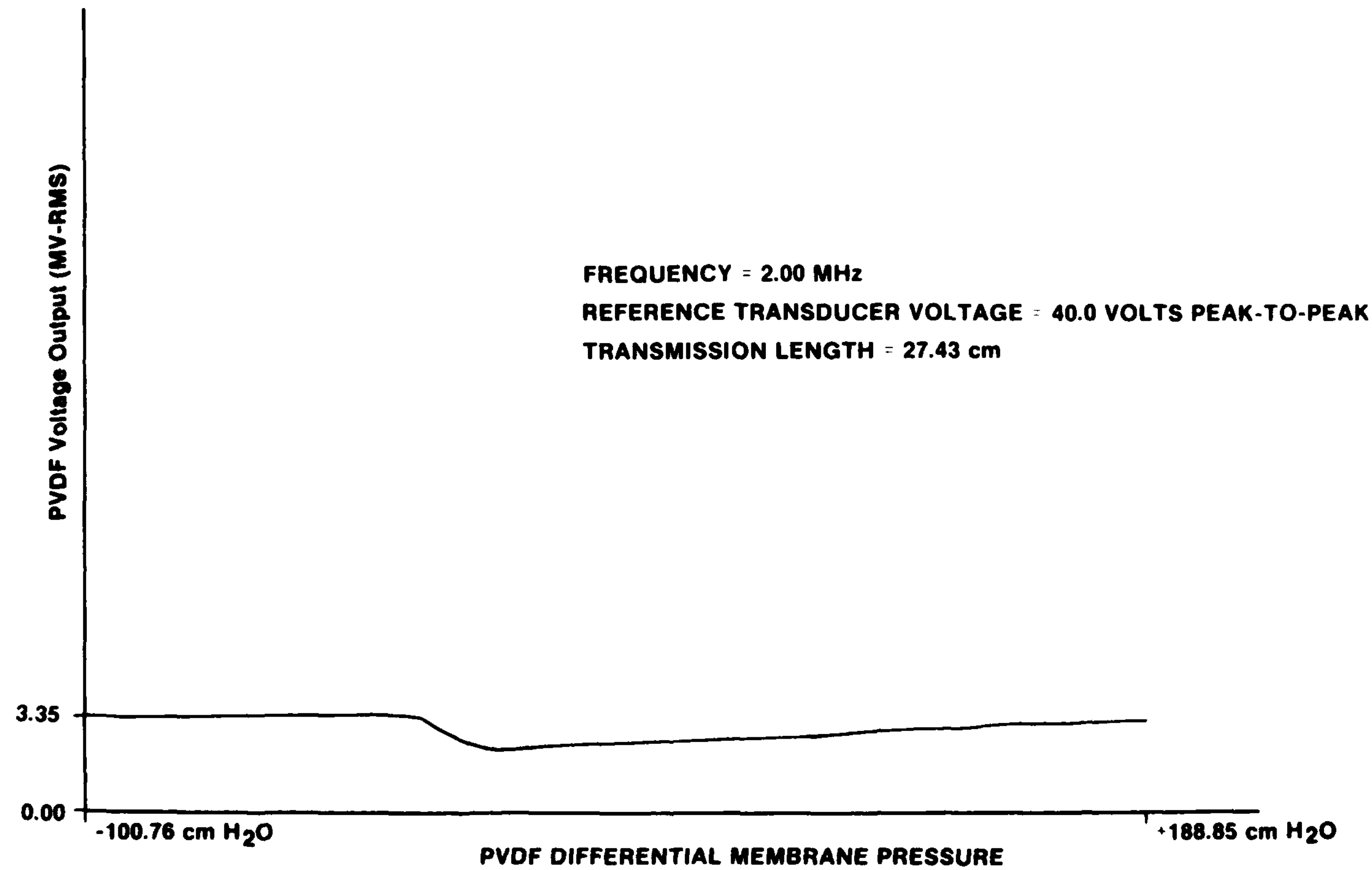

Figure 23. Test B2.00

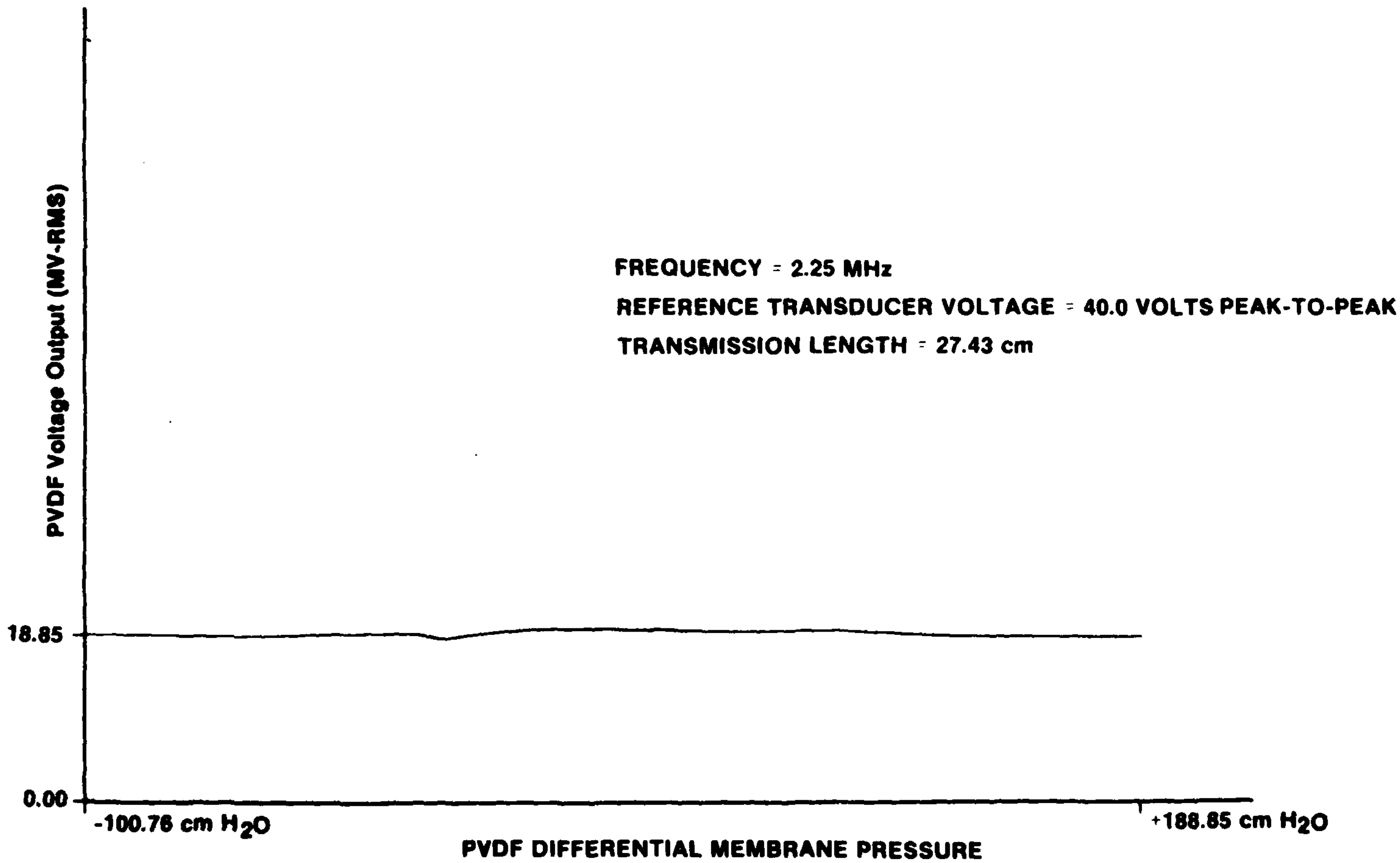

Figure 24. Test B2.25

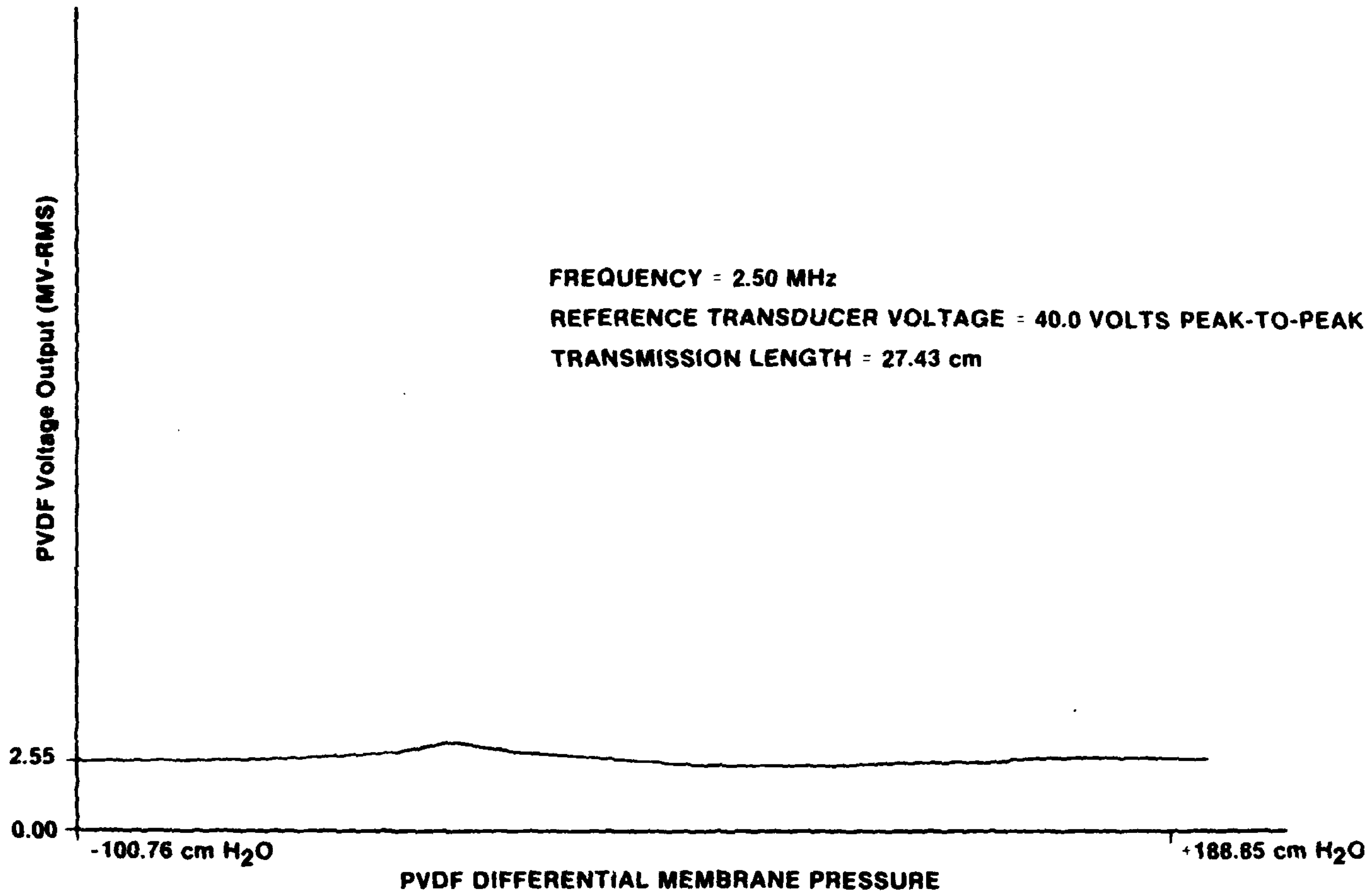

Figure 25. Test B2.50

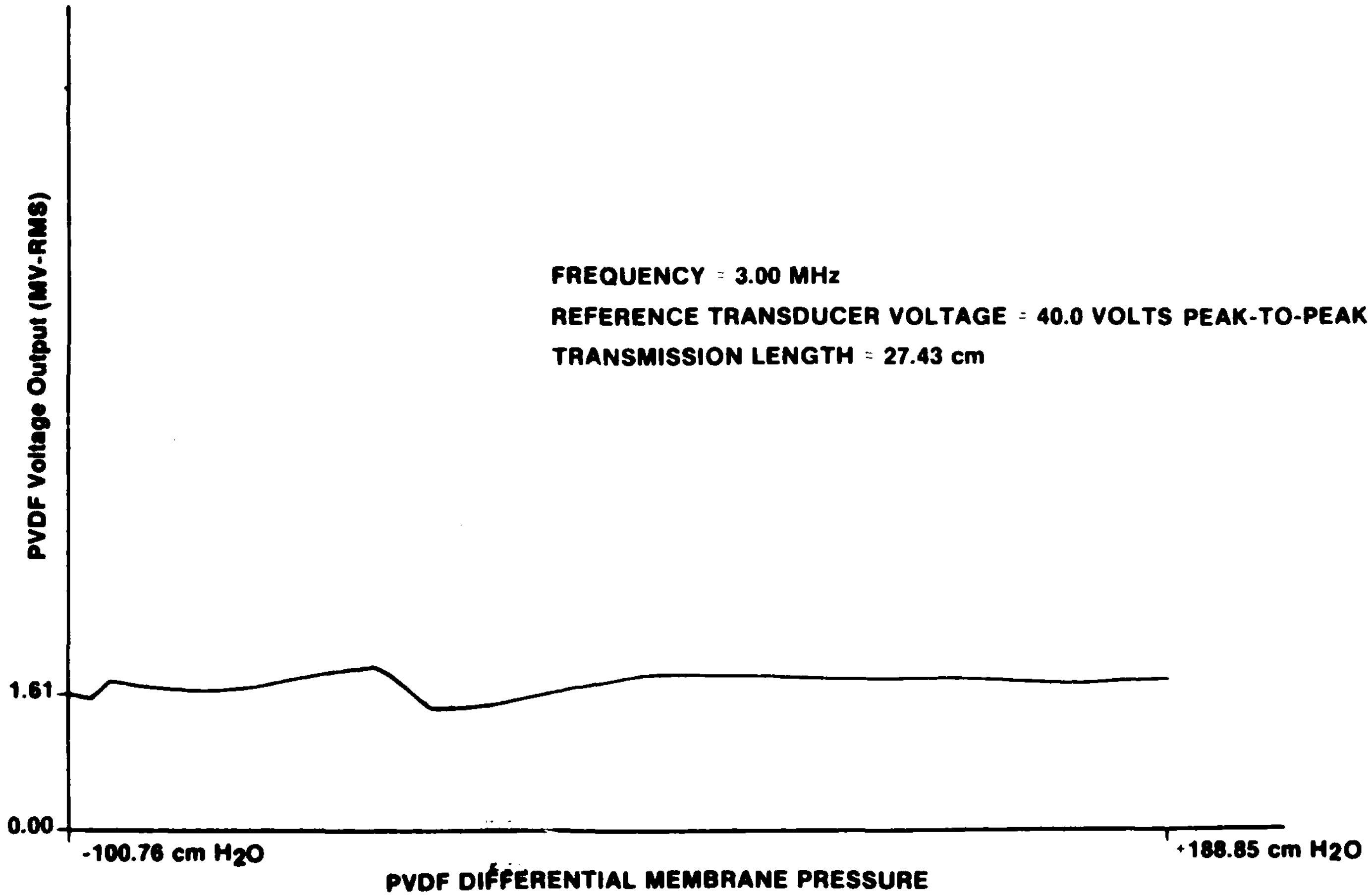

Figure 26. Test B3.00

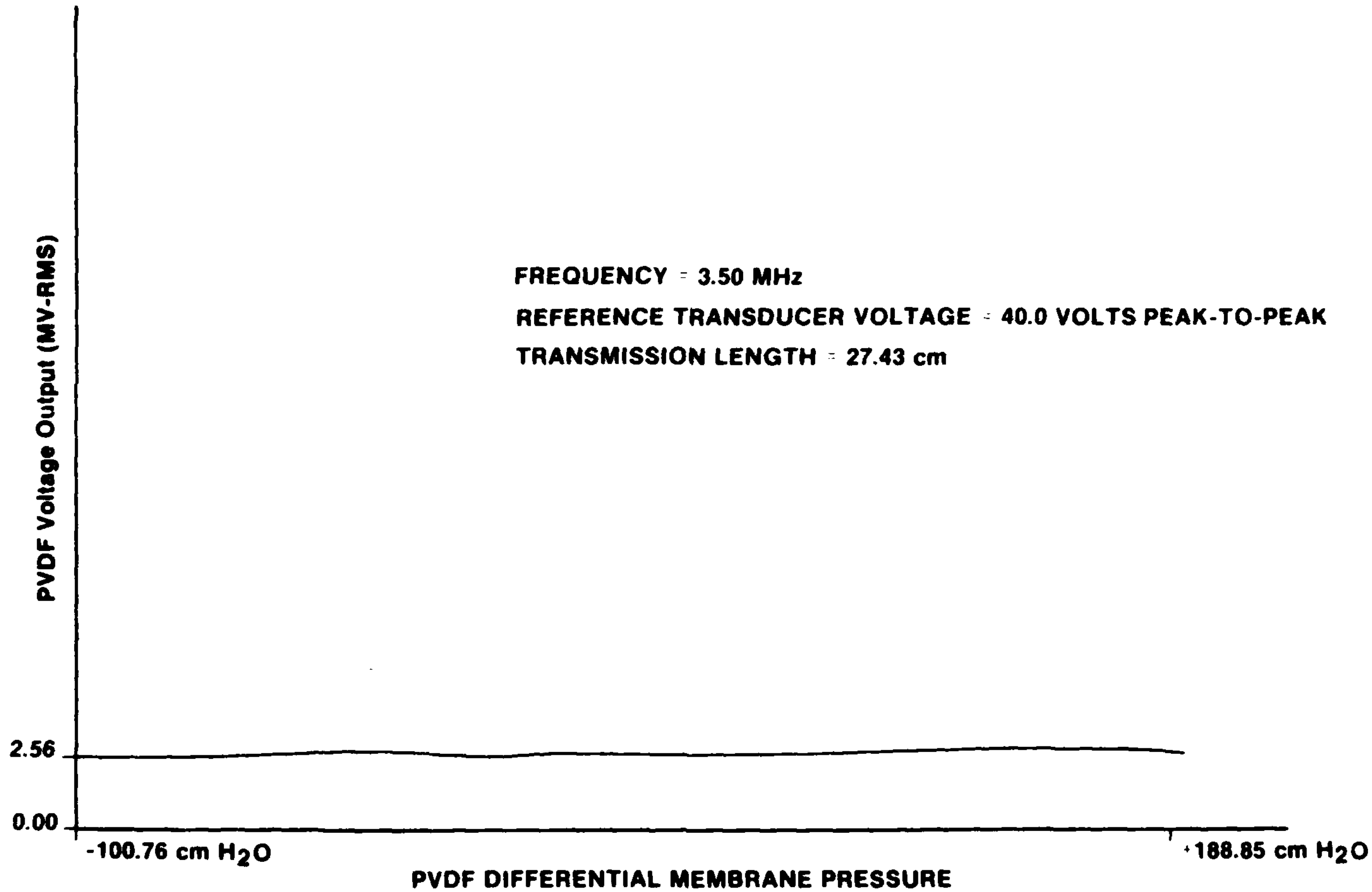

Figure 27. Test B3.50

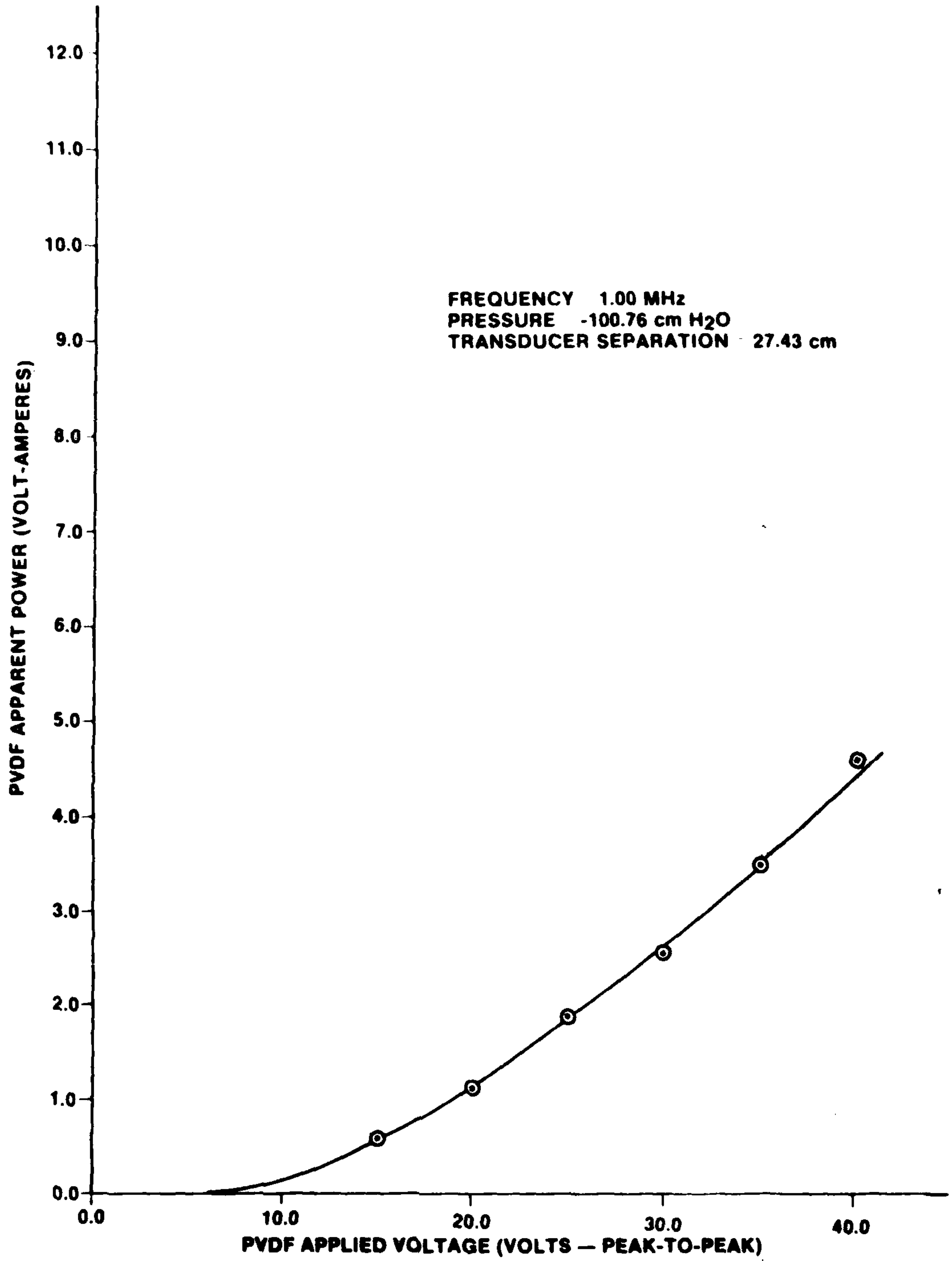

Figure 28. Test C1.00

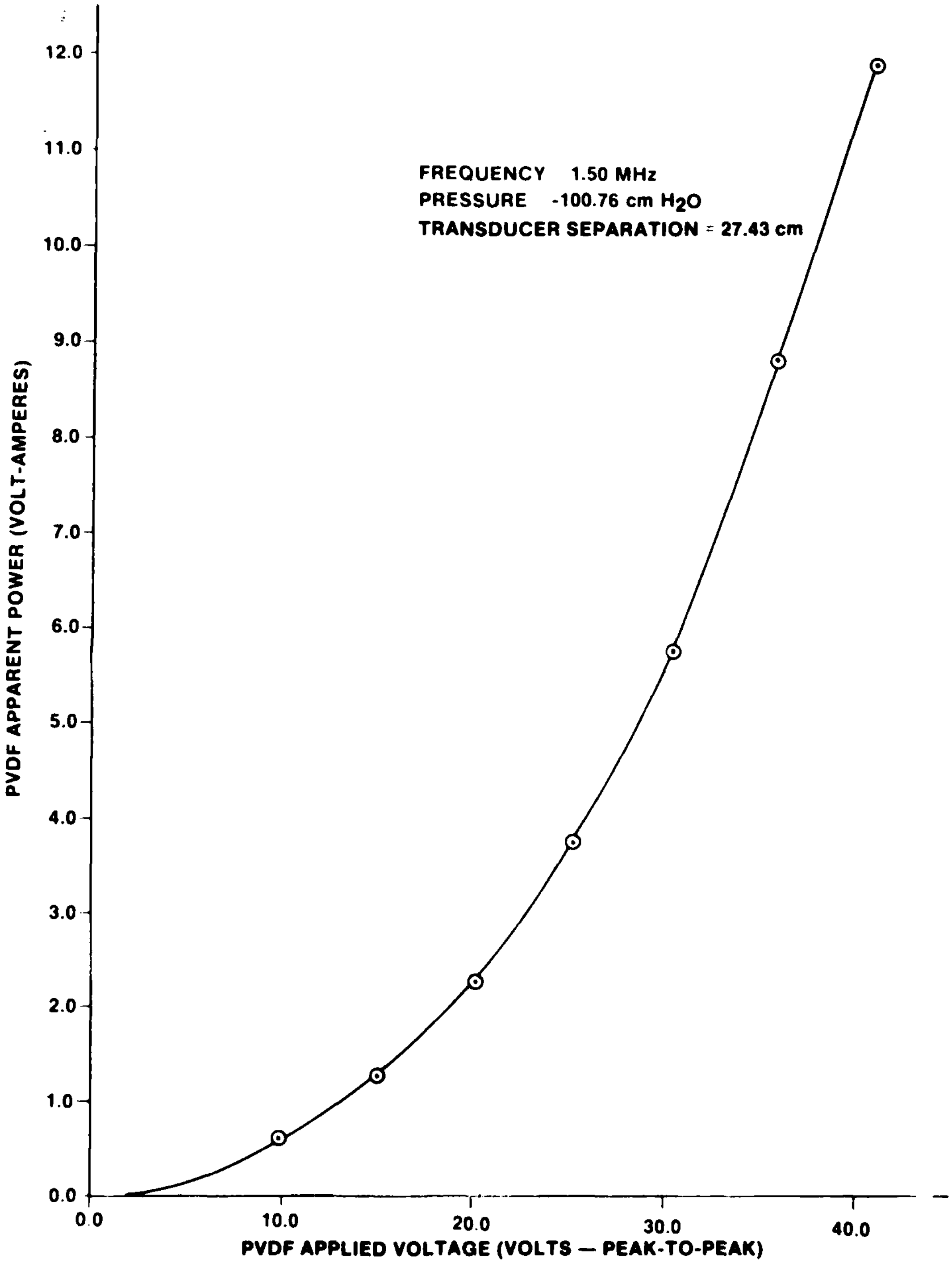

Figure 29. Test C1.50

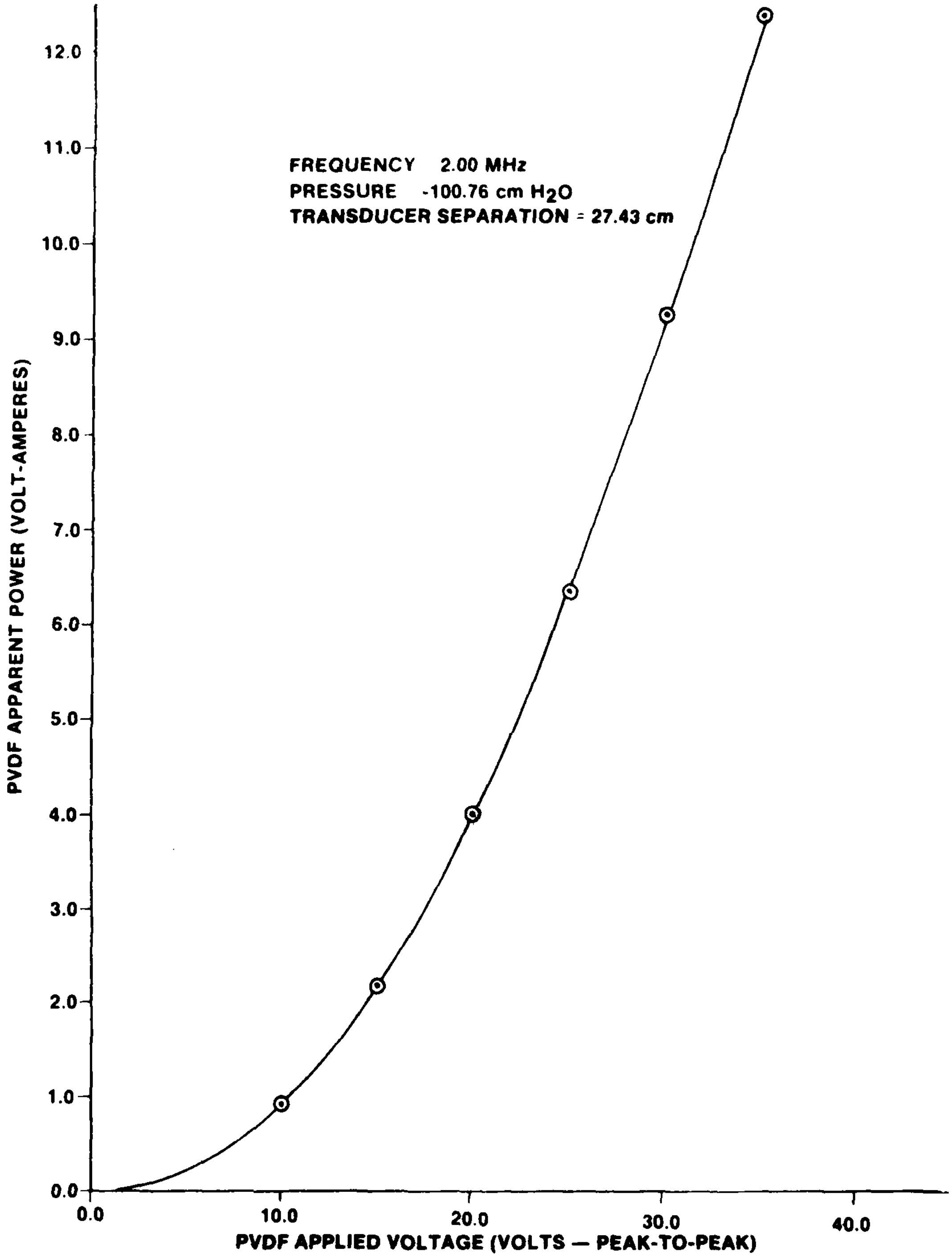

Figure 30. Test C2.00

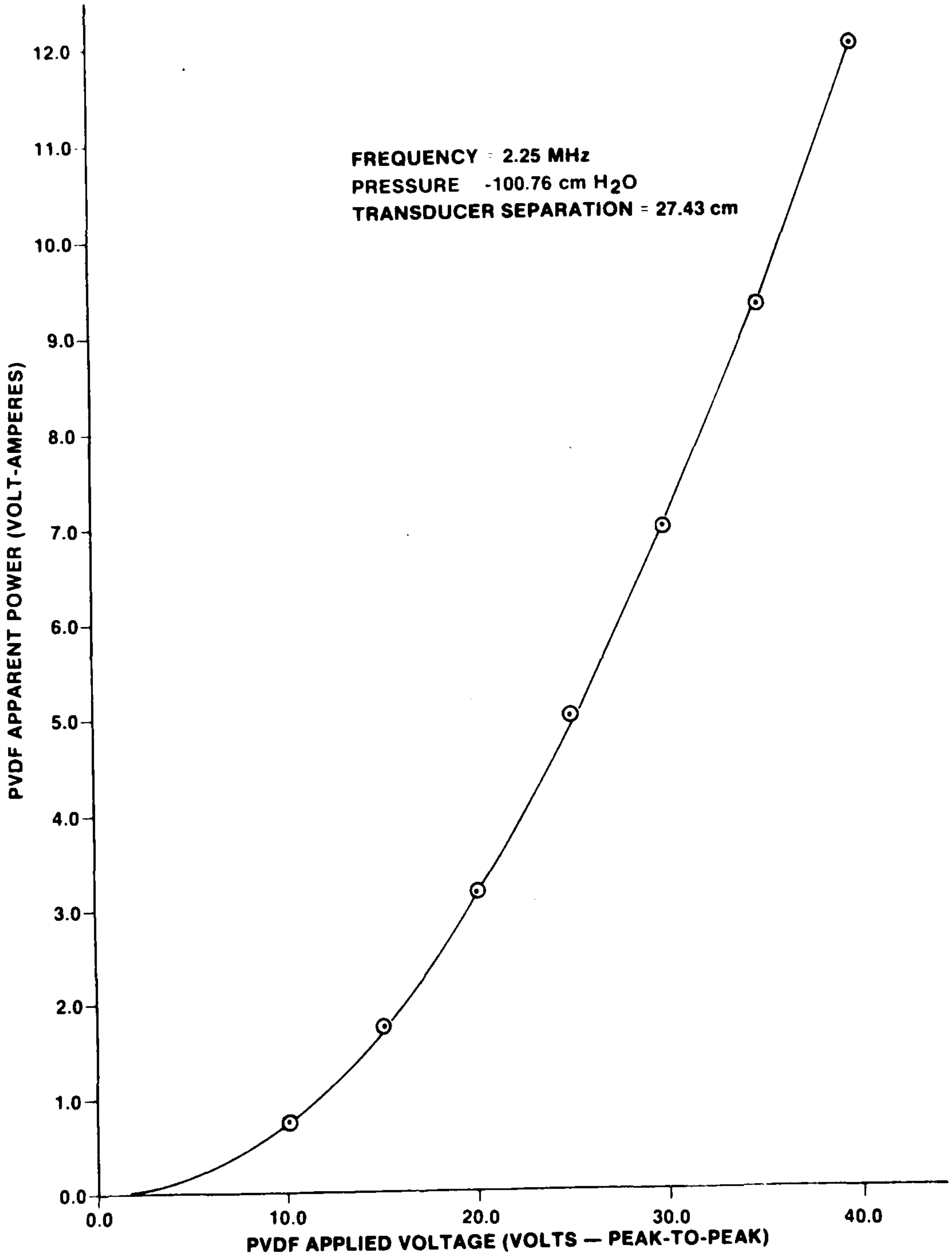

Figure 31. Test C2.25

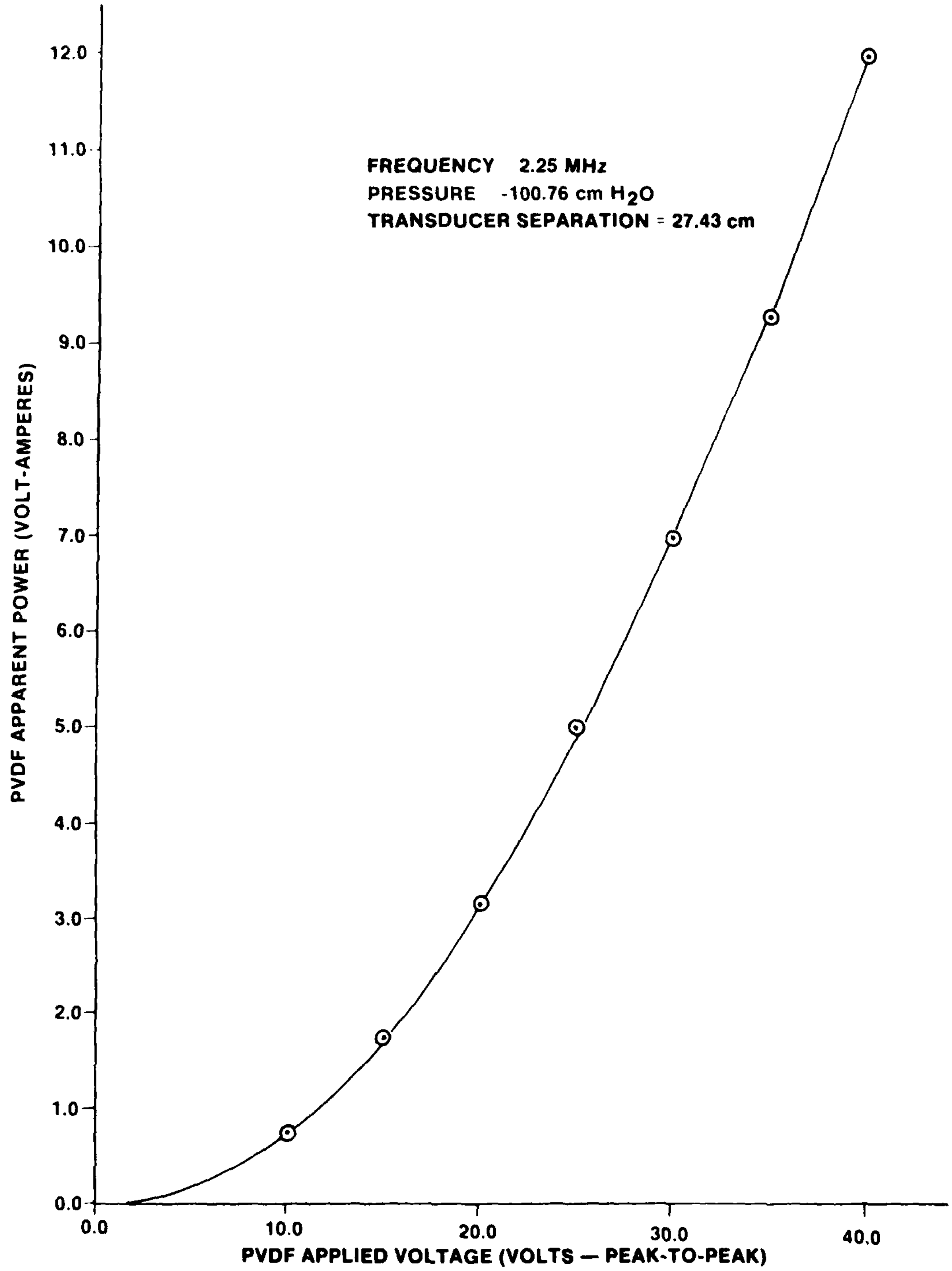

Figure 31. Test C2.25

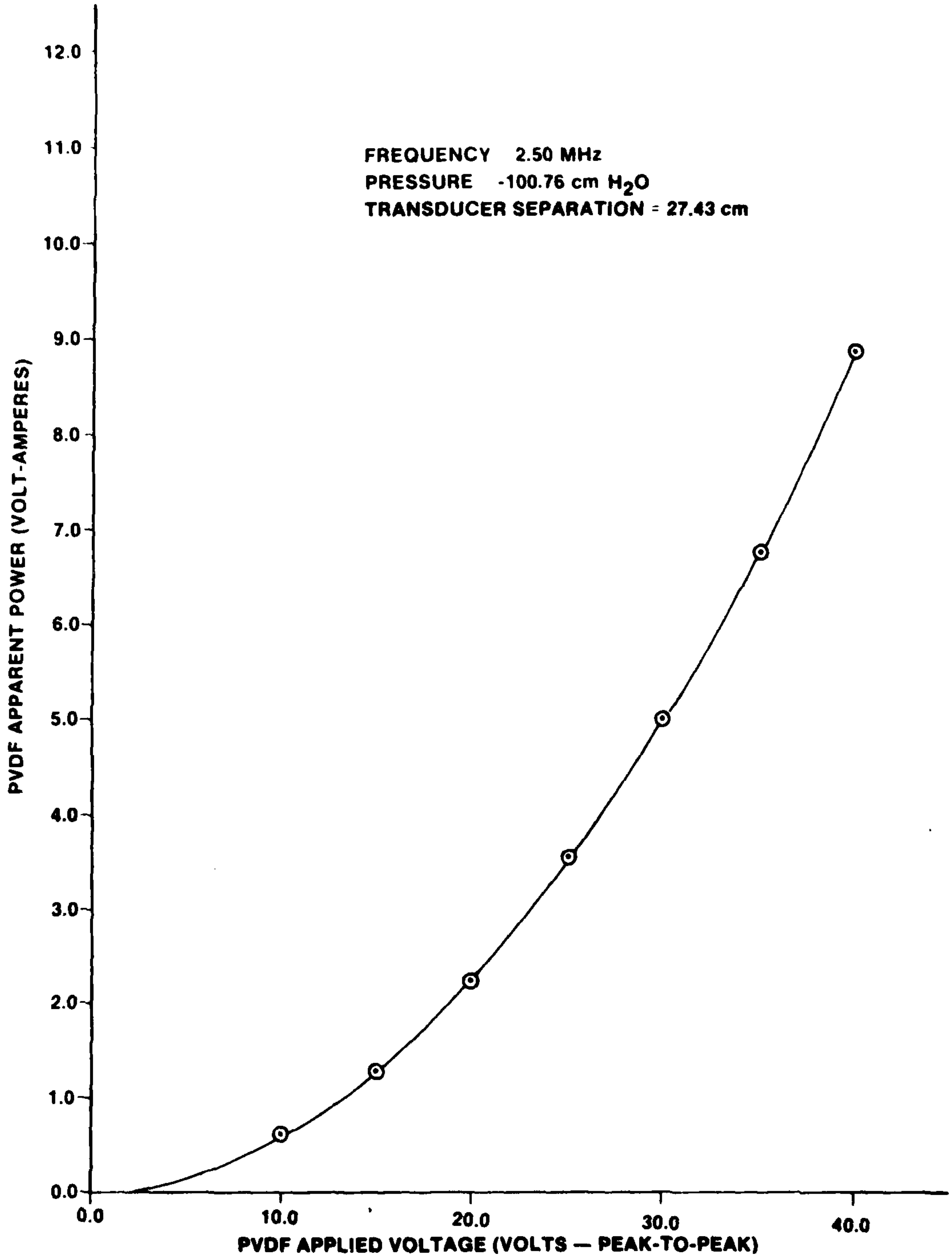

Figure 32. Test C2.50

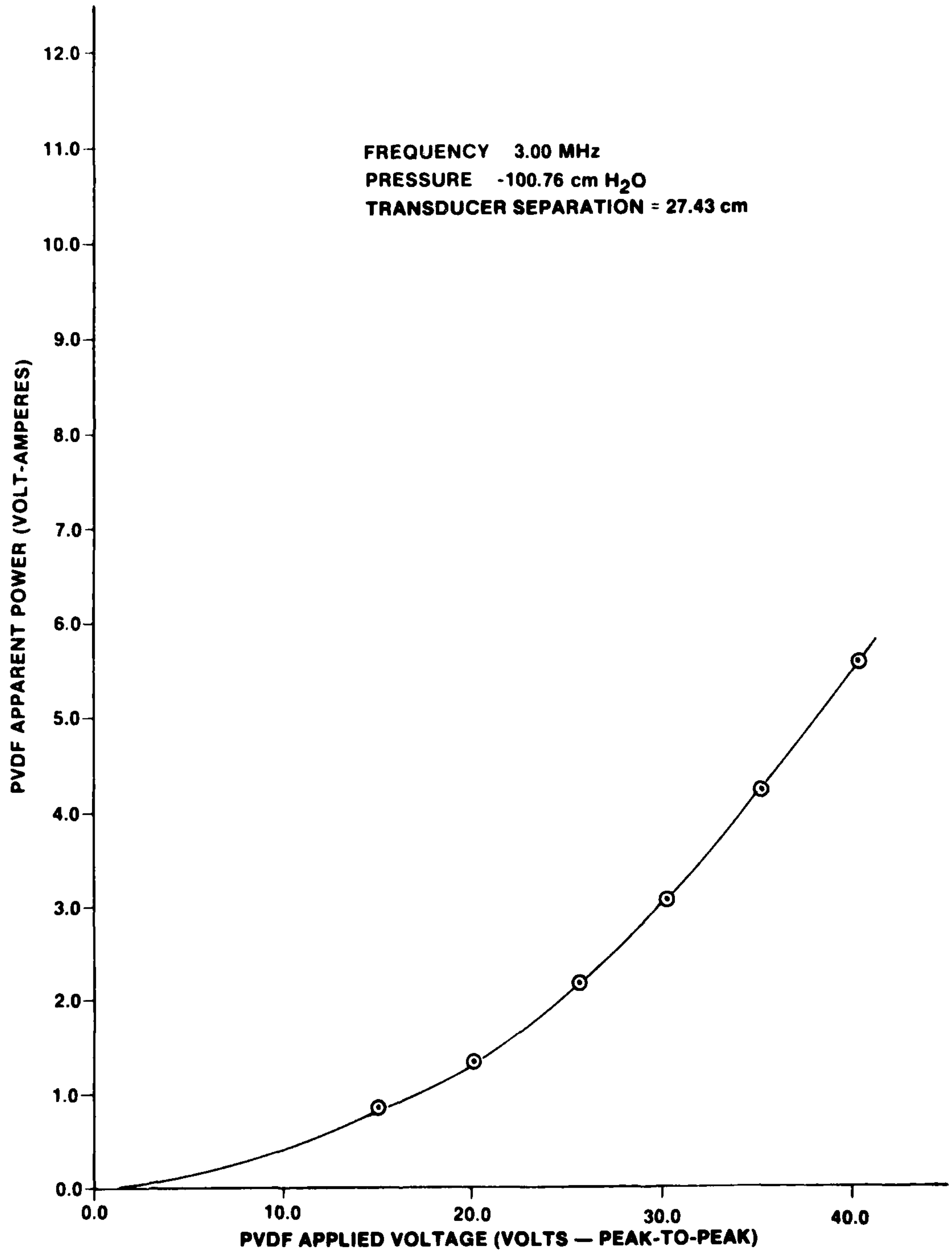

Figure 33. Test C3.00

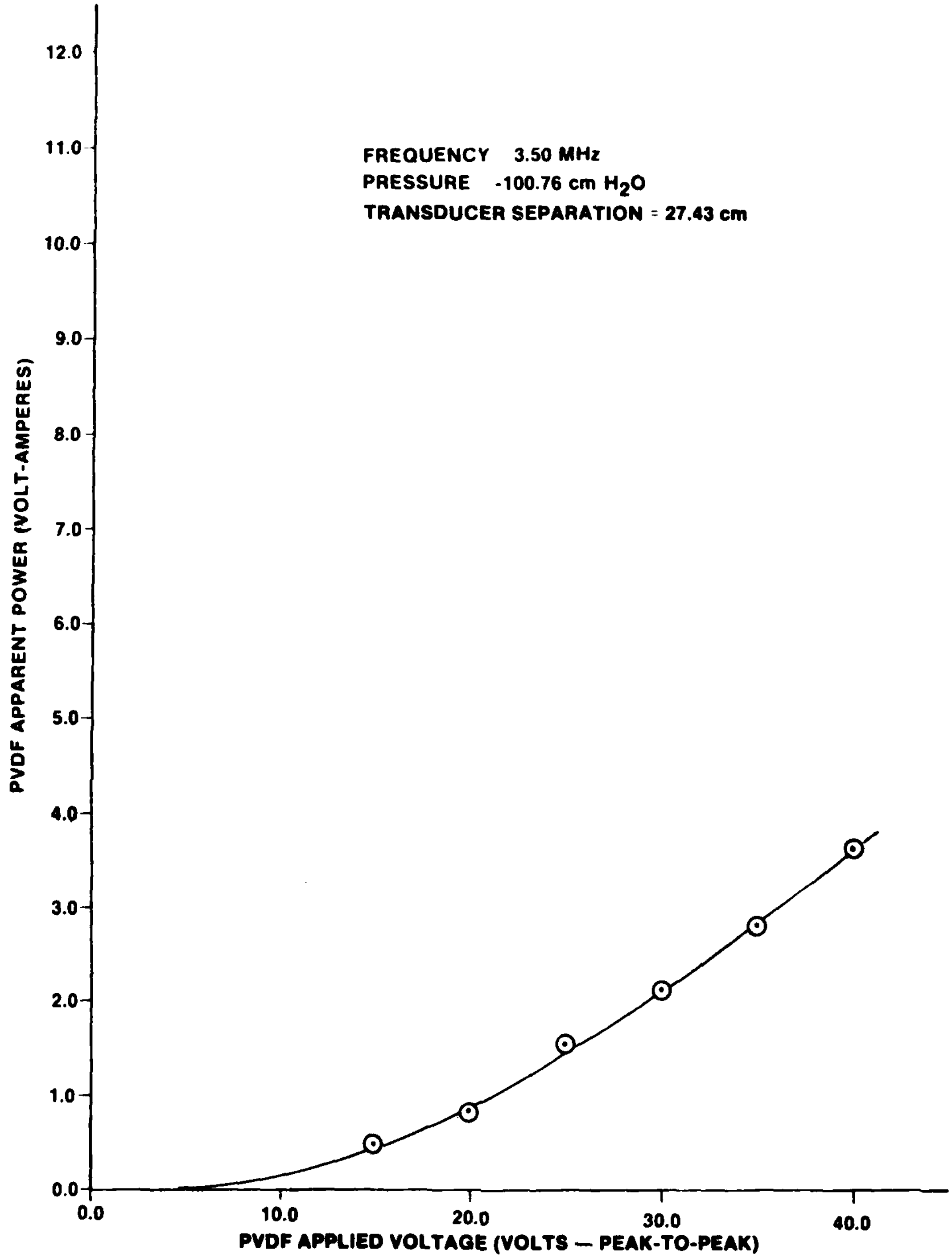

Figure 34. Test C3.50

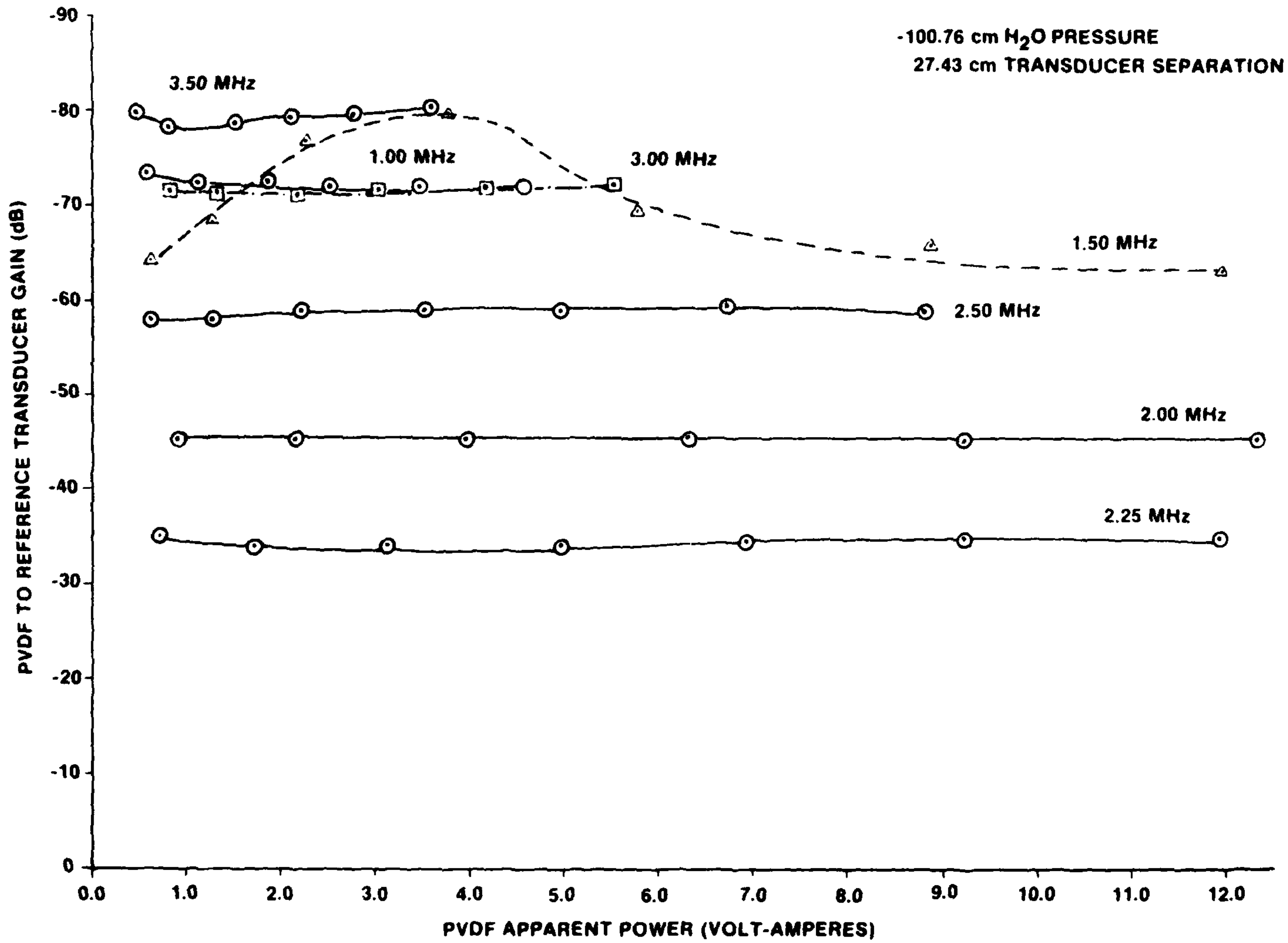

Figure 35. PVDF to reference transducer gain versus PVDF apparent power.

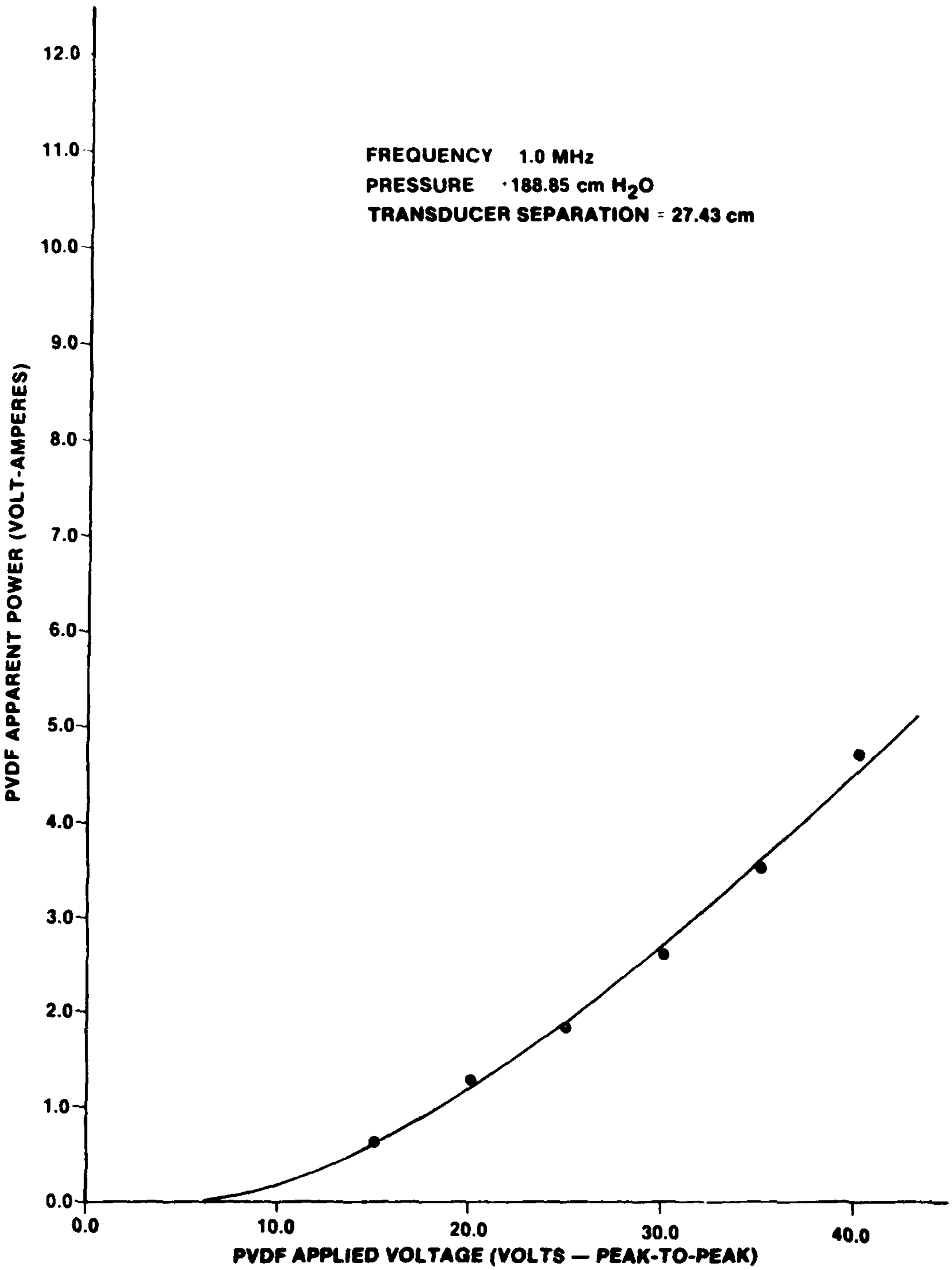

Figure 36. Test D1.00.

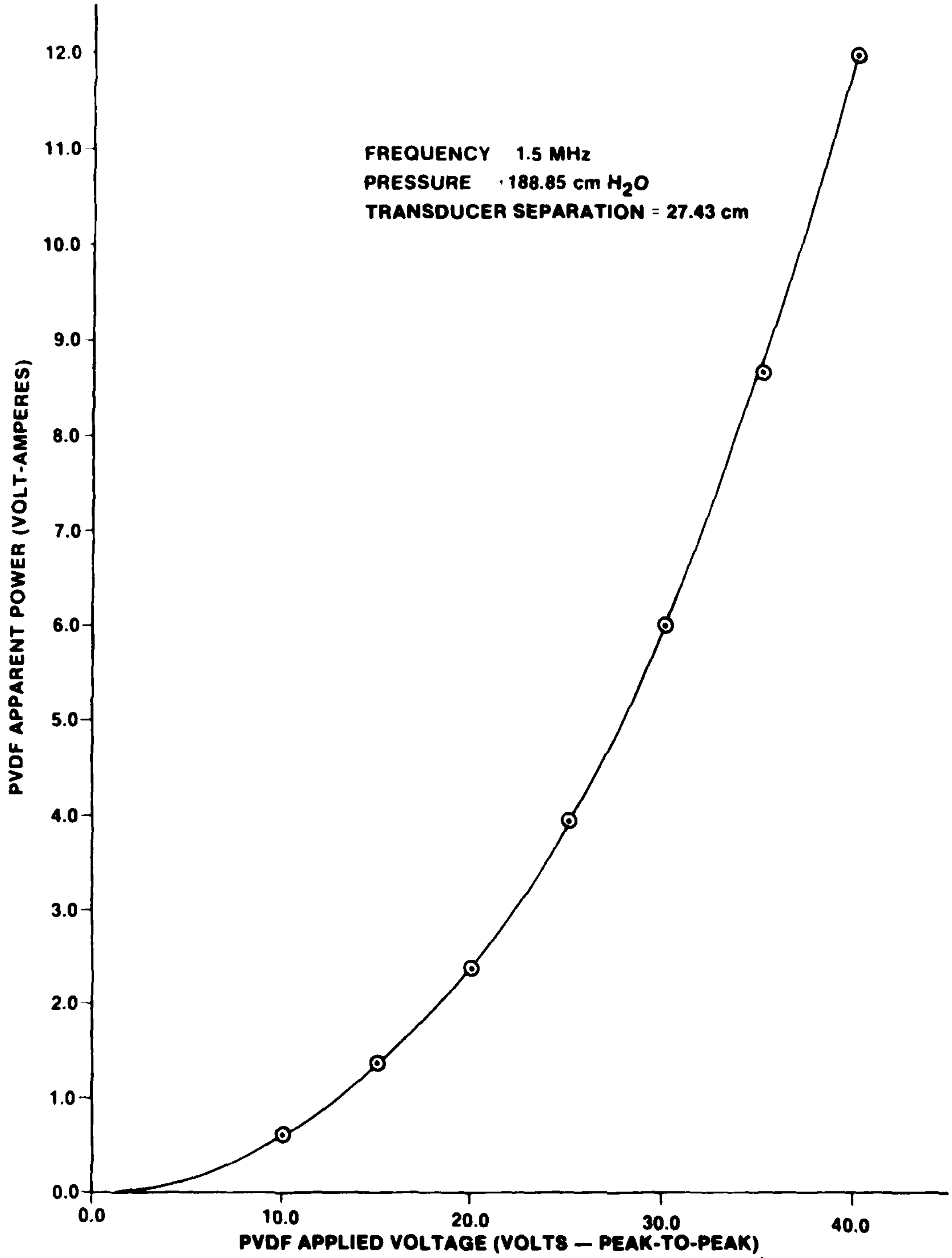

Figure 37. Test D1.50.

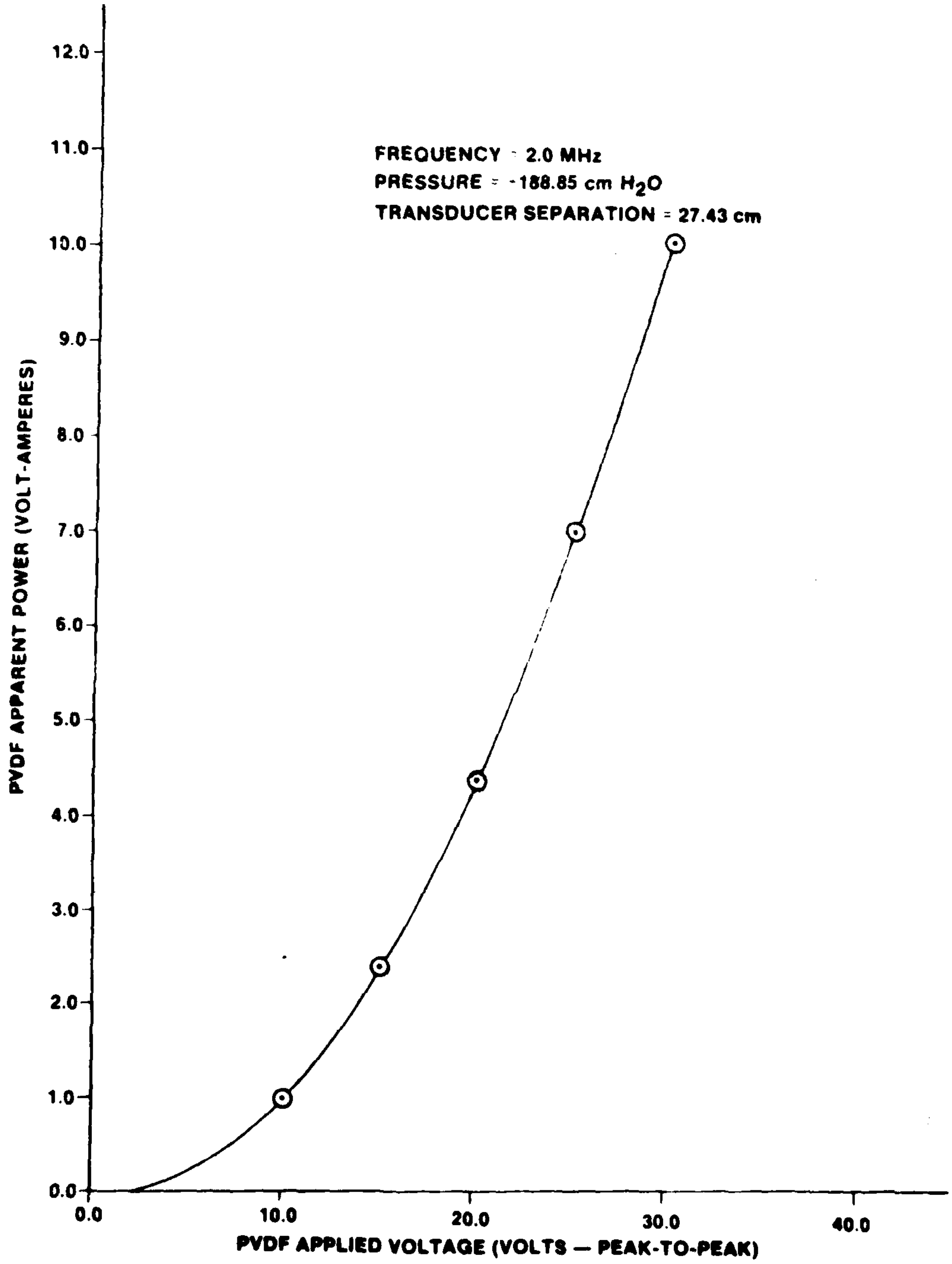

Figure 38. Test D2.00.

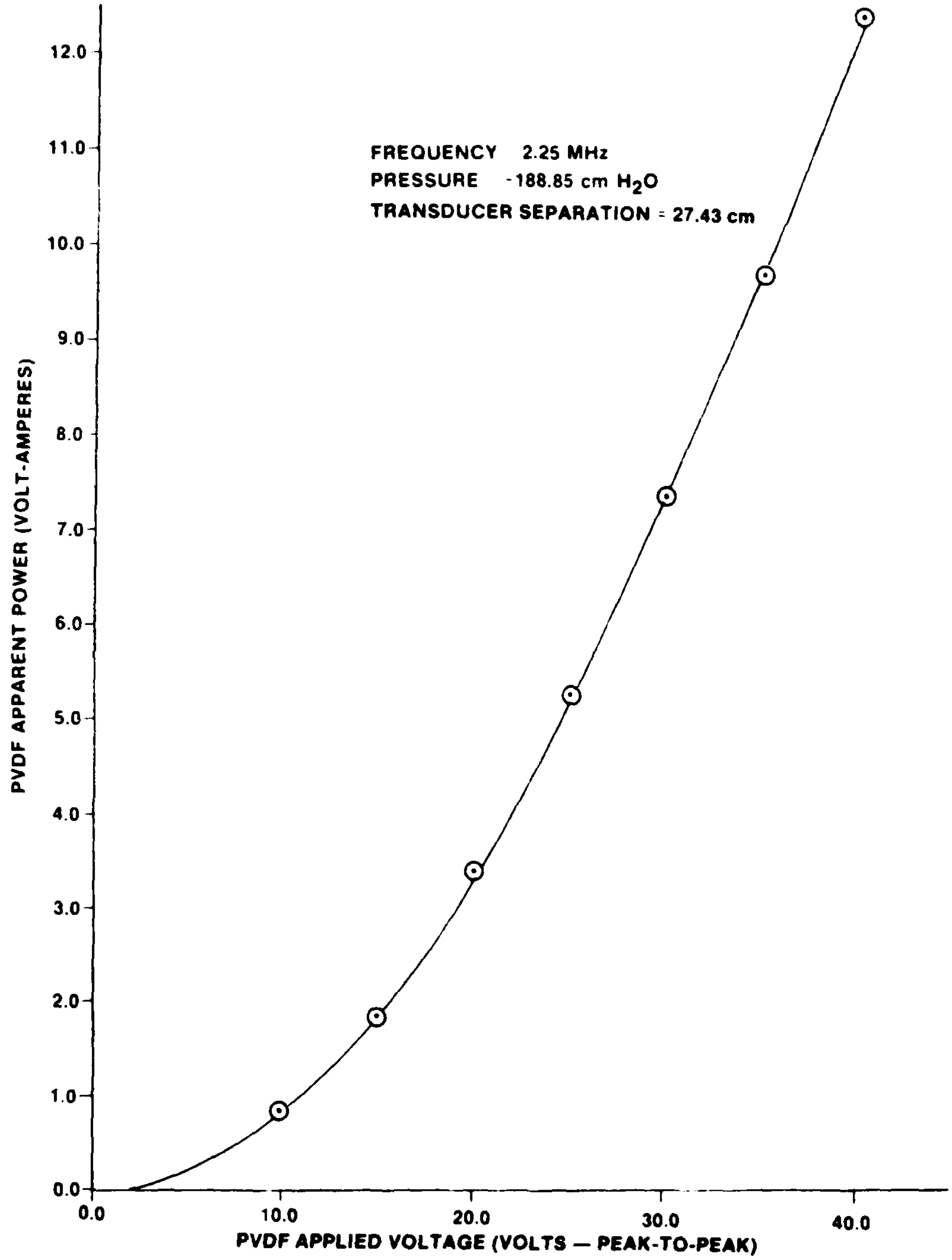

Figure 39. Test D2.25.

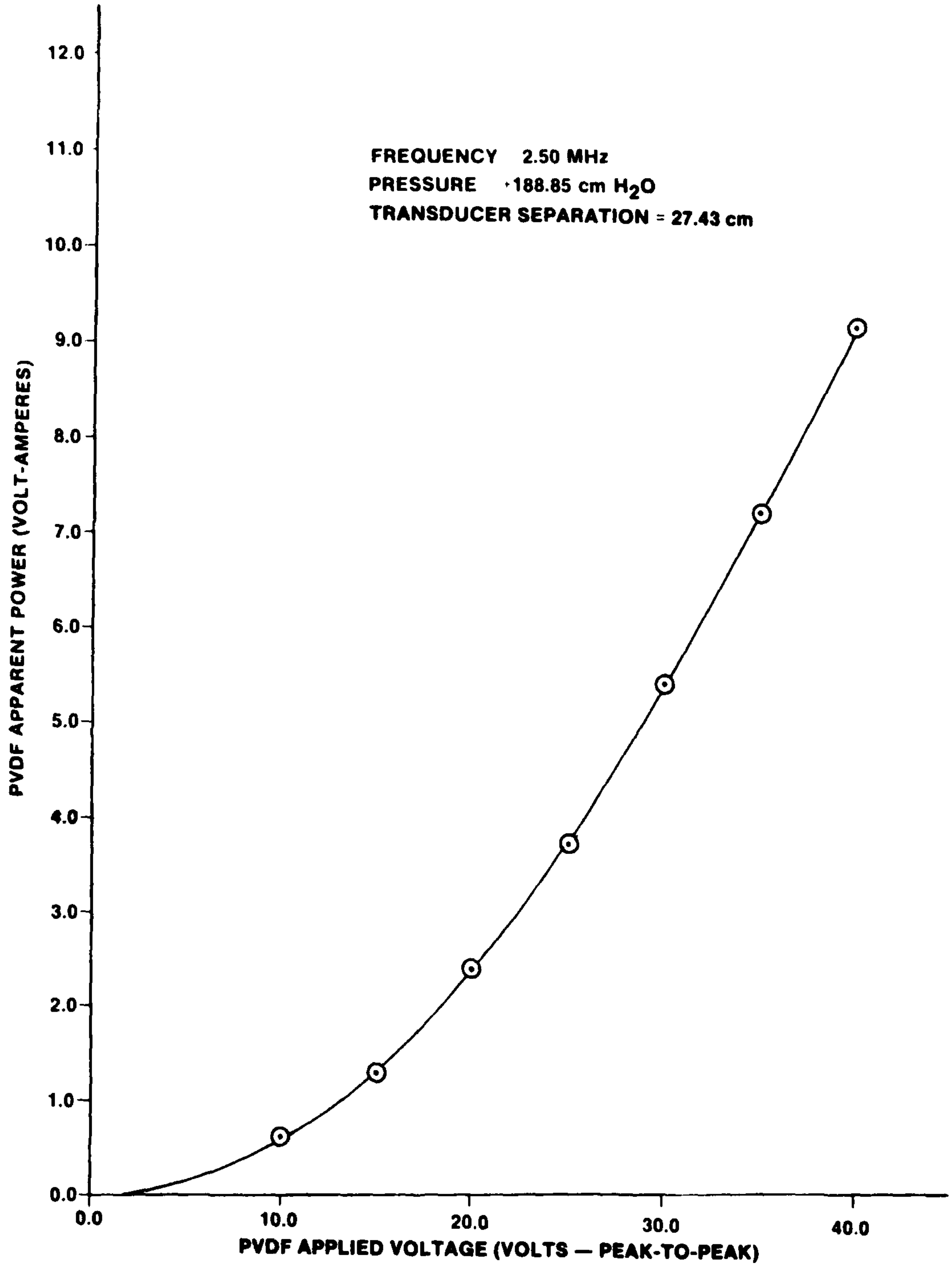

Figure 40. Test D2.50.

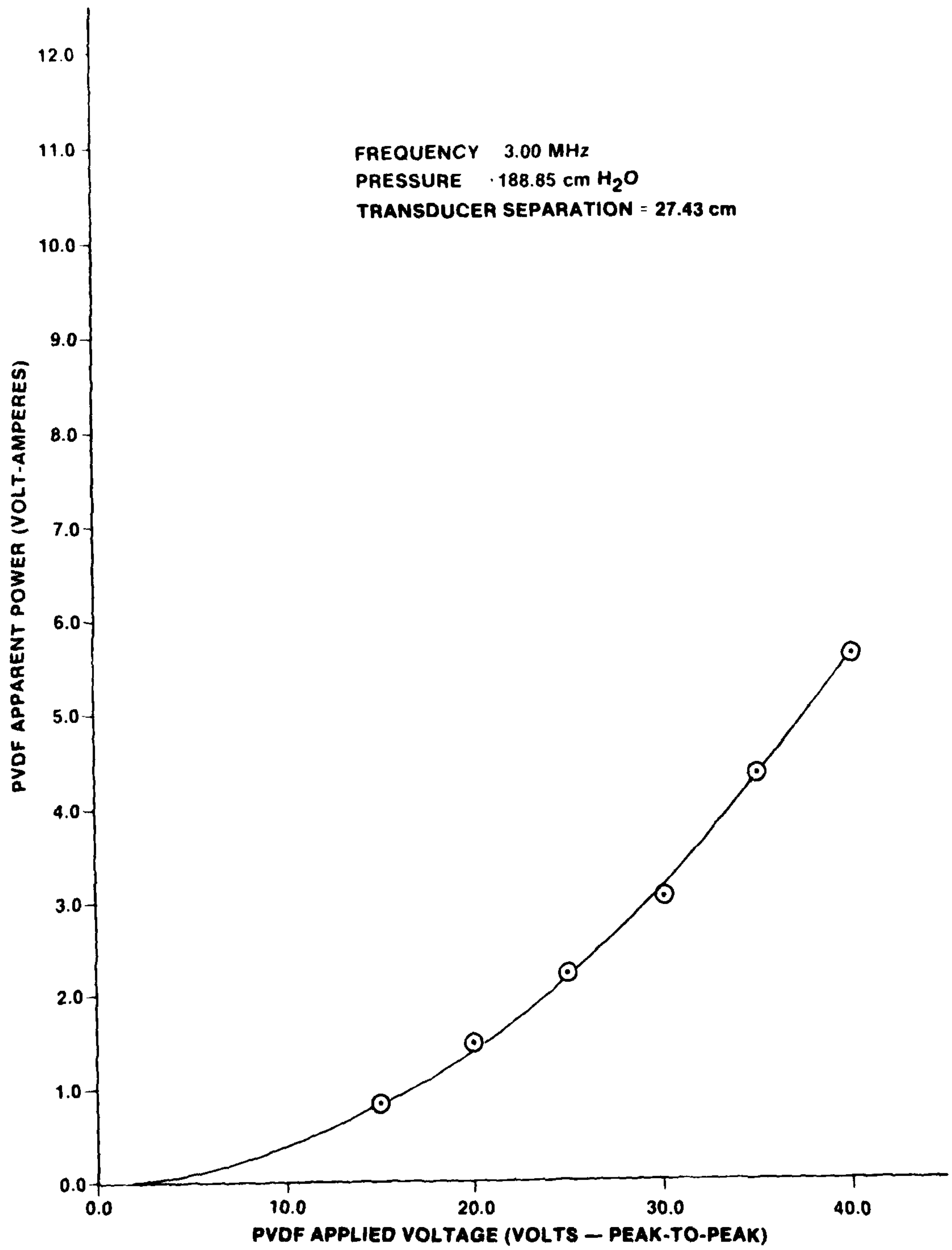

Figure 41. Test D3.00.

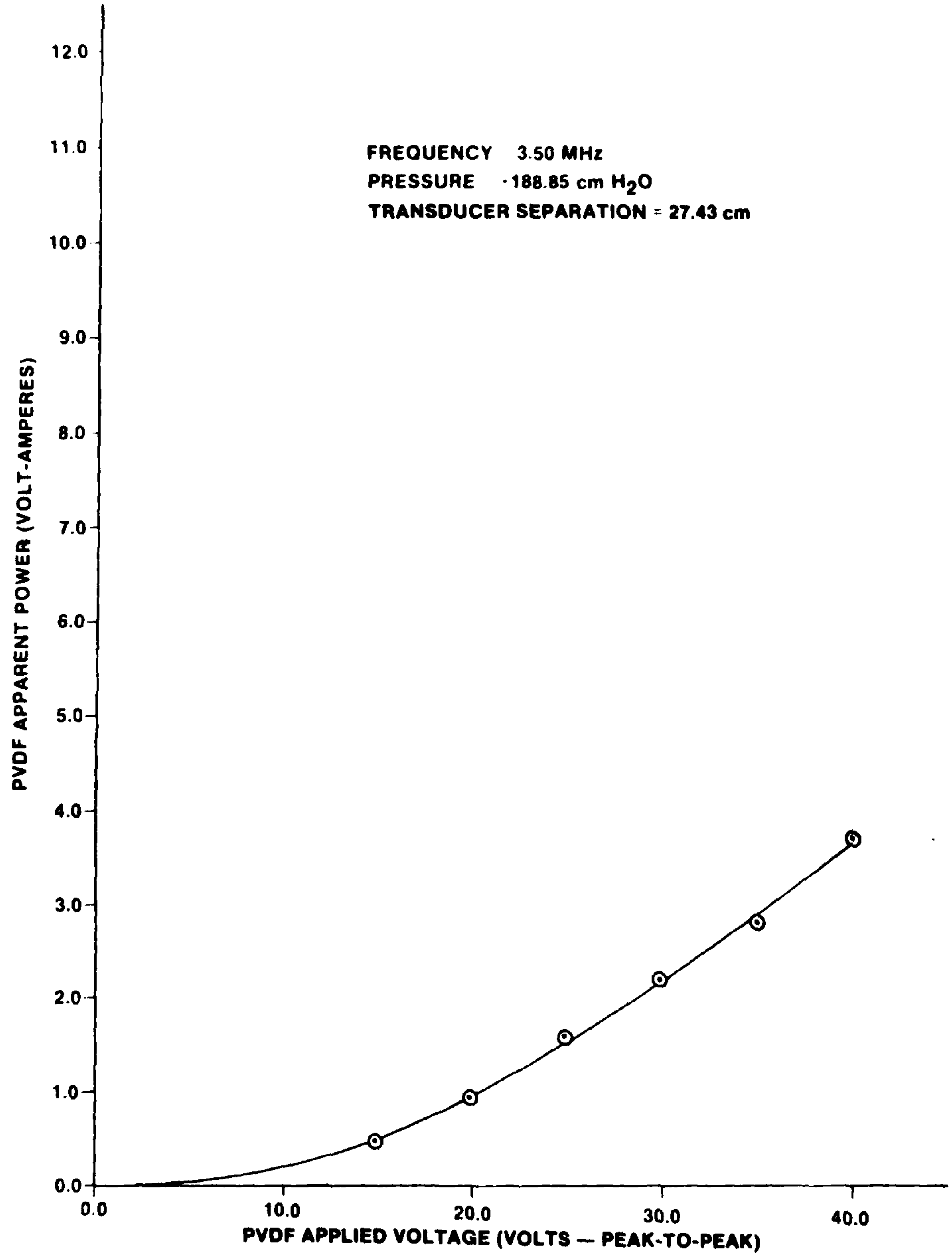

Figure 42. Test D3.50.

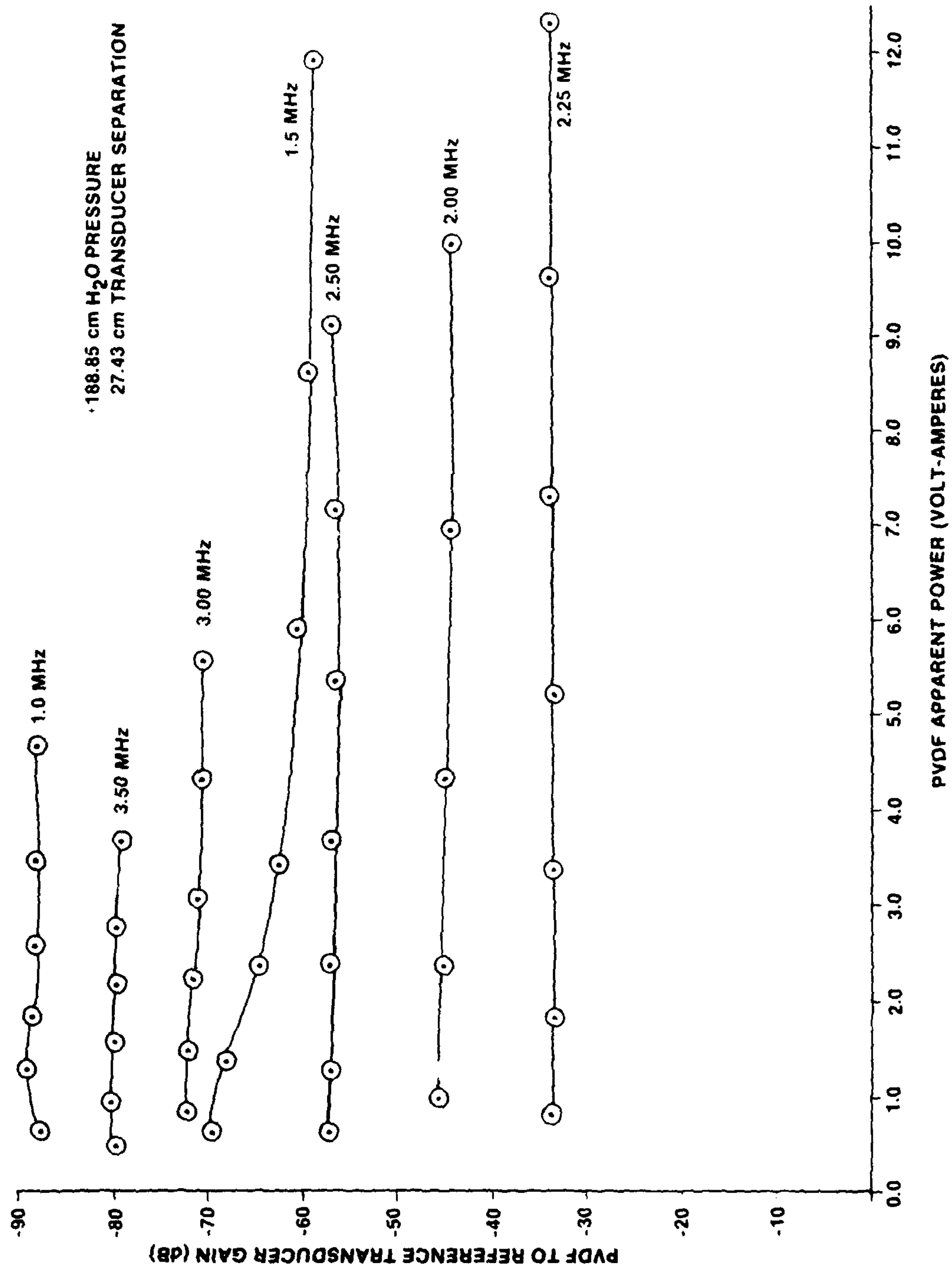

Figure 43. PVDF to reference transducer gain versus PVDF apparent power.

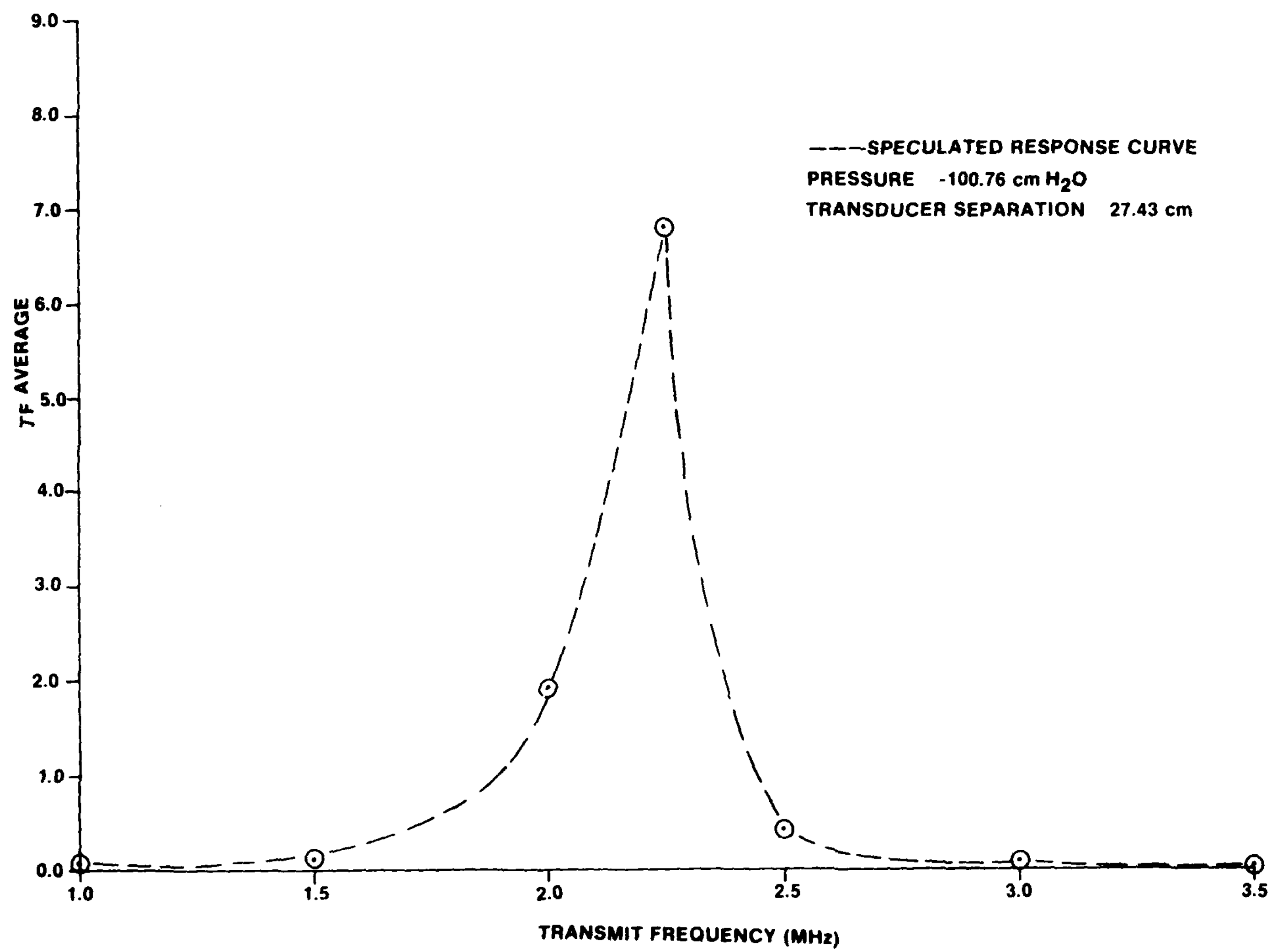

Figure 44. τ_F **versus frequency for -100.76 cm H_2O differential membrane pressure.**

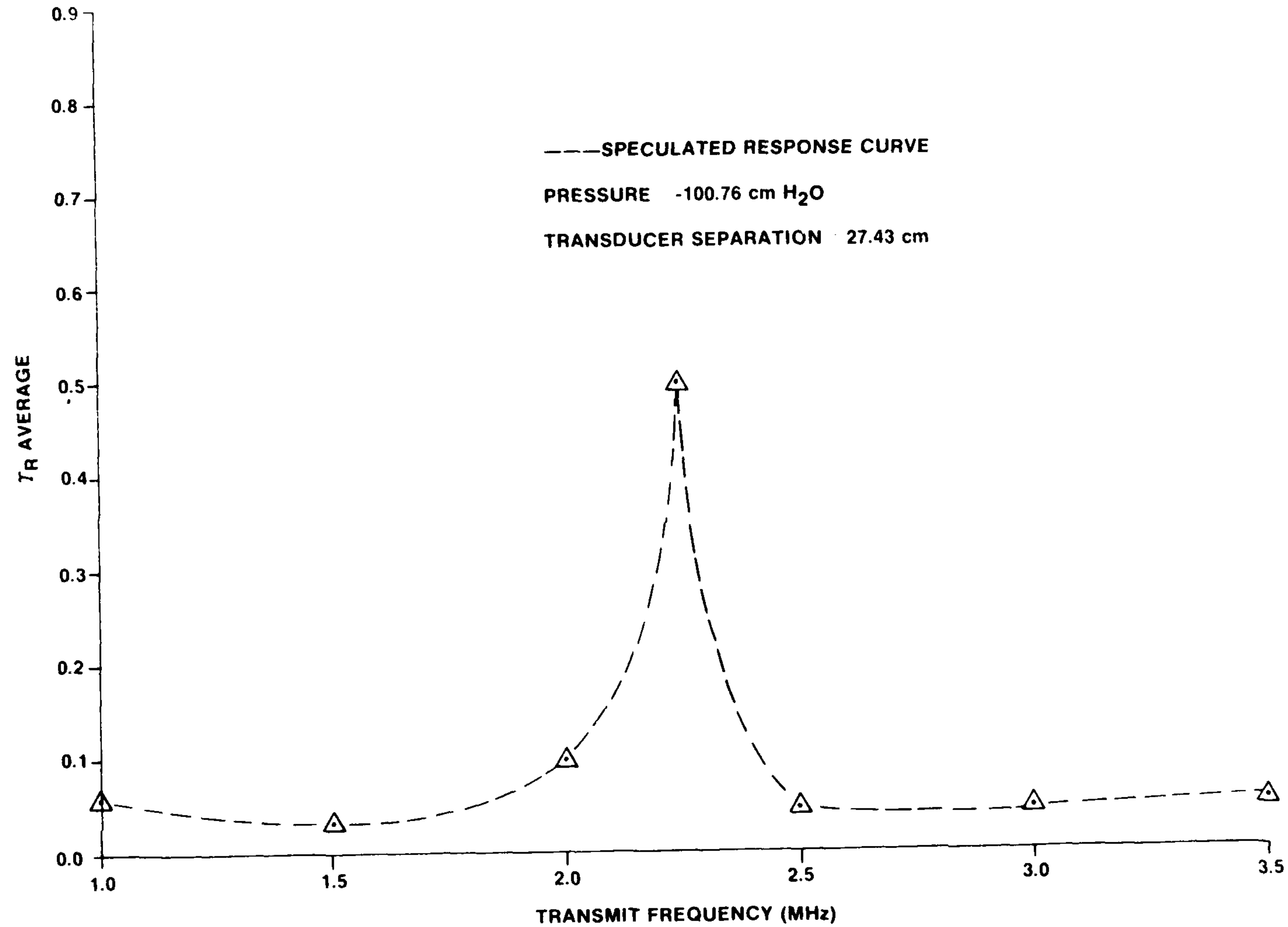

Figure 45. TR versus frequency for -100.76 cm H_2O differential membrane pressure.

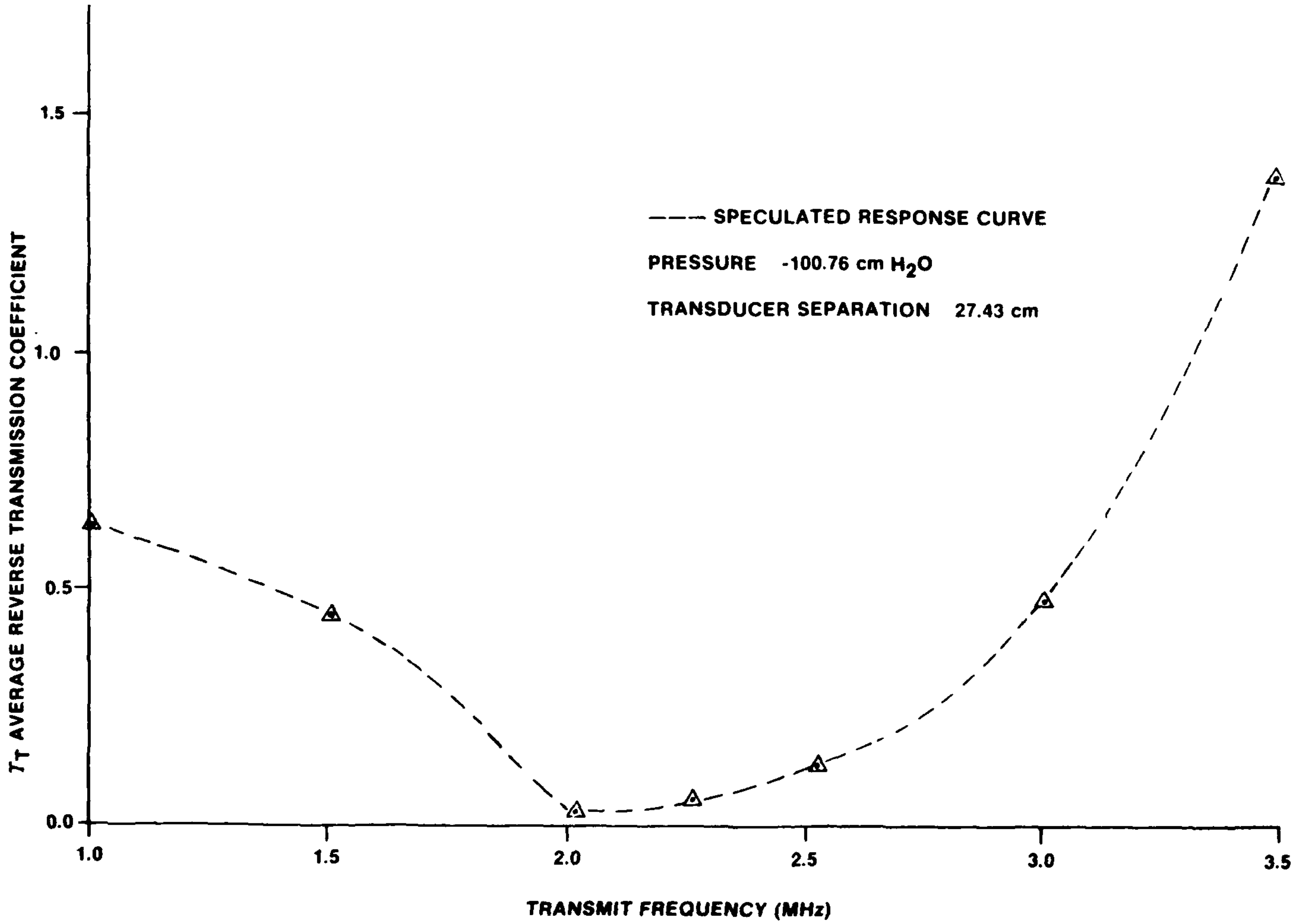

Figure 46. T_T versus frequency for -100.76 cm H_2O differential membrane pressure.

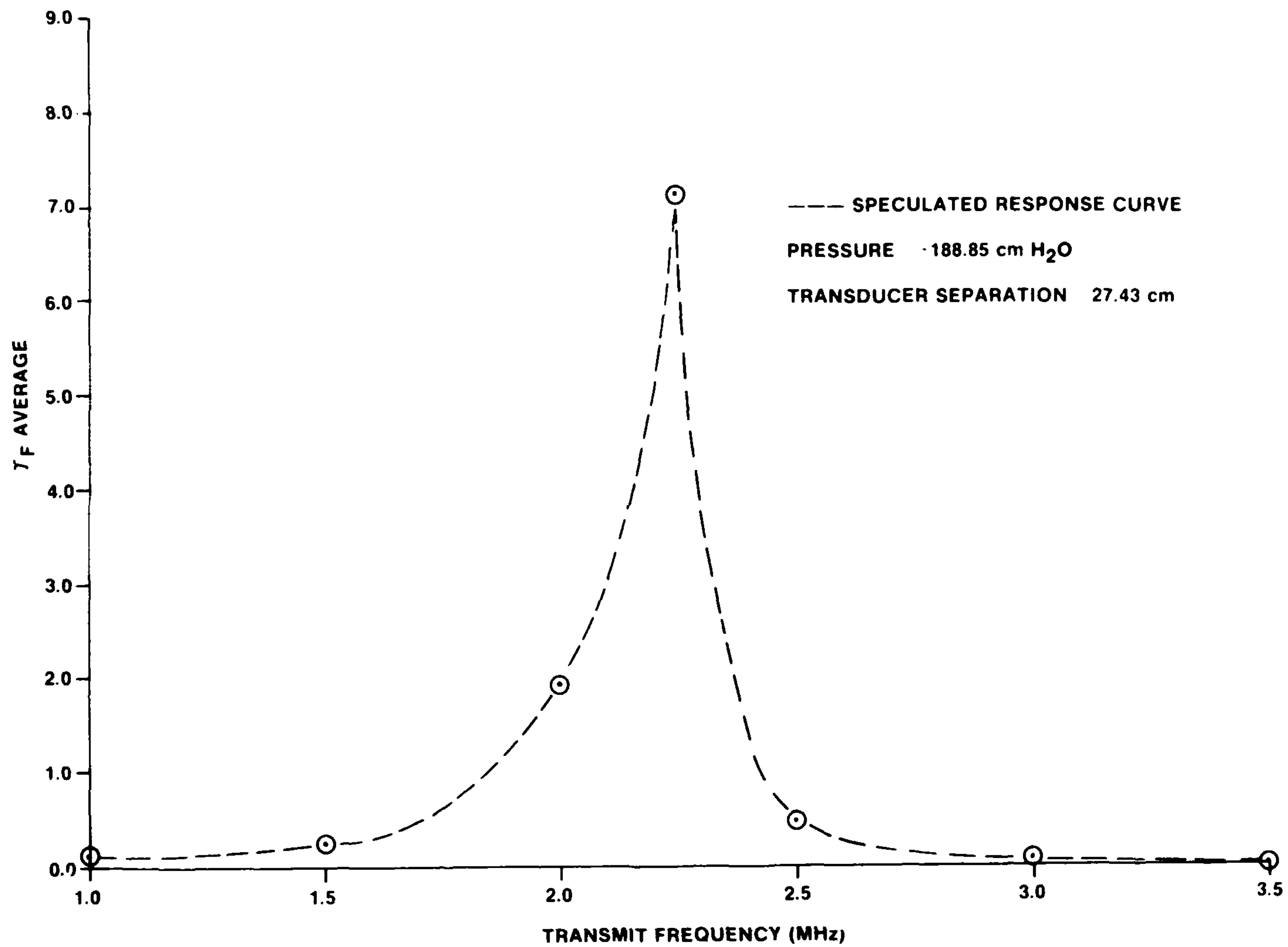

Figure 47. T_F versus frequency for +188.85 cm H_2O differential membrane pressure.

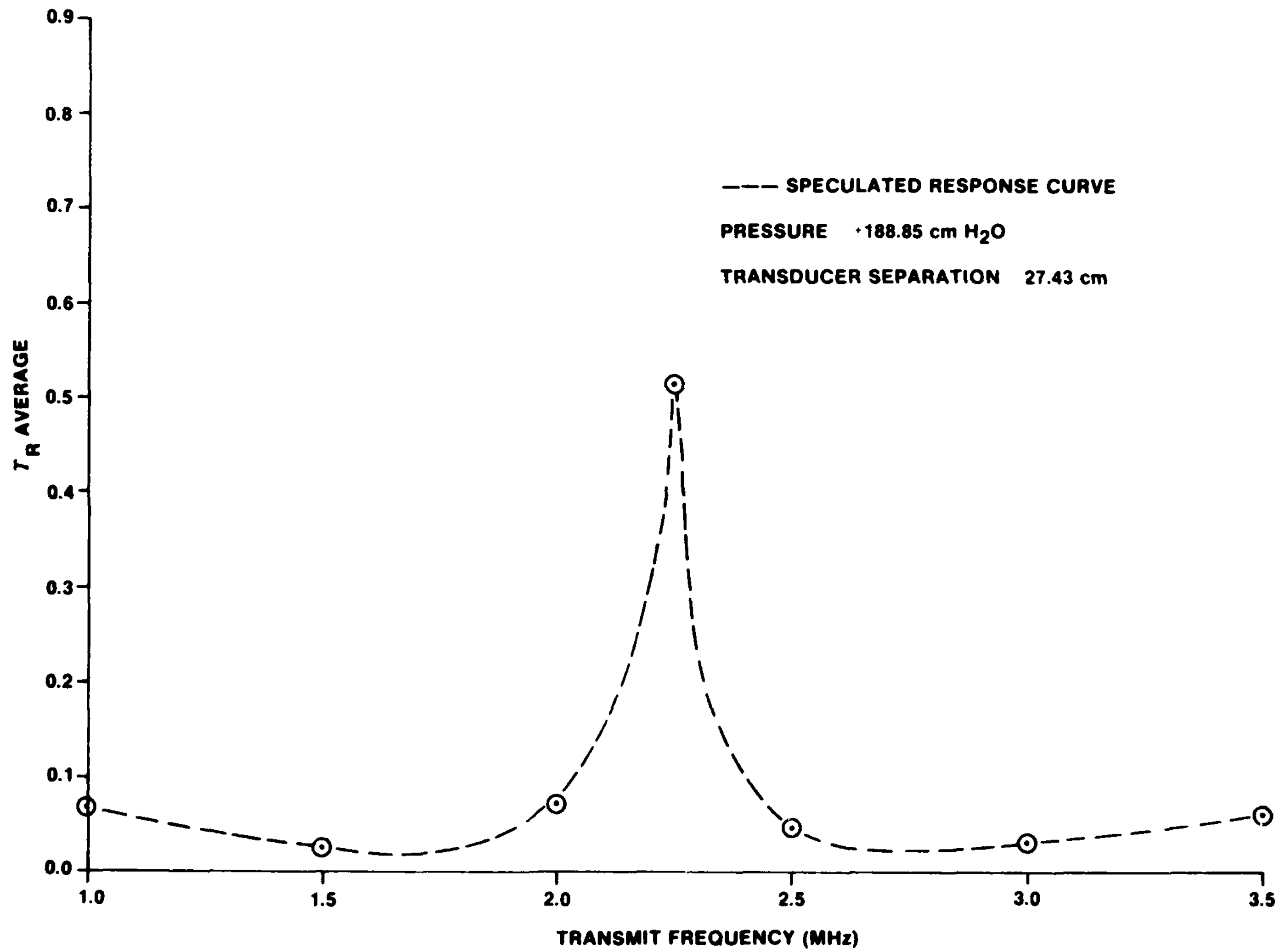

Figure 48. T_R **versus frequency for +188.85 cm** H_2O **differential membrane pressure.**

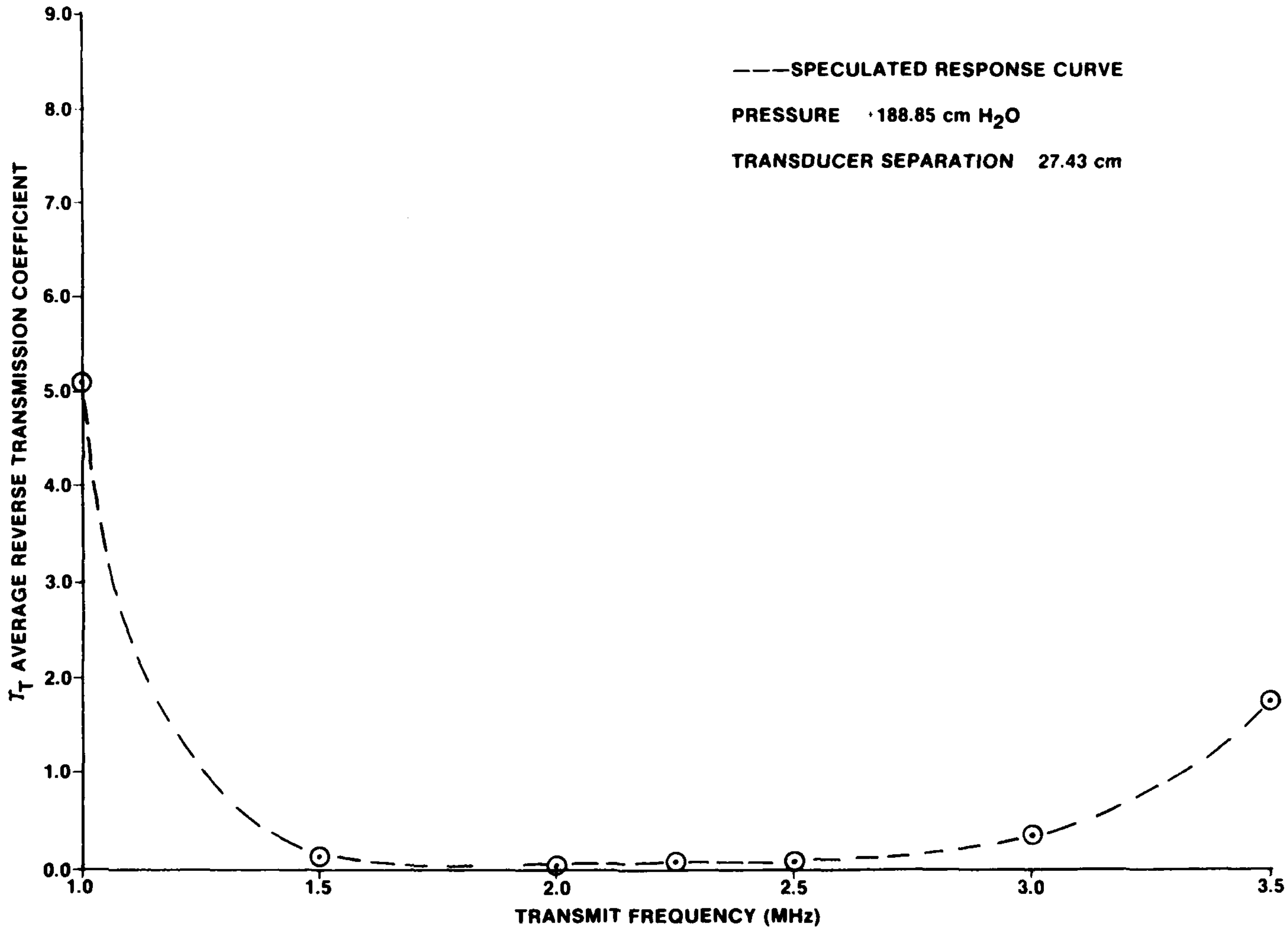

Figure 49. τ_T **versus frequency for +188.85 cm H_2O differential membrane pressure.**

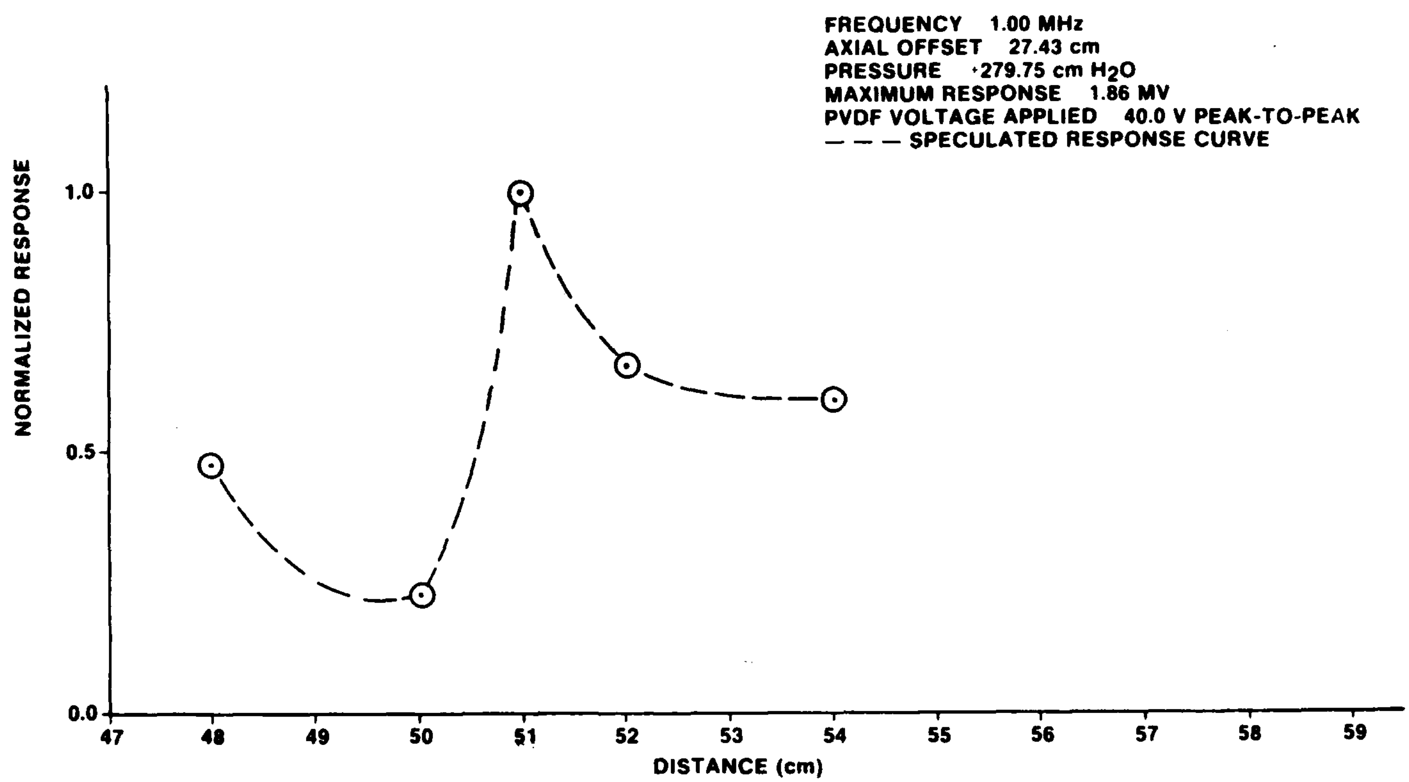

Figure 50. Scan test G1.00.

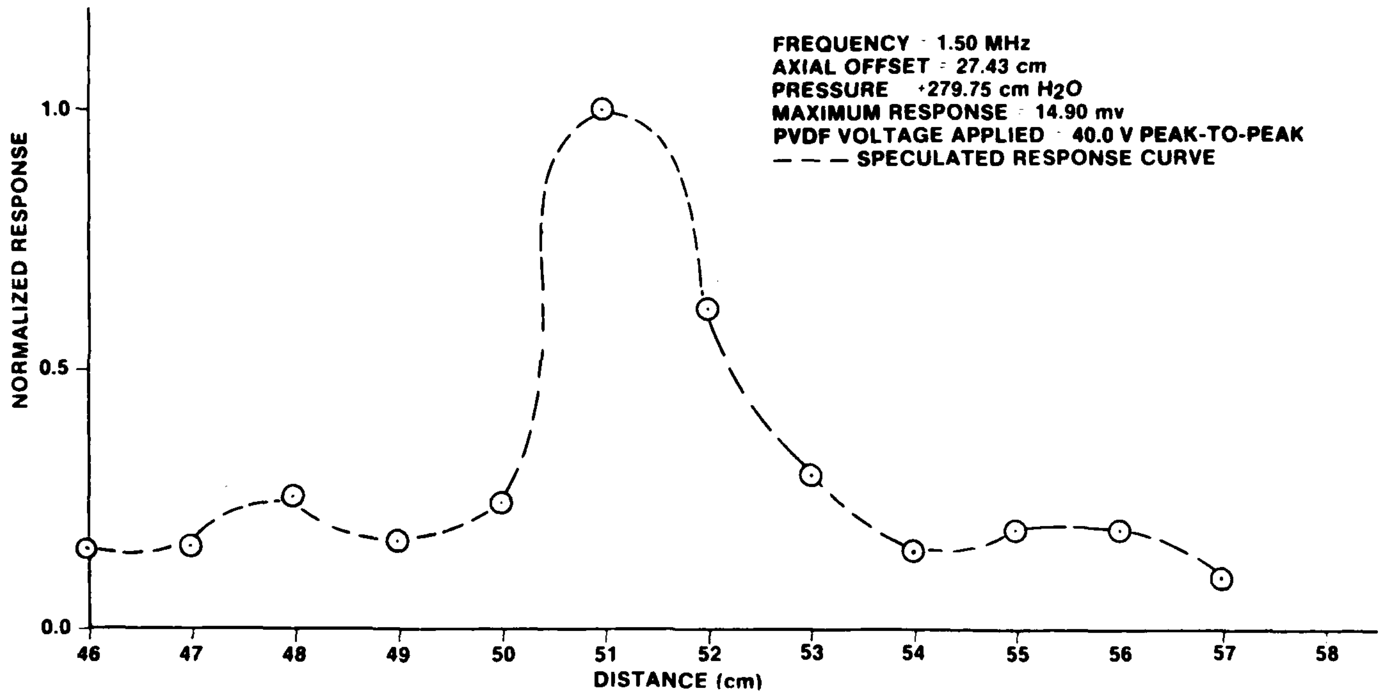

Figure 51. Scan test G1.50.

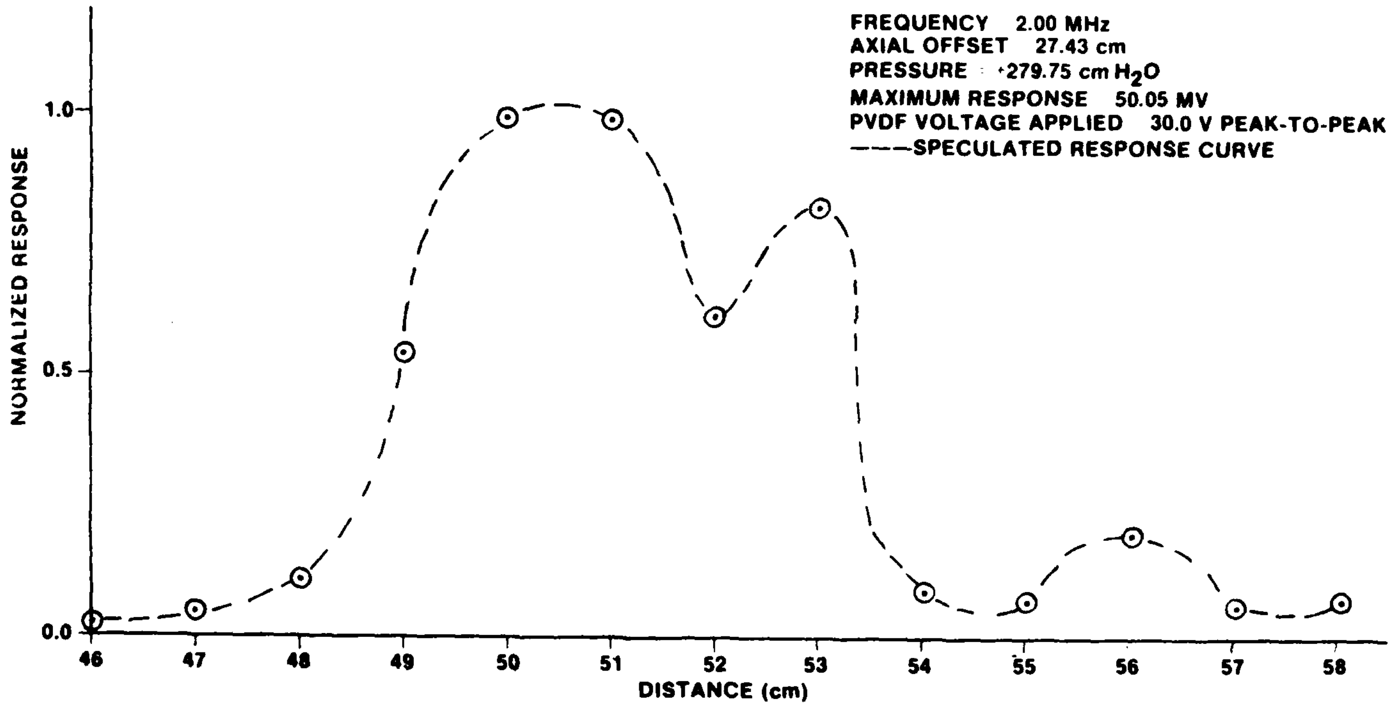

Figure 52. Scan test G2.00.

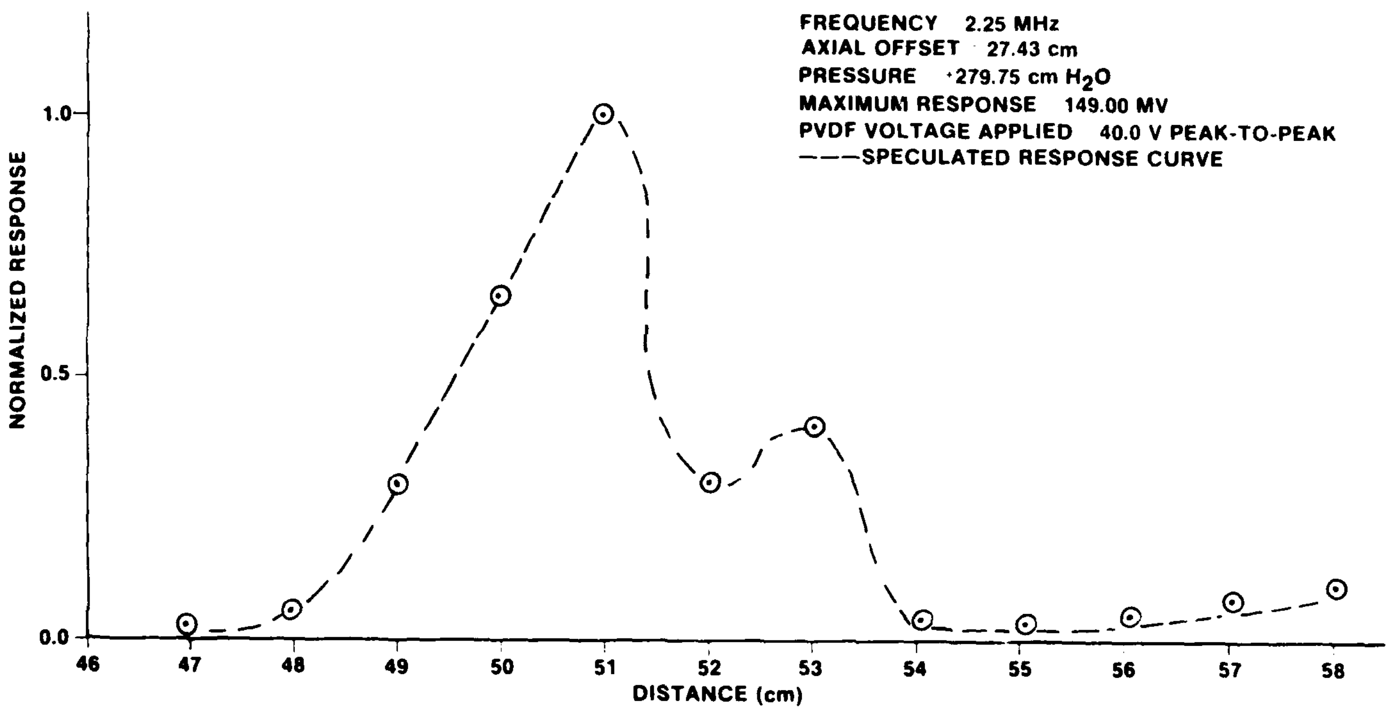

Figure 53. Scan test G2.25.

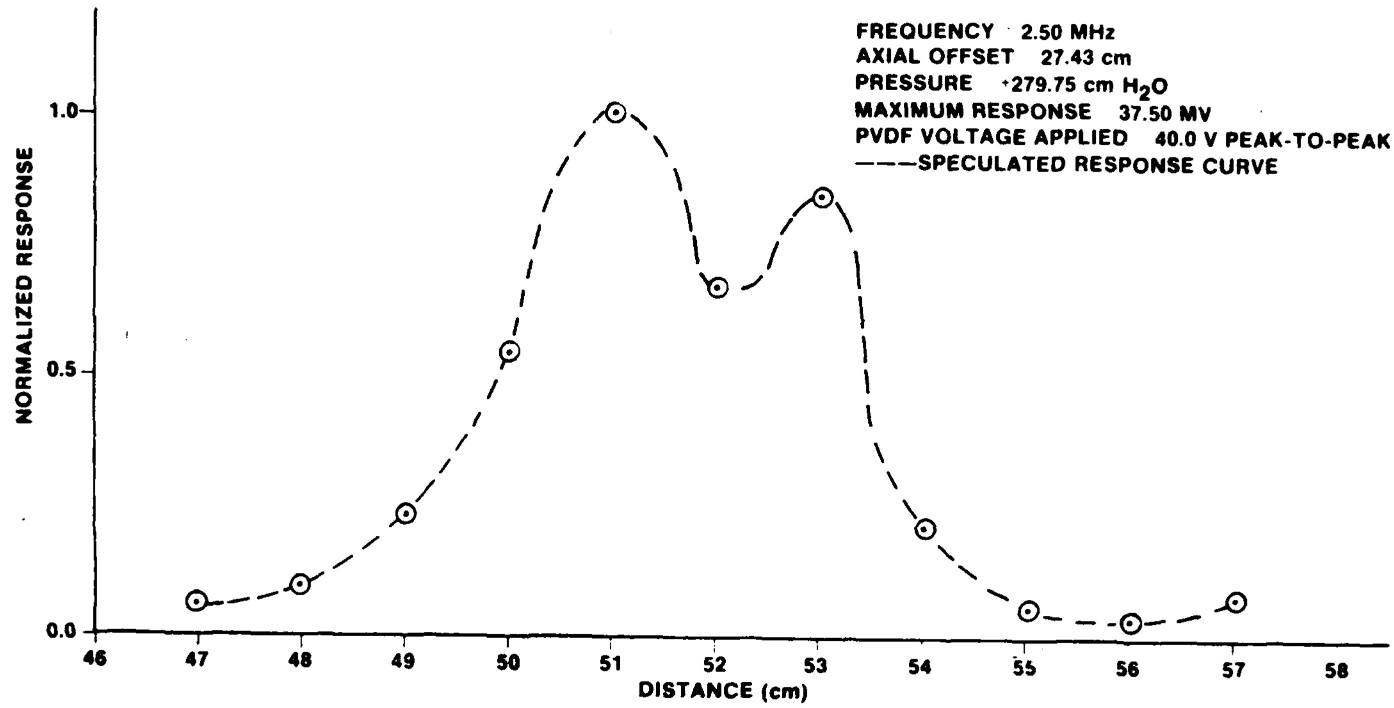

Figure 54. Scan test G2.50.

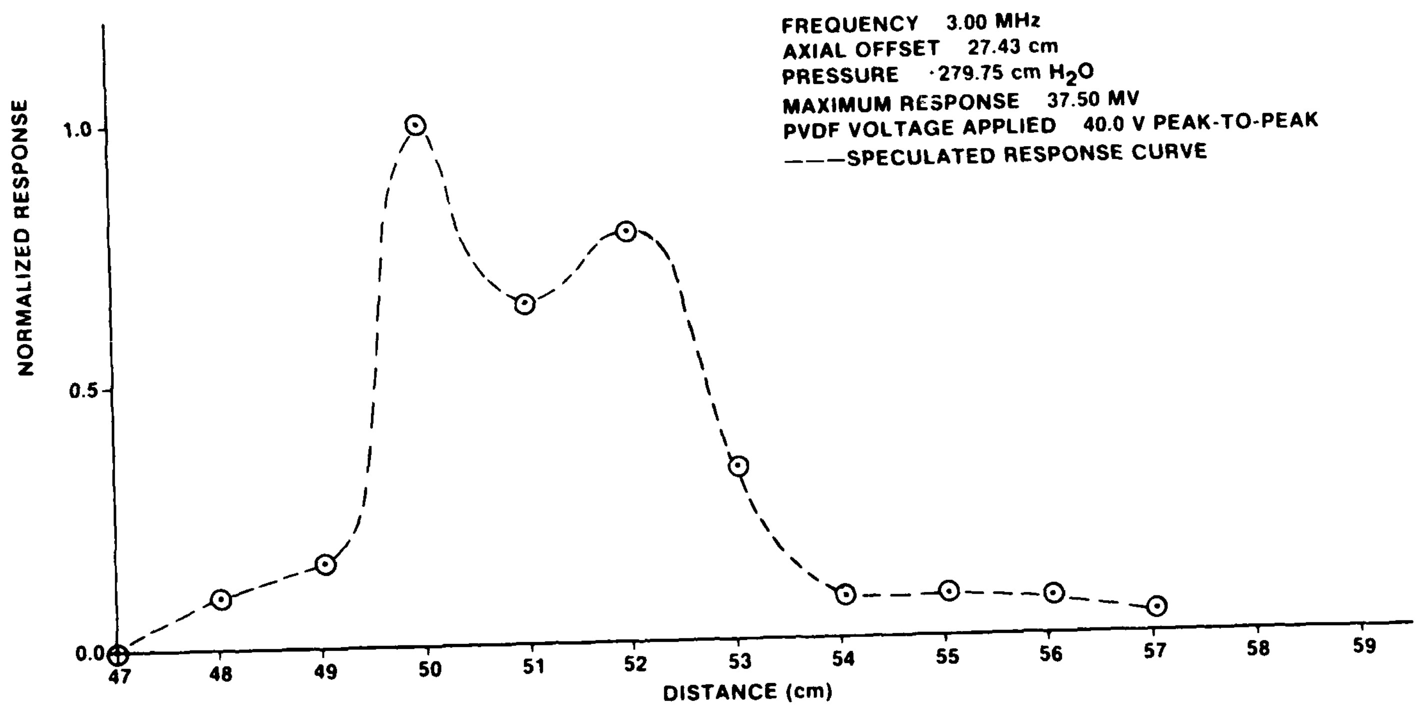

Figure 55. Scan test G3.00

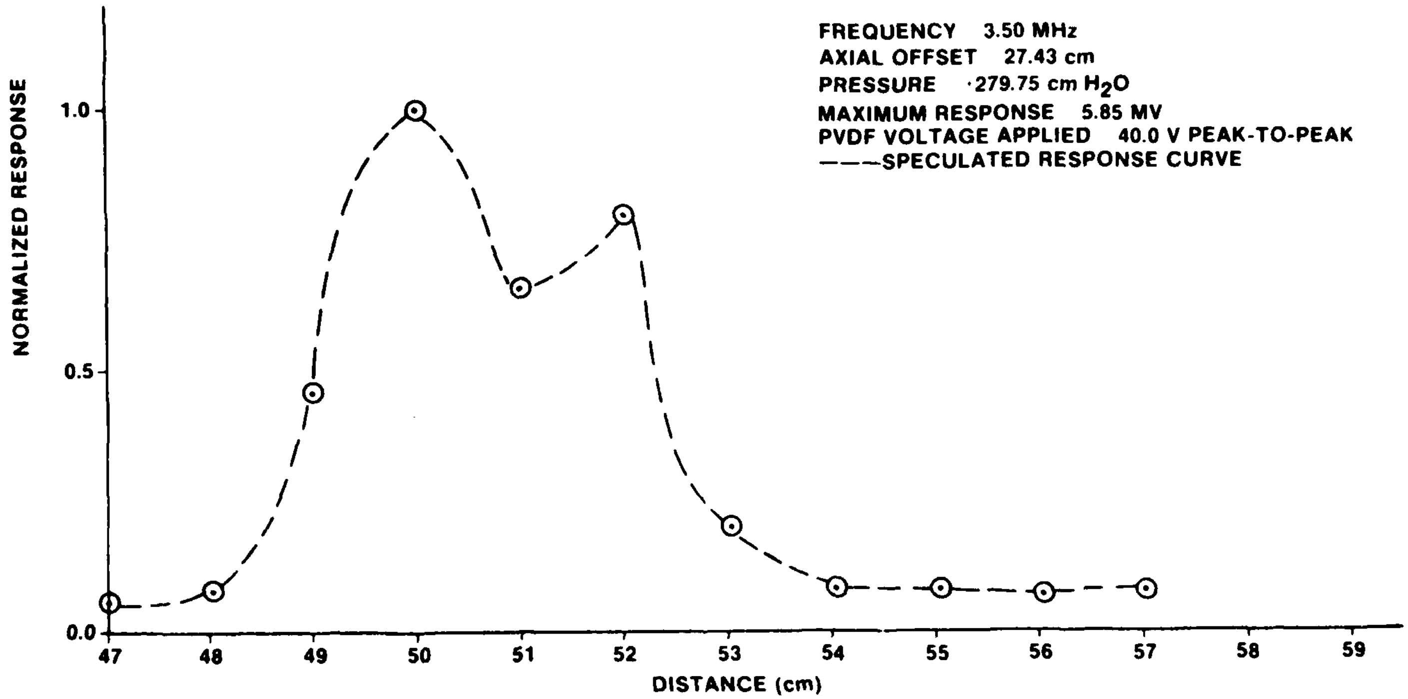

Figure 56. Scan test G3.50.

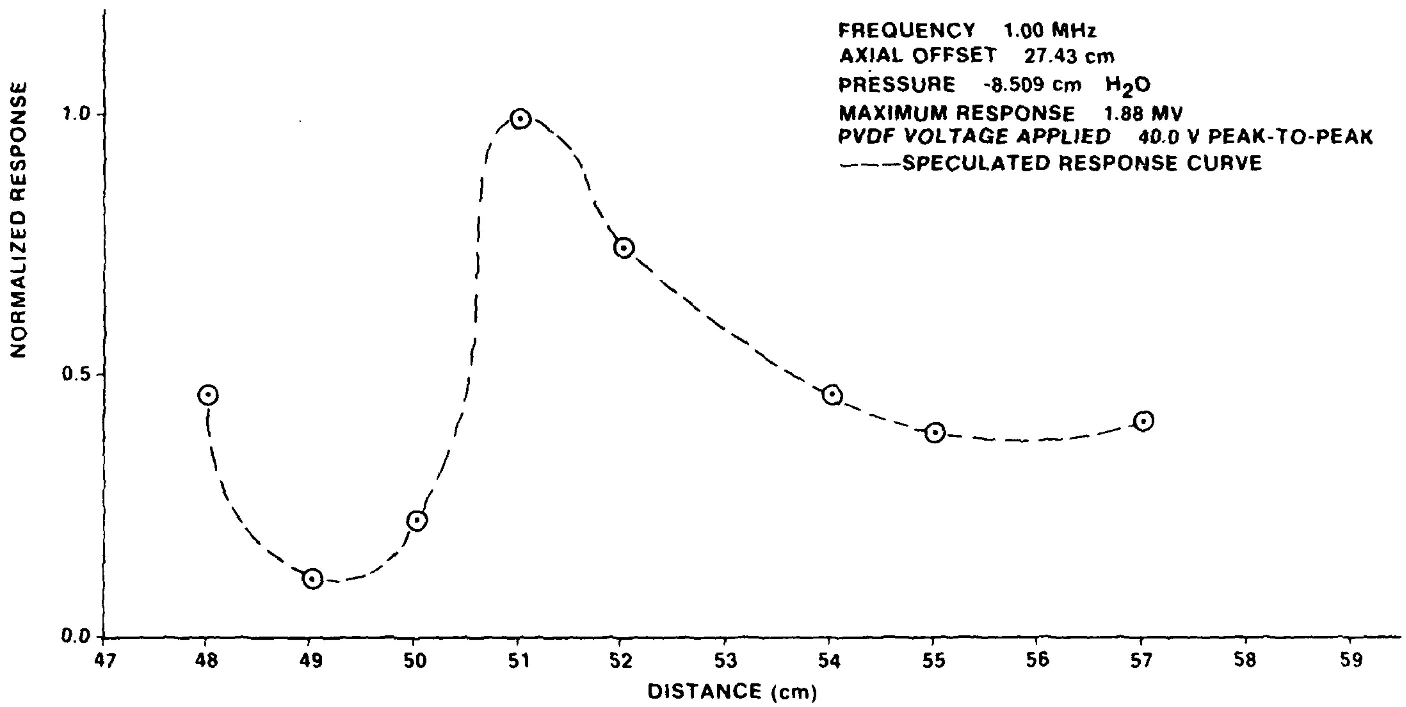

Figure 57. Scan test H1.00.

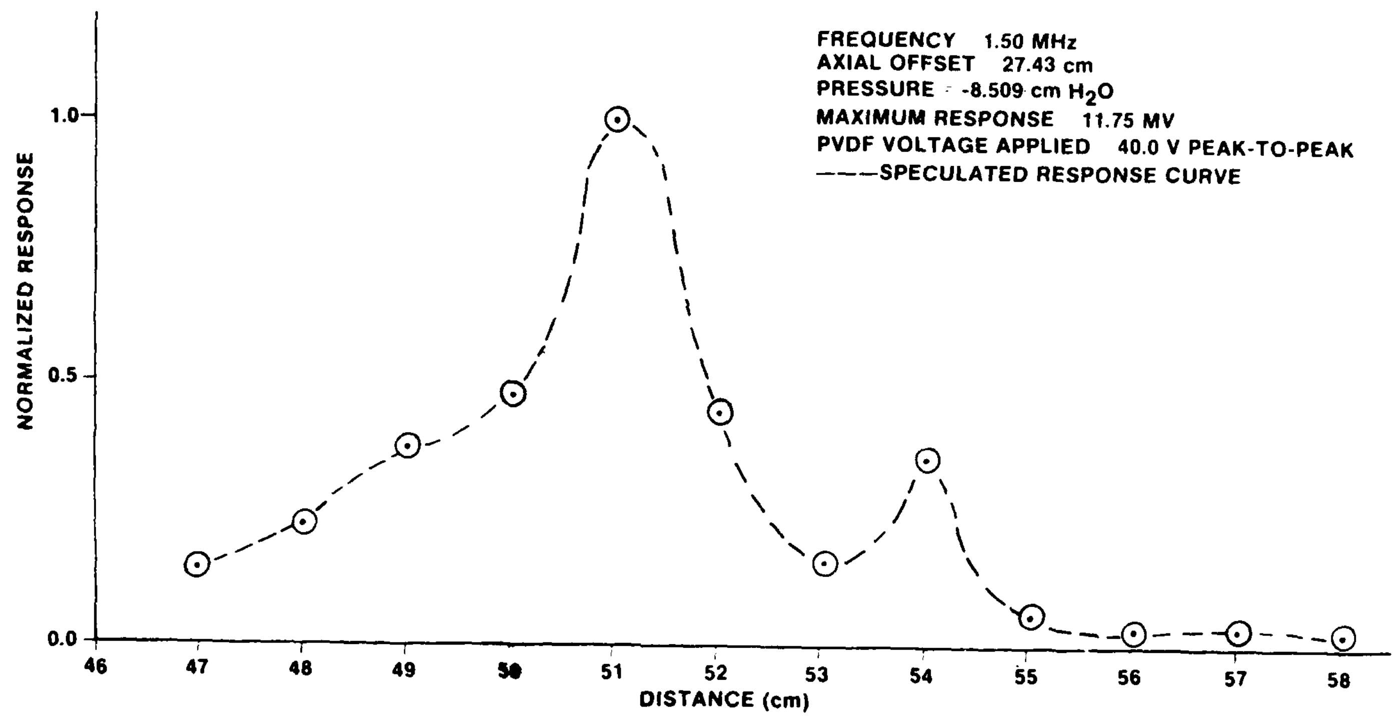

Figure 58. Scan test H1.50.

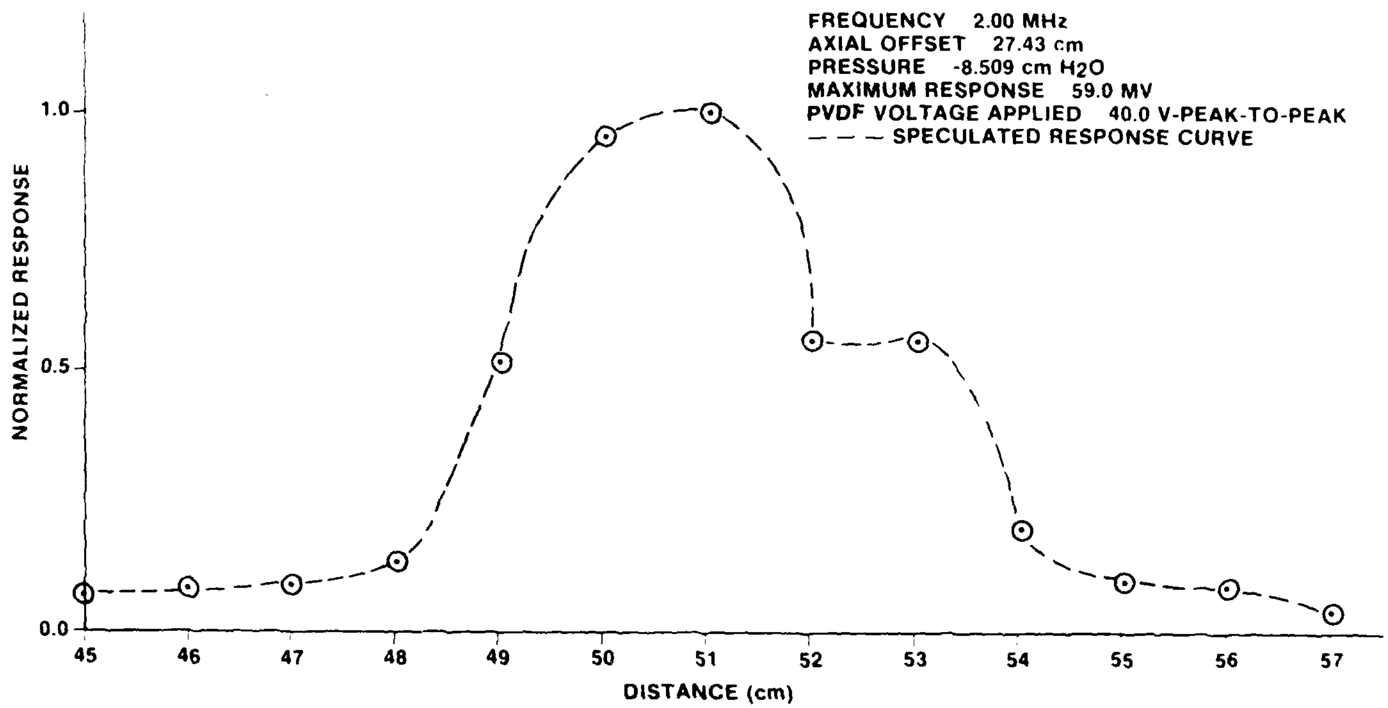

Figure 59. Scan test H2.00.

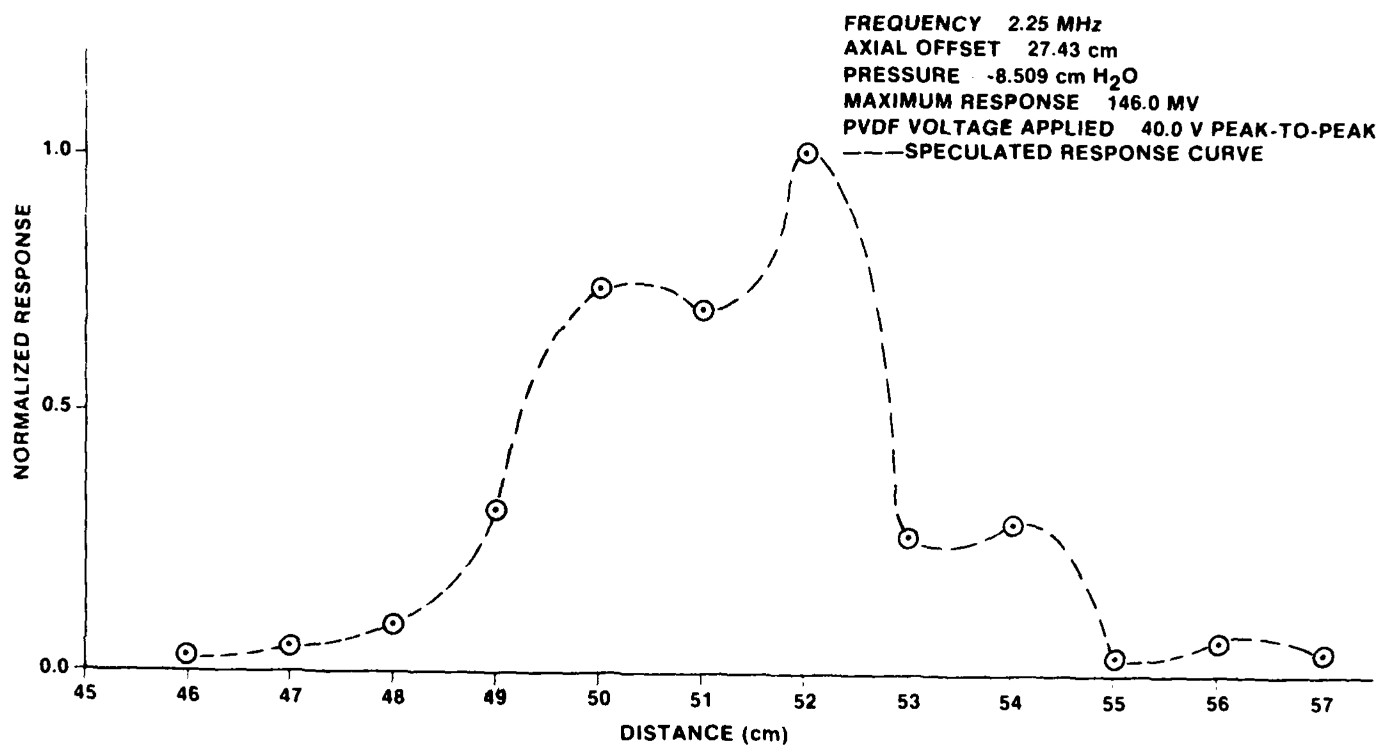

Figure 60. Scan test H2.25.

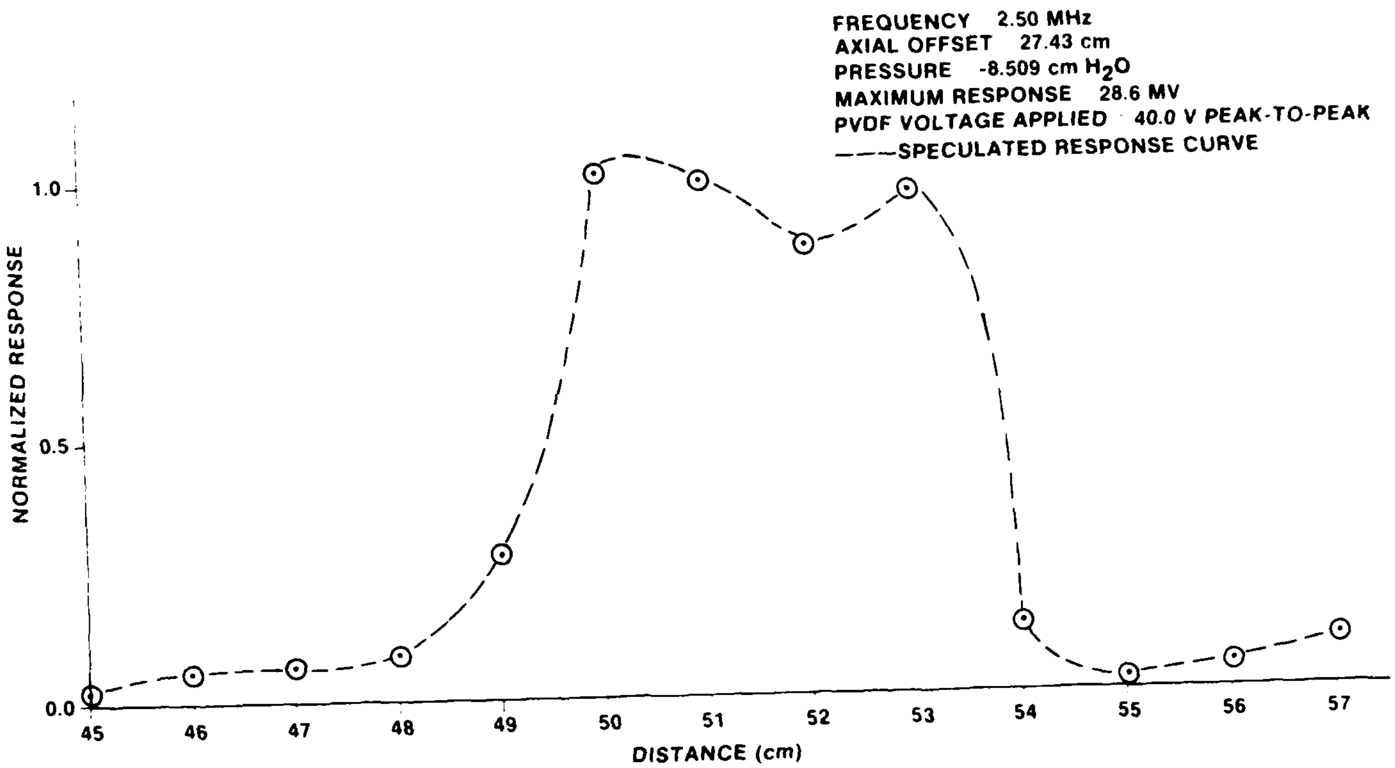

Figure 61. Scan test H2.50.

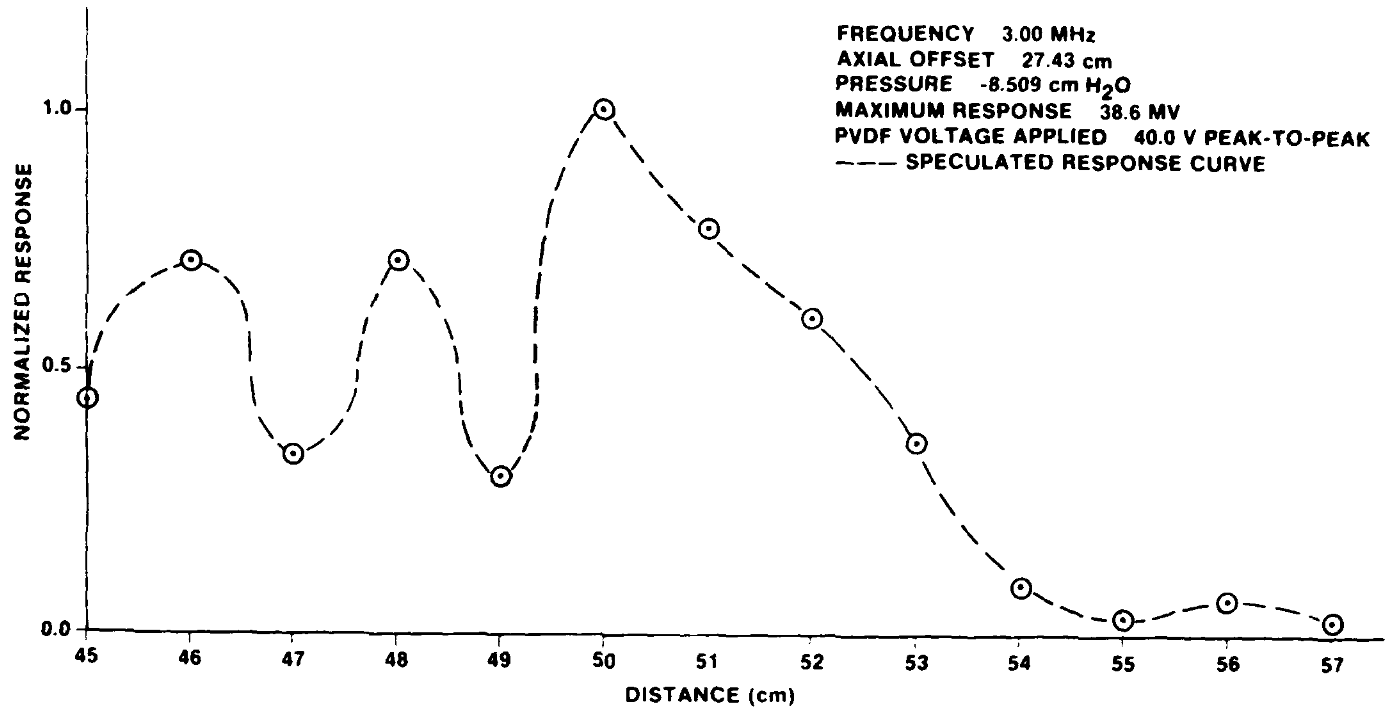

Figure 62. Scan test H3.00.

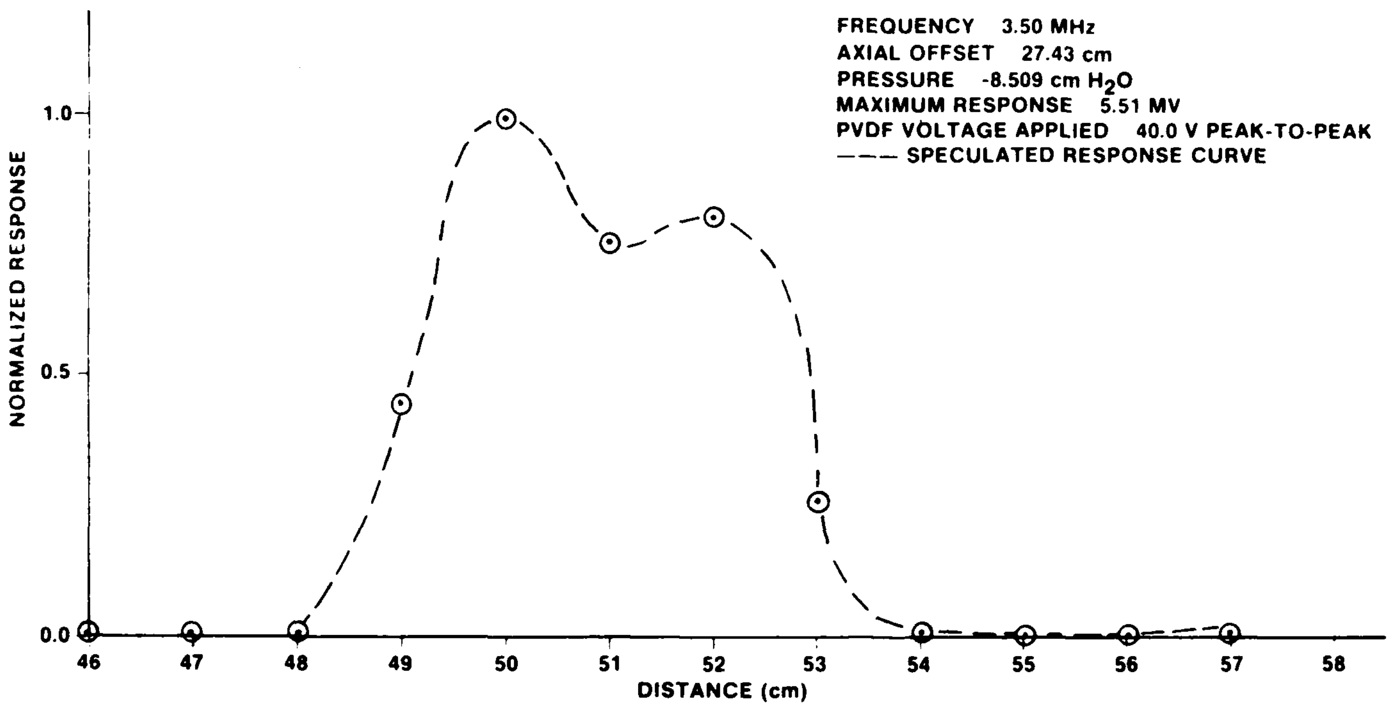

Figure 63. Scan test H3.50.

Figure 64. Scan test I1.00.

Figure 65. Scan test I1.50.

Figure 66. Scan test I2.00.

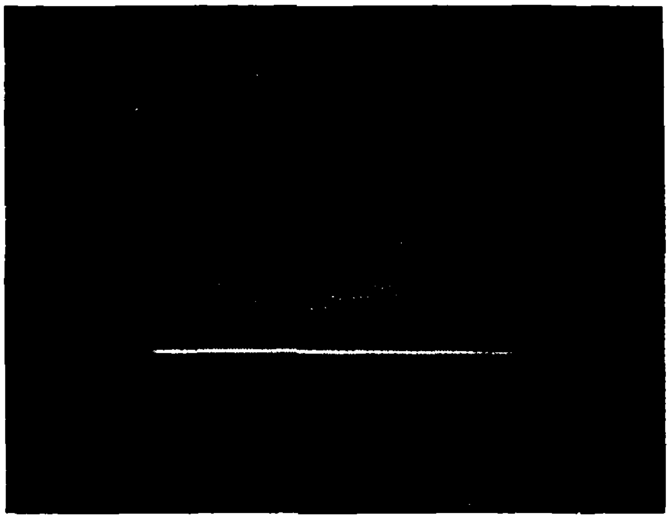

Figure 67. Scan test I2.25.

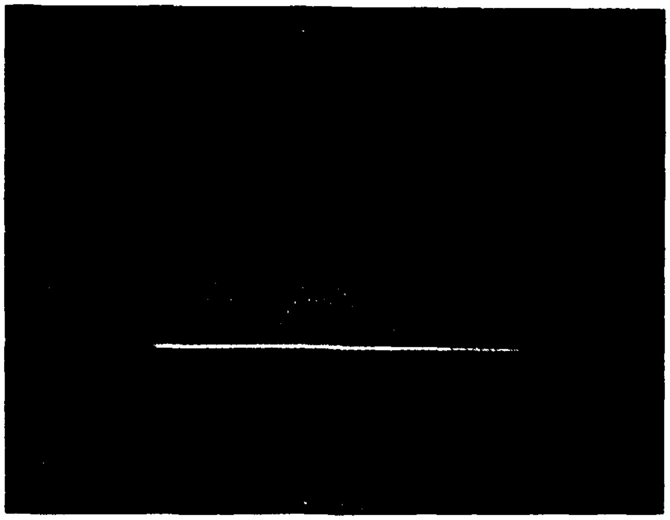

Figure 68. Scan test 12.50.

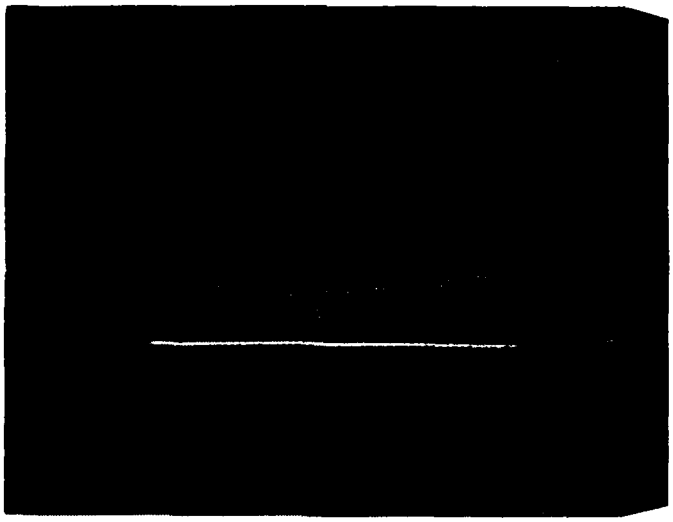

Figure 69. Scan test 13.00.

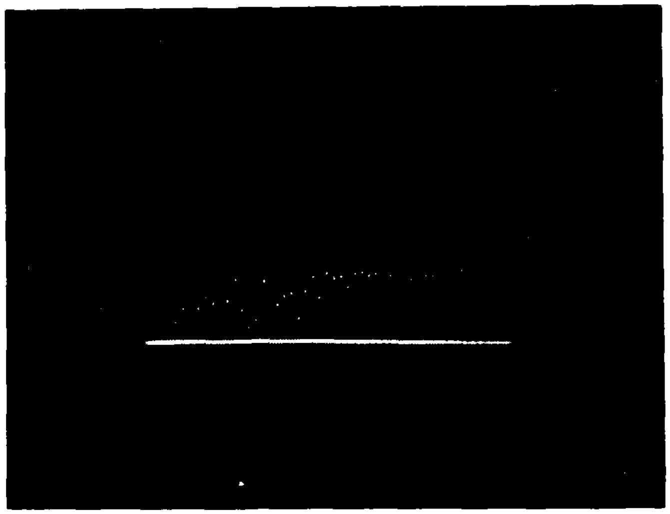

Figure 70. Scan test I3.50.

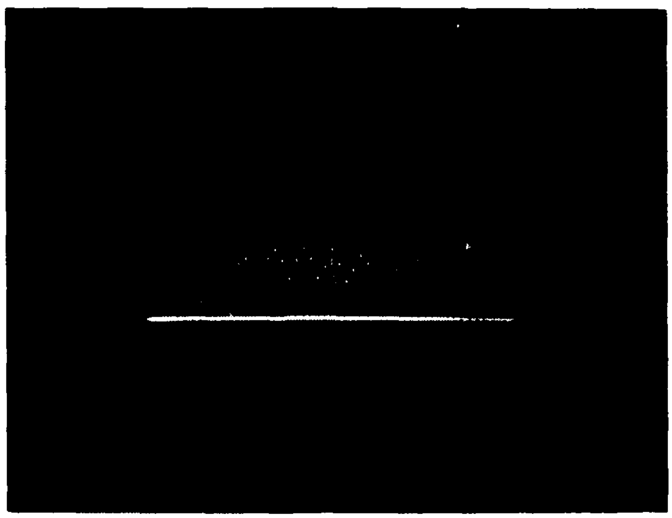

Figure 71. Scan test J1.00.

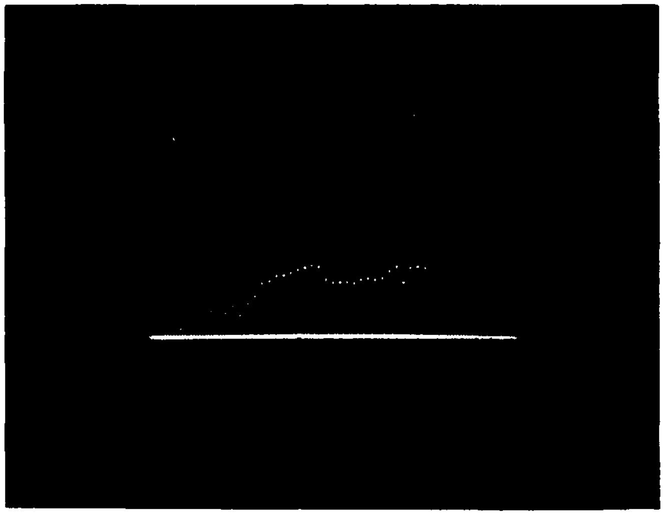

Figure 72. Scan test J1.50.

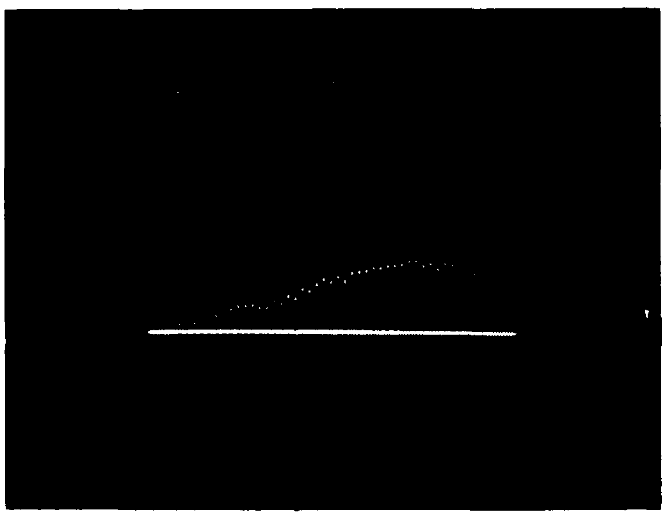

Figure 73. Scan test J2.00.

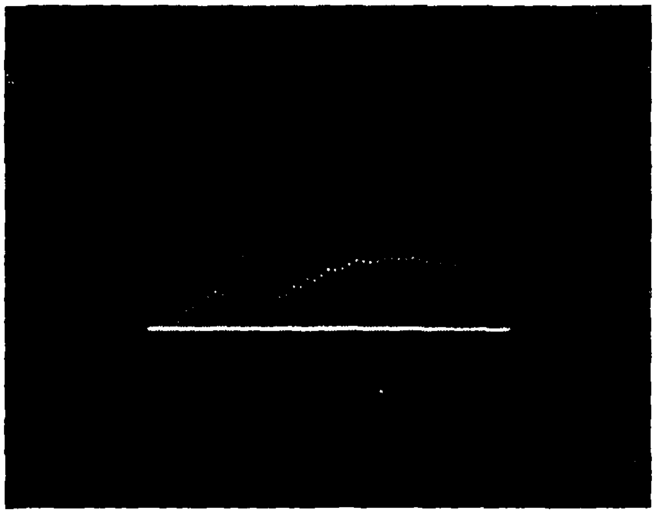

Figure 74. Scan test J2.25.

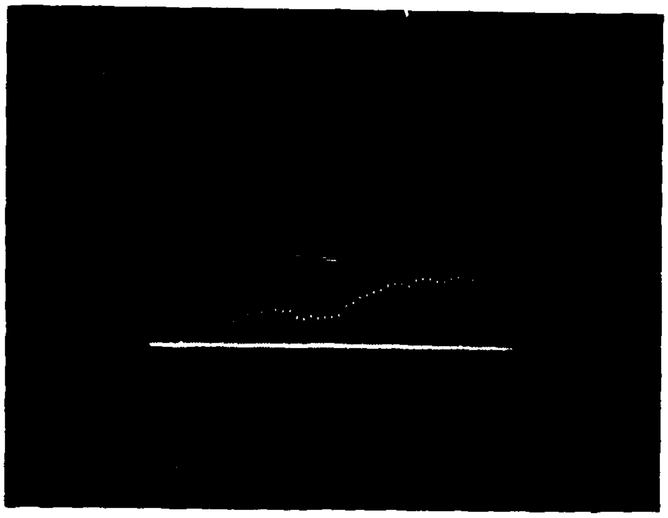

Figure 75. Scan test J2.50.

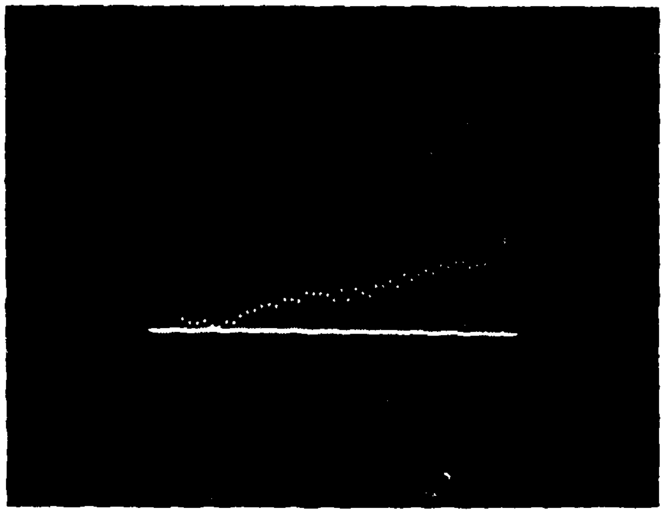

Figure 76. Scan test J3.00.

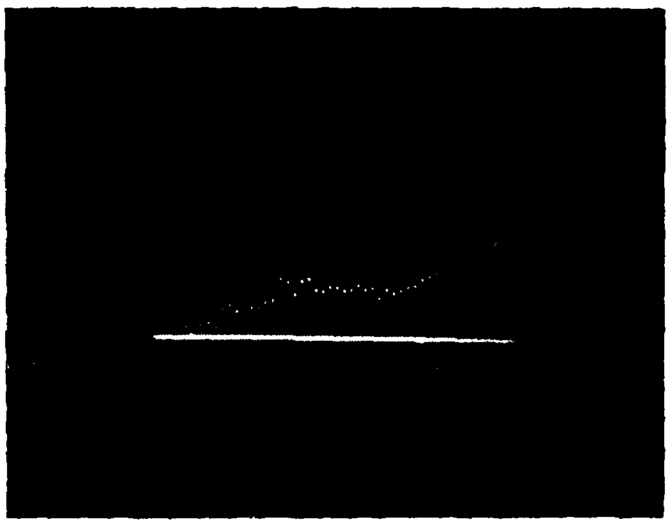

Figure 77. Scan test J3.50.

TABLE 1. PIEZOELECTRIC PROPERTIES OF VARIOUS MATERIALS

PIEZOELECTRIC MATERIAL	DENSITY g/cm^3	DIELECTRIC PERMITTIVITY ϵ	d CGS ESU $X10^{-8}$
QUARTZ	2.66	4.5	6
ROCHELLE SALT	1.77	350	825
PZT CERAMICS	7.5	1700	384
PVDF	-	10	20
PVDF (PIONEER ELECTRONICS CORP.)	1.79	12	80

TABLE 2. τ_F, τ_R AND τ_T AT 1.0 MHz FOR -100.76 cm H_2O DIFFERENTIAL MEMBRANE PRESSURE

TRANSMITTER VOLTAGE (PEAK-TO-PEAK VOLTS)	RECEIVER VOLTAGE (MV-RMS)		τ_F	τ_R	τ_T
	AEROTECH	PVDF			
10.0	-	-	-	-	-
15.0	1.13	-	.075	-	-
20.0	1.74	1.28	.087	.064	.735
25.0	2.21	1.54	.088	.061	.696
30.0	2.71	1.78	.090	.059	.656
35.0	3.21	1.97	.091	.056	.613
40.0	3.60	2.18	.090	.054	.605
AVERAGES →			.086	.058	.661

AD-A082 025 ARMY MISSILE COMMAND REDSTONE ARSENAL AL TECHNOLOGY LAB F/G 17/1
A POLYVINYLIDENE FLUORIDE DIFFERENTIAL MEMBRANE PRESSURE ACOUST--ETC(U)
SEP 79 J A SCHAEFFEL
UNCLASSIFIED DRSMI-T-79-25 NL

2 .. 2

END
DATE
FILMED
4 80
DTIC

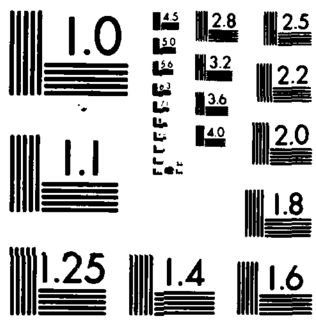

MICROCOPY RESOLUTION TEST CHART

NATIONAL BUREAU OF STANDARDS-1963-A

TABLE 3. τ_F, τ_R AND τ_T AT 1.50 MHz FOR -100.76 cm H_2O DIFFERENTIAL MEMBRANE PRESSURE

TRANSMITTER VOLTAGE (PEAK-TO-PEAK VOLTS)	RECEIVER VOLTAGE (MV-RMS)		τ_F	τ_R	τ_T
	AEROTECH	PVDF			
10.0	2.23	-	.223	-	-
15.0	2.04	0.66	.136	.044	.323
20.0	1.04	0.95	.052	.047	.913
25.0	0.93	0.97	.037	.038	1.043
30.0	3.61	1.01	.120	.033	.279
35.0	6.25	0.99	.178	.028	.158
40.0	9.99	0.96	.249	.006	.096
AVERAGES →			.142	.032	.468

TABLE 4. τ_F, τ_R AND τ_T AT 2.00 MHz FOR -100.76 cm H_2O DIFFERENTIAL MEMBRANE PRESSURE

TRANSMITTER VOLTAGE (PEAK-TO-PEAK VOLTS)	RECEIVER VOLTAGE (MV-RMS)		τ_F	τ_R	τ_T
	AEROTECH	PVDF			
10.0	18.8	.96	1.880	.0960	.051
15.0	28.9	1.46	1.926	.0973	.050
20.0	38.5	1.98	1.925	.0990	.051
25.0	48.0	2.33	1.920	.0932	.048
30.0	56.5	2.85	1.883	.0950	.050
35.0	66.1	3.39	1.888	.0968	.051
40.0	-	3.92	-	.0980	-
AVERAGES →			1.903	.096	.050

TABLE 5. τ_F, τ_R AND τ_T AT 2.25 MHz FOR -100.76 cm H_2O DIFFERENTIAL MEMBRANE PRESSURE

TRANSMITTER VOLTAGE (PEAK-TO-PEAK VOLTS)	RECEIVER VOLTAGE (MV-RMS)		τ_F	τ_R	τ_T
	AEROTECH	PVDF			
10.0	64.0	4.99	6.40	.499	.077
15.0	108.0	7.35	7.20	.490	.068
20.0	144.0	9.95	7.20	.497	.069
25.0	178.0	12.45	7.12	.498	.069
30.0	206.0	15.20	6.86	.506	.073
35.0	232.0	17.75	6.62	.507	.076
40.0	257.0	20.05	6.42	.501	.078
		AVERAGES →	6.83	.499	.072

TABLE 6. τ_F, τ_R AND τ_T AT 2.50 MHz FOR -100.76 cm H_2O DIFFERENTIAL MEMBRANE PRESSURE

TRANSMITTER VOLTAGE (PEAK-TO-PEAK VOLTS)	RECEIVER VOLTAGE (MV-RMS)		τ_F	τ_R	τ_T
	AEROTECH	PVDF			
10.0	4.51	0.465	.451	.046	.103
15.0	6.70	0.670	.446	.044	.100
20.0	8.30	0.899	.415	.044	.108
25.0	9.99	1.180	.399	.047	.118
30.0	12.35	1.460	.411	.048	.118
35.0	13.71	1.760	.391	.050	.128
40.0	16.35	1.970	.408	.049	.120
AVERAGES →			.417	.046	.113

TABLE 7. τ_F, τ_R AND τ_T AT 3.00 MHz FOR -100.76 cm H_2O DIFFERENTIAL MEMBRANE PRESSURE

TRANSMITTER VOLTAGE (PEAK-TO-PEAK VOLTS)	RECEIVER VOLTAGE (MV-RMS) AEROTECH	RECEIVER VOLTAGE (MV-RMS) PVDF	τ_F	τ_R	τ_T
10.0	-	.425	-	.042	-
15.0	1.48	.625	.098	.041	.422
20.0	1.92	.820	.096	.041	.427
25.0	2.42	1.160	.096	.046	.479
30.0	2.82	1.440	.094	.048	.510
35.0	3.25	1.680	.092	.048	.516
40.0	3.65	1.960	.091	.049	.536
		AVERAGES ⟶	.094	.045	.481

TABLE 8. τ_F, τ_R AND τ_T AT 3.50 MHz FOR -100.76 cm H_2O DIFFERENTIAL MEMBRANE PRESSURE

TRANSMITTER VOLTAGE (PEAK-TO-PEAK VOLTS)	RECEIVER VOLTAGE (MV-RMS)		τ_F	τ_R	τ_T
	AEROTECH	PVDF			
10.0	-	.425	-	.042	-
15.0	1.48	.625	.098	.041	.422
20.0	1.92	.820	.096	.041	.427
25.0	2.42	1.160	.096	.046	.479
30.0	2.82	1.440	.094	.048	.510
35.0	3.25	1.680	.092	.048	.516
40.0	3.65	1.960	.091	.049	.536
AVERAGES →			.094	.045	.481

TABLE 9. τ_F, τ_R AND τ_T AT 1.0 MHz FOR +188.85 cm H_2O DIFFERENTIAL MEMBRANE PRESSURE

TRANSMITTER VOLTAGE (PEAK-TO-PEAK VOLTS)	RECEIVER VOLTAGE (MV-RMS)		τ_F	τ_R	τ_T
	AEROTECH	PVDF			
10.0	-	-	-	-	-
15.0	.22	-	.014	-	-
20.0	.25	1.24	.012	.062	4.960
25.0	.33	1.63	.013	.065	4.939
30.0	.41	2.03	.013	.067	4.951
35.0	.48	2.46	.013	.070	5.125
40.0	.56	2.84	.014	.071	5.071
	AVERAGES →		.013	.067	5.009

TABLE 10. τ_F, τ_R AND τ_T AT 1.50 MHz FOR +188.85 cm H_2O DIFFERENTIAL MEMBRANE PRESSURE

TRANSMITTER VOLTAGE (PEAK-TO-PEAK VOLTS)	RECEIVER VOLTAGE (MV-RMS)		τ_F	τ_R	τ_T
	AEROTECH	PVDF			
10.0	1.18	-	.118	-	-
15.0	2.05	.66	.136	.044	.321
20.0	3.99	.64	.199	.032	.160
25.0	6.48	.44	.259	.017	.067
30.0	9.48	.56	.316	.018	.059
35.0	12.95	.79	.370	.022	.061
40.0	15.75	1.09	.393	.027	.069
	AVERAGES →		.255	.026	.122

TABLE 11. τ_F, τ_R AND τ_T AT 2.00 MHz FOR +188.85 cm H_2O DIFFERENTIAL MEMBRANE PRESSURE

TRANSMITTER VOLTAGE (PEAK-TO-PEAK VOLTS)	RECEIVER VOLTAGE (MV-RMS)		τ_F	τ_R	τ_T
	AEROTECH	PVDF			
10.0	18.40	.74	1.84	.074	.040
15.0	28.25	1.13	1.88	.075	.040
20.0	39.00	1.57	1.95	.078	.040
25.0	50.00	1.84	2.00	.073	.036
30.0	62.00	2.22	2.06	.074	.035
35.0	-	2.62	-	.074	-
40.0	-	3.06	-	.076	-
		AVERAGES →	1.94	.074	.038

TABLE 12. τ_F, τ_R AND τ_T AT 2.25 MHz FOR +188.85 cm H_2O DIFFERENTIAL MEMBRANE PRESSURE

TRANSMITTER VOLTAGE (PEAK-TO-PEAK VOLTS)	RECEIVER VOLTAGE (MV-RMS)		τ_F	τ_R	τ_T
	AEROTECH	PVDF			
10.0	73.0	5.10	7.300	.510	.069
15.0	112.0	7.49	7.466	.499	.066
20.0	148.0	11.35	7.400	.567	.076
25.0	182.0	12.75	7.280	.510	.070
30.0	211.0	15.43	7.033	.514	.073
35.0	238.0	17.98	6.800	.513	.075
40.0	268.0	20.61	6.700	.515	.076
AVERAGES ⟶			7.139	.518	.072

TABLE 13. τ_F, τ_R AND τ_T AT 2.50 MHz FOR +188.85 cm H_2O DIFFERENTIAL MEMBRANE PRESSURE

TRANSMITTER VOLTAGE (PEAK-TO-PEAK VOLTS)	RECEIVER VOLTAGE (MV-RMS)		τ_F	τ_R	τ_T
	AEROTECH	PVDF			
10.0	4.85	.449	.485	.044	.092
15.0	7.15	.721	.476	.048	.100
20.0	9.75	.965	.487	.048	.098
25.0	12.40	1.250	.496	.050	.100
30.0	15.15	1.475	.505	.049	.097
35.0	17.65	1.650	.504	.047	.093
40.0	19.65	1.870	.491	.046	.095
AVERAGES →			.492	.047	.096

TABLE 14. τ_F, τ_R AND τ_T AT 3.00 MHz FOR +188.85 cm H_2O DIFFERENTIAL MEMBRANE PRESSURE

TRANSMITTER VOLTAGE (PEAK-TO-PEAK VOLTS)	RECEIVER VOLTAGE (MV-RMS)		τ_F	τ_R	τ_T
	AEROTECH	PVDF			
10.0	-	.360	-	.036	-
15.0	1.32	.540	.088	.036	.409
20.0	1.73	.681	.086	.034	.393
25.0	2.24	.865	.089	.034	.386
30.0	2.85	.980	.095	.032	.343
35.0	3.55	1.125	.101	.032	.316
40.0	4.02	1.240	.100	.031	.308
AVERAGES →			.093	.033	.359

TABLE 15. τ_F, τ_R AND τ_T AT 3.50 MHz FOR +188.85 cm H_2O DIFFERENTIAL MEMBRANE PRESSURE

TRANSMITTER VOLTAGE (PEAK-TO-PEAK VOLTS)	RECEIVER VOLTAGE (MV-RMS)		τ_F	τ_R	τ_T
	AEROTECH	PVDF			
10.0	-	-	-	-	-
15.0	.54	.855	.036	.057	1.583
20.0	.68	1.270	.034	.063	1.867
25.0	.89	1.670	.035	.066	1.876
30.0	1.09	1.980	.036	.066	1.816
35.0	1.29	2.230	.036	.063	1.728
40.0	1.52	2.520	.038	.063	1.657
AVERAGES →			.035	.063	1.754

TABLE 16. I AND J TEST SERIES DATA

TEST NUMBER	MINIMUM TRANSDUCER SPACING (cm)	MAXIMUM TRANSDUCER SPACING (cm)	PVDF APPLIED VOLTAGE (VOLTS PEAK-TO-PEAK)	AEROTECH TRANSDUCER MAXIMUM RESPONSE (MV-RMS)
I1.00	2.651	44.65	40.0	3.80
I1.50	1.651	44.65	40.0	14.20
I2.00	1.651	44.65	30.0	51.00
I2.25	1.651	44.65	40.0	63.00
I2.50	1.651	44.65	40.0	12.80
I3.00	1.651	44.65	40.0	21.65
I3.50	1.651	44.65	40.0	5.85
J1.00	2.651	44.65	40.0	3.24
J1.50	1.651	44.65	40.0	17.70
J2.00	2.651	44.65	25.0	59.90
J2.25	2.651	44.65	40.0	206.00
J2.50	2.651	44.65	40.0	48.50
J3.00	2.651	44.65	40.0	44.20
J3.50	2.651	44.65	40.0	8.55

SYMBOLS

Symbol	Definition
a	Membrane radius.
D	Diameter of circular radiator.
d_{ij}	Piezoelectric modulii
E	Membrane modulus of elasticity.
E_i	Electric field strength.
I_{RMS}	RMS current flow through PVDF transducer.
N	Near field length.
P	Differential membrane pressure.
P_{app}	Apparent power consumed by PVDF transducer.
P_i	Polarization per unit area.
r	Membrane transducer focal radius.
t	Membrane thickness.
V_A	Peak-to-peak voltage applied to reference transducer.
V_{ARMS}	RMS voltage output of reference transducer.
V_{PRMS}	RMS voltage input to or output from PVDF transducer.
V_{PVDF}	Peak-to-peak voltage applied to the PVDF transducer.
V_{RMS}	RMS voltage applied to the PVDF transducer.
w	Membrane deflection.
β	Transmission gain in transmitting ultrasound from PVDF to reference transducer.
ϵ_j	Matrix representation of strain.
Θ	Acoustical radiator divergence angle.
λ	Ultrasonic wavelength.
γ	Angle of acoustical radiator divergence.
σ_j	Matrix representation of applied stress.
T_F	PVDF transducer transmission coefficient.
T_R	Reference transmission coefficient.
T_T	Reverse transmission coefficient.

DISTRIBUTION

	No. of Copies
Defense Metals Information Center Battelle Memorial Institute 505 King Avenue Columbus, Ohio 43201	1
Defense Technical Information Center Cameron Station Alexandria, Virginia 22314	12
Commander US Army Foreign Science and Technology Center ATTN: DRXST-SD3 220 Seventh Street, NE Charlottesville, Virginia 22901	1
Office of Chief of Research and Development Department of the Army ATTN: DARD-ARS-P Washington, DC 20301	1
Commander US Army Electronics Command ATTN: DRSEL-PA-P	1
-CT-DT	1
-PP, Mr. Sulkolove Fort Monmouth, New Jersey 07703	1
Commander US Army Natick Laboratories Kansas Street ATTN: STSNLT-EQR Natick, Massachusetts 01760	1
Commander US Army Mobility Equipment Research and Development Center Fort Belvoir, Virginia 22060	1

DISTRIBUTION (Continued)

	No. of Copies
Director USA Mobility Equipment Research and Development Center Coating and Chemical Laboratory ATTN: STSFB-CL Aberdeen Proving Ground, Maryland 21005	1
Commander Edgewood Arsenal ATTN: SAREA-TS-A Aberdeen Proving Ground, Maryland 21010	1
Commander Picatinny Arsenal ATTN: SARPA-TS-S, Mr. M. Costello Dover, New Jersey 07801	1
Commander Rock Island Arsenal Research and Development ATTN: 9320 Rock Island, Illinois 61201	1
Commander Watervliet Arsenal Watervliet, New York 12189	1
Commander US Army Aviation Systems Command ATTN: DRSAV-EE -MT, Mr. Vollmer St. Louis, Missouri 63166	1 1
Commander US Army Aeronautical Depot Maintenance Center (Mail Stop) Corpus Christi, Texas 78403	1
Commander US Army Test and Evaluation Command ATTN: DRSTE-RA Aberdeen Proving Ground, Maryland 21005	1
Commander ATTN: STEAP-MT Aberdeen Proving Ground, Maryland 21005	1

DISTRIBUTION (Continued)

	No. of Copies
Chief Bureau of Naval Weapons Department of the Navy Washington, DC 20360	1
Chief Bureau of Ships Department of the Navy Washington, DC 20315	1
Naval Research Laboratory ATTN: Dr. M. M. Krafft Code 8430 Washington, DC 20375	1
Commander Wright Air Development Division ATTN: ASRC Wright-Patterson AFB, Ohio 45433	1
Director Air Force Materiel Laboratory ATTN: AFML-DO-Library Wright-Patterson AFB, Ohio 45433	1
Director, Army Materials and Mechanics Research Center ATTN: DRXMR-PL	1
-MT, Mr. Farrow Watertown, Massachusetts 02172	1
Commander White Sands Missile Range ATTN: STEWS-AD-L White Sands Missile Range, New Mexico 88002	1
Deputy Commander US Army Nuclear Agency ATTN: MONA-ZB Fort Bliss, Texas 79916	1
Jet Propulsion Laboratory California Institute of Technology ATTN: Library/Acquisitions 111-113 4800 Oak Grove Drive Pasadena, California 91103	1

DISTRIBUTION (Continued)

	No. of Copies
Sandia Laboratories ATTN: Library P.O. Box 969 Livermore, California 94550	1
Commander US Army Air Defense School ATTN: ATSA-CD-MM Fort Bliss, Texas 79916	1
Technical Library Naval Ordnance Station Indian Head, Maryland 20640	1
Commander US Army Material Development and Readiness Command ATTN: DRCMT Washington, DC 20315	1
Headquarters SAC/NRI (Stinfo Library) Offutt Air Force Base, Nebraska 68113	1
Commander Rock Island Arsenal ATTN: SARRI-RLPL-Technical Library Rock Island, Illinois 61201	1
Commander (Code 233) Naval Weapons Center ATTN: Library Division China Lake, California 93555	1
Department of the Army US Army Research Office ATTN: Information Processing Office P.O. Box 12211 Research Triangle Park, North Carolina 27709	1
ADTC (DLDSL) Eglin Air Force Base, Florida 32542	1

DISTRIBUTION (Continued)

	No. of Copies
University of California Los Alamos Scientific Laboratory ATTN: Reports Library P.O. Box 1663 Los Alamos, New Mexico 87545	1
Commander US Army Materiel Development and Readiness Command ATTN: DRCRD DRCDL 5001 Eisenhower Avenue Alexandria, Virginia 22333	1 1
Director Defense Advanced Research Projects Agency 1400 Wilson Boulevard Arlington, Virginia 22209	1
Commander US Army Research Office ATTN: DRXRO-PH, Dr. R. Lontz P.O. Box 12211 Research Triangle Park, North Carolina 27709	2
US Army Research and Standardization Group (Europe) ATTN: DRXSN-E-RX, Dr. Alfred K. Nedoluha Box 65 FPO New York 09510	2
Headquarters Department of the Army Office of the DCS for Research Development and Acquisition Room 3A474, The Pentagon ATTN: DAMA-ARZ Washington, DC 20310	2
US Army Materiel Systems Analysis Activity ATTN: DRXSY-MP Aberdeen Proving Ground, MD 21005	1
IIT Research Institute ATTN: GACIAC 10 West 35th Street Chicago, Illinois 60616	1

DISTRIBUTION (Concluded)

	No. of Copies
DRSMI-LP, Mr. Voigt	1
DRSMI -T, Dr. Kobler	1
-TL, Mr. Lewis	1
-TLA, Mr. Pettey	1
-TLA, Dr. Mullinix	1
Mr. Schaeffel	50
-EA	2
-EAA	2
-EAS	1
-EAM	1
-EAP	1
-EAB	1
-EAT	3
-ICBB	1
-TBD	3
-TI (Record Set)	1
(Reference Copy)	1